

NASA/TM-2003-206892, Vol. 27



## SeaWiFS Postlaunch Technical Report Series

*Stanford B. Hooker and Elaine R. Firestone, Editors*

### Volume 27, BENCAL Cruise Report

*Ray Barlow, Heather Sessions, Nonkubela Silulwane, Hermann Engel,  
Stanford B. Hooker, James Aiken, James Fishwick, Victor Martinez-Vicente,  
André Morel, Malik Chami, Joséphine Ras, Stewart Bernard, Maya Pfaff,  
James W. Brown, and Alexandra Fawcett*

National Aeronautics and  
Space Administration

Goddard Space Flight Center  
Greenbelt, Maryland 20771

---

September 2003

## The NASA STI Program Office ... in Profile

Since its founding, NASA has been dedicated to the advancement of aeronautics and space science. The NASA Scientific and Technical Information (STI) Program Office plays a key part in helping NASA maintain this important role.

The NASA STI Program Office is operated by Langley Research Center, the lead center for NASA's scientific and technical information. The NASA STI Program Office provides access to the NASA STI Database, the largest collection of aeronautical and space science STI in the world. The Program Office is also NASA's institutional mechanism for disseminating the results of its research and development activities. These results are published by NASA in the NASA STI Report Series, which includes the following report types:

- **TECHNICAL PUBLICATION.** Reports of completed research or a major significant phase of research that present the results of NASA programs and include extensive data or theoretical analysis. Includes compilations of significant scientific and technical data and information deemed to be of continuing reference value. NASA's counterpart of peer-reviewed formal professional papers but has less stringent limitations on manuscript length and extent of graphic presentations.
- **TECHNICAL MEMORANDUM.** Scientific and technical findings that are preliminary or of specialized interest, e.g., quick release reports, working papers, and bibliographies that contain minimal annotation. Does not contain extensive analysis.
- **CONTRACTOR REPORT.** Scientific and technical findings by NASA-sponsored contractors and grantees.
- **CONFERENCE PUBLICATION.** Collected papers from scientific and technical conferences, symposia, seminars, or other meetings sponsored or cosponsored by NASA.
- **SPECIAL PUBLICATION.** Scientific, technical, or historical information from NASA programs, projects, and mission, often concerned with subjects having substantial public interest.
- **TECHNICAL TRANSLATION.** English-language translations of foreign scientific and technical material pertinent to NASA's mission.

Specialized services that complement the STI Program Office's diverse offerings include creating custom thesauri, building customized databases, organizing and publishing research results... even providing videos.

For more information about the NASA STI Program Office, see the following:

- Access the NASA STI Program Home Page at <http://www.sti.nasa.gov/STI-homepage.html>
- E-mail your question via the Internet to [help@sti.nasa.gov](mailto:help@sti.nasa.gov)
- Fax your question to the NASA Access Help Desk at (301) 621-0134
- Write to:  
NASA Access Help Desk  
NASA Center for Aerospace Information  
7121 Standard Drive  
Hanover, MD 21076-1320



## SeaWiFS Postlaunch Technical Report Series

Stanford B. Hooker, Editor  
*NASA Goddard Space Flight Center, Greenbelt, Maryland*

Elaine R. Firestone, Senior Scientific Technical Editor  
*Science Applications International Corporation, Beltsville, Maryland*

## Volume 27, BENCAL Cruise Report

Ray Barlow, Heather Sessions, Nonkqubela Silulwane, and Hermann Engel  
*Marine and Coastal Management, Cape Town, South Africa*

Stanford B. Hooker  
*NASA Goddard Space Flight Center, Greenbelt, Maryland*

James Aiken, James Fishwick, and Victor Martinez-Vicente  
*Plymouth Marine Laboratory, Plymouth, United Kingdom*

André Morel, Malik Chami, and Joséphine Ras  
*LOV Observatoire Océanologique de Villefranche, Villefranche-sur-Mer, France*

Stewart Bernard and Maya Pfaff  
*University of Cape Town, Cape Town, South Africa*

James W. Brown  
*RSMAS University of Miami, Miami, Florida*

Alexandra Fawcett  
*Saturn Solutions, Ltd., Southampton, United Kingdom*

**ISSN 1522-8789**

---

Available from:

NASA Center for AeroSpace Information  
7121 Standard Drive  
Hanover, MD 21076-1320  
Price Code: A17

National Technical Information Service  
5285 Port Royal Road  
Springfield, VA 22161  
Price Code: A10

## PREFACE

The concept of the Benguela Calibration (BENCAL) cruise for the calibration and validation of ocean color satellite observations emerged from a number of preexisting multilateral, international, and interagency collaborations. Such activities were also strongly encouraged through the Sensor Intercomparison and Merger for Biological and Interdisciplinary Oceanic Studies (SIMBIOS) Project, and many of the scientists involved in the precruise planning discussions were SIMBIOS investigators. Indeed, these collaborations were a prerequisite for an internal coherency or consistency that allow a meaningful merging of data delivered by the various satellite ocean color sensors.

Previous collaborations and activities at sea included the Atlantic Meridional Transect (AMT) cruises along with several others. Cruises of particular interest include: AMT-5—the Sea-viewing Wide Field-of-view Sensor (SeaWiFS) Atlantic Characterization Experiment—which occurred from the UK to the Falklands Islands in September–October 1997 (Aiken et al. 1998); AMT-6, from Cape Town to the UK in May–June 1998; the Benguela Environment Fisheries Interaction and Training (BENEFIT) cruises in the Benguela ecosystem off the coast of south west Africa, on the research vessel (R/V) *Meteor* in October 2000 and on the Fisheries Research Ship (FRS) *Africana* in February 2002; and the PROSOPE† cruise on *Thalassa*, from the Moroccan upwelling zone to the central Mediterranean Sea in September 1999 (Claustre et al. 2002).

The imminent launch of the Medium Resolution Imaging Spectrometer (MERIS), on board the European Space Agency (ESA) Environmental Satellite (ENVISAT), was the primary inspiration for the renewed collaboration. Throughout the period before the ENVISAT launch, it was obvious to the MERIS and AATSR‡ Validation Team (MAVT) and the NASA partners, that no matter when the launch date, a calibration and validation cruise in Case-1 waters, particularly in highly productive waters, would be a necessity at an early date. High concentration waters in near proximity to a major port and home to a deep water research vessel would allow radiometric calibration and algorithm validation over the widest range of phytoplankton biomass. Few opportunities existed in the Northern Hemisphere close to the coastal zones of most European MAVT members. In fact, no dedicated ship time and no adequate ship, large enough for a cooperative effort involving several research teams, were available within the European community.

The availability of the FRS *Africana*, flagship of the Marine and Coastal Management (MCM§) fleet of fisheries research vessels, for a dedicated marine optics cruise in the Benguela ecosystem off the coast of southwest Africa in October 2002, was the perfect opportunity. The juxtaposition of four stars in the firmament by summer 2002, provided a unique opportunity to intercalibrate the SeaWiFS instrument (launched August 1997) with the newer sensors, that is, the Moderate Resolution Imaging Spectroradiometer (MODIS) aboard the Terra spacecraft (December 1999), MERIS (February 2002), and a second MODIS instrument on board the Aqua satellite (April 2002). Note that had the Japanese Global Imager (GLI) launched on its original schedule, the hand dealt would have been a royal flush instead of four aces.

The cruise timing was critical given that the SeaWiFS data-buy contract was due to expire in December 2002. The SeaWiFS data set has had the benefit of routine lunar calibrations that establish data stability, independent of the Earth-viewing data, and has been refined through four complete reprocessings. Consequently, it provides the best available basis for an ocean color satellite intercomparison experiment. The initial cruise was sponsored by the MCM group and planned under the initiative of Dr. Ray Barlow as Chief Scientist. Thanks to the financial support of both ESA and NASA, the duration of the cruise was significantly increased, and the transportation of people (two from the US, three from the UK, and three from France), as well as a considerable

† The *Productivité des Systèmes Océaniques Pélagiques* (Productivity of Pelagic Oceanic Systems) cruise is documented at the following Web address: <http://www.obs-vlfr.fr/jgofs/html/prosope/home.htm>.

‡ The Advanced Along Track Scanning Radiometer.

§ MCM is the marine branch of the South African Department of Environmental Affairs and Tourism.

## BENCAL Cruise Report

amount of scientific equipment was made possible. Finally, with the emphasis put on state-of-the-art *in situ* optical instruments and bio-optical measurements, the experiment was given the name BENCAL to emphasize the location and the primary objective.

All the partners had prepared well, which was the key to the successes achieved. Like all oceanographic research, BENCAL had its difficulties and setbacks, but ultimately good fortune played a significant part. The extended range of phytoplankton biomass and the optical properties encountered in the area, along with the excellent sunny weather, a marvelous research vessel (the *Africana*), plus the expertise of her captain, officers, and crew were all factors in the success of the field campaign. Having clear skies is crucial for satellite validation studies and cannot be taken for granted. An earlier cruise near the BENCAL site by some members of the BENCAL group (AMT-6), encountered heavy concentrations of absorbing aerosols (dust and smoke) which made SeaWiFS comparisons difficult. Most of all, the success can be attributed to the collaborations of the scientific party who worked together, long and hard to support each other, and to the patient efficiency of the Chief Scientist in organizing the planning of sometimes rather incompatible operations. Of course the financial support for this cruise from the main sponsors—MCM, NASA, and ESA—was essential and much appreciated.

The BENCAL cruise had several auspicious historical precedents. The Scientific Committee on Oceanographic Research (SCOR) Working Group 15 on Photosynthetic Radiant Energy in the Ocean, chaired by J.E. Tyler, made arrangements to use the USC *Discoverer*. In cooperation with the United Nations Educational, Scientific, and Cultural Organization (UNESCO) and the International Association for the Physical Sciences of the Ocean (IAPSO), SCOR funded the international *Discoverer* expedition (May 1970), with two principal objectives. The first objective was to obtain a complete and accurate documentation of the available radiant energy flux as a function of time and depth at every station, by using all types of optical instrumentation. It also included the intercomparison of instruments and methods. The second objective was to determine photosynthesis at several depths by three methods, all executed under carefully controlled light conditions: a) the *in situ* method, b) the simulated *in situ* method (deck incubator), and c) a laboratory method (*P* versus *E* curve).

The BENCAL cruise coincided with the thirtieth anniversary of the Optical Oceanography Symposium, organized by N. Jerlov and E. Steemann Nielsen, and held in Copenhagen in June 1972. The *Discoverer* expedition and the Copenhagen symposium in many regards heralded the birth of modern marine bio-optics and the prospect of remote sensing of the oceans, particularly of ocean color.

Finally, South African oceanographers submitted a proposal as a response to the Announcement of Opportunity published by NASA for participation in the Nimbus-7 Coastal Zone Color Scanner (CZCS) program. This proposal was one of two international proposals accepted by NASA. The emphasis of South Africa's contribution to the CZCS program was placed on the Benguela system, and resulted in a series of cruises (1978–1982) in support of the CZCS mission. These activities and results were presented in a book, edited by L.V. Shannon, *South African Ocean Colour and Upwelling Experiment*, published in 1985 by the Sea Fisheries Research Institute in Cape Town. About 20 years later, a newer ship with the same name, sailing in the same area, with a different science team, continued the tradition, but this time there were four global ocean color satellites providing coverage. As a community, we have come a long way in 20 years.

Greenbelt, Maryland  
April 2003

—C. R. McClain  
SIMBIOS Project Manager



## ABSTRACT

This report documents the scientific activities on board the South African Fisheries Research Ship (FRS) *Africana* during an ocean color calibration and validation cruise in the Benguela upwelling ecosystem (BENCAL), 4–17 October 2002. The cruise, denoted *Africana* voyage 170, was staged in the southern Benguela between Cape Town and the Orange River within the region 14–18.5°E, 29–34°S, with 15 scientists participating from seven different international organizations. Uniquely in October 2002, four high-precision ocean color sensors were operational, and these included the Moderate Resolution Imaging Spectroradiometer (MODIS) instruments on the Aqua and Terra spacecraft, the Medium Resolution Imaging Spectrometer (MERIS), and the Sea-viewing Wide Field-of-view Sensor (SeaWiFS). SeaWiFS imagery was transmitted daily to the ship to assist in choosing the vessel's course and selecting stations for bio-optical deployments. There were four primary objectives of the cruise. The first was to conduct bio-optical measurements with above- and in-water optical instruments to vicariously calibrate the satellite sensors. The second was to interrelate diverse measurements of the apparent optical properties (AOPs) at satellite sensor wavelengths with inherent optical properties (IOPs) and bio-optically active constituents of seawater such as particles, pigments, and dissolved compounds. The third was to determine the interrelationships between optical properties, phytoplankton pigment composition, photosynthetic rates, and primary production, while the fourth objective was to collect samples for a second pigment round-robin intercalibration experiment. Weather conditions were generally very favorable, and a range of hyperspectral and fixed wavelength AOP instruments were deployed during daylight hours. Various IOP instruments were used to determine the absorption, attenuation, scattering, and backscattering properties of particulate matter and dissolved substances, while a Fast Repetition Rate Fluorometer (FRRF) was deployed to acquire data on phytoplankton photosynthetic activity. Hydrographic profiling was conducted routinely during the cruise, and seawater samples were collected for measurements of salinity, oxygen, inorganic nutrients, pigments, particulate organic carbon, suspended particulate material, and primary production. Location of stations and times of optical deployments were selected to coincide with satellite overpasses whenever possible, and to cover a large range in trophic conditions.

## 1. INTRODUCTION

The Benguela Current flows along the west coast of southern Africa and is one of four major eastern boundary current systems in the world ocean. The oceanography of the region is dominated by coastal upwelling and the Benguela Current is unique in that it is bounded on both the poleward and equatorward ends by warm water regimes (Nelson and Hutchings 1983, Shannon 1985, and Shannon and Nelson 1996). The Benguela ecosystem (14–37°S) displays substantial seasonal, interannual, and decadal variability which significantly impact its biological resources. The northern boundary of the Benguela ecosystem, the Angolan–Benguela frontal zone, is a permanent feature and characteristically maintained between 14–17°S. The southern boundary is considered to be the Agulhas retroflection area between 36–37°S. This warm boundary moves during the year, and tropical Agulhas water leaks into the South Atlantic, mostly in the form of eddies and filaments, which are shed from the Agulhas Current as it retroflects to the east (Duncombe Rae 1991, Nelson et al. 1998, and Garzoli et al. 1999).

The extent and intensity of coastal upwelling throughout the Benguela is primarily determined by the wind and pressure fields, and together with topographic features and

the orientation of the coast, results in the formation of a number of upwelling cells (Nelson and Hutchings 1983, Hutchings 1992, and Shannon and Nelson 1996). The largest cell, located off Luderitz, is characterized by high turbulence and is one of the most intense upwelling cells in the world ocean. Upwelling in the south tends to be more ephemeral and seasonal. Between 18–34°S, there is a well-developed longshore thermal front, or series of fronts, which coincides approximately with the seaward boundary of the general upwelling area (Shannon and Nelson 1996). South of Luderitz, a single front is usually well defined, which although spatially and temporally variable, coincides approximately with the shelf edge. Farther north, the front is more diffuse and multiple fronts are sometimes evident. Upwelling filaments, with a life span of days to several weeks, and generally orientated perpendicular to the coast, cause the front to become highly convoluted (Shannon and Nelson 1996).

As a consequence of upwelling, primary production is high. Average primary production estimates for the northern Benguela are  $1.2 \text{ gC m}^{-2} \text{ d}^{-1}$  and  $2.0 \text{ gC m}^{-2} \text{ d}^{-1}$  for the southern Benguela (Brown et al. 1991). The phytoplankton communities are generally dominated by diatoms, although some studies have highlighted the importance of nanoflagellates (Mitchell-Innes and Winter 1987,

and Brown et al. 1991). Diatoms tend to dominate inshore in nutrient-rich waters, while nanoflagellates are more important offshore on the seaward side of the fronts. Red tide blooms occur throughout the region, particularly during quiescent periods in aged upwelled water as stratification increases (Pitcher et al. 1998). Phytoplankton abundance is highly variable with low values around 27–28°S at the base of the Luderitz cell and high values downstream of the cell and other cells farther south.

During active upwelling, the highest concentrations of chlorophyll *a* occur off the coast of Namibia (50 km), but during quiescent periods the phytoplankton is located close to the coast (Brown et al. 1991). Chlorophyll *a* levels are generally lower off Namibia than in South African waters, because the phytoplankton are more uniformly distributed with less well-defined chlorophyll fronts at the oceanic boundary. In the southern Benguela, maximum concentrations tend to occur inshore, although significant levels can extend to 100 km offshore following periods of active upwelling. Chlorophyll *a* concentrations in recently upwelled water, maturing upwelled water, and aged water are less than 1, 1–20, and 5–30 mg m<sup>-3</sup>, respectively (Barlow 1982).

The Sea-viewing Wide Field-of-view Sensor (SeaWiFS) has been used to observe mesoscale variations in chlorophyll *a* concentration in support of *in situ* measurements in the Benguela ecosystem (Barlow et al. 2001). During May–June 1998, an Atlantic Meridional Transect (AMT) cruise was staged from Cape Town to the UK (AMT-6), and a suite of optical and pigment measurements were conducted to provide SeaWiFS calibration and validation data. The AMT-6 expedition was the first cruise to provide a comprehensive bio-optical data set for the Benguela and the idea of undertaking a dedicated optical cruise in the region was discussed by scientists from the Marine and Coastal Management (MCM), Plymouth Marine Laboratory (PML), *Laboratoire d'Océanographie de Villefranche* (LOV), and the National Aeronautics and Space Administration (NASA).

After considerable planning, ship time was requested and allocated on board the South African Fisheries Research Ship (FRS) *Africana*, and funding was obtained from NASA Goddard Space Flight Center (GSFC)† and the European Space Agency (ESA). The satellite calibration and validation cruise in the Benguela ecosystem (BENCAL) was staged from 4–18 October 2002 in the southern Benguela between Cape Town and the Orange River, with 15 scientists participating from four different countries (Appendix A).

Uniquely in October 2002, four high-precision satellite ocean color sensors were operational, thereby providing an opportunity for the vicarious calibration and intercomparison of all sensors simultaneously. These included the

MODIS instruments aboard the Aqua and Terra spacecraft (MODIS-A and MODIS-T, respectively), the MERIS sensor, and the SeaWiFS instrument. Furthermore, state-of-the-art optical instrumentation was available to the scientific team, allowing an intercalibration of a range of ground sensors and techniques. Another advantage of a Benguela cruise was the fact that the coastal waters along the west coast of South Africa are mostly Case-1, because there are no major rivers delivering sediment runoff onto the shelf. Consequently, the euphotic zone would contain particles of truly marine origin.

As part of the cruise planning, consideration was also given to conducting a pigment intercomparison based on high performance liquid chromatography (HPLC) methods. The first SeaWiFS HPLC Analysis Round-Robin Experiment (SeaHARRE-1) involved four HPLC laboratories (Claustre et al. 2003), and the samples were collected in upwelled waters off Morocco and in the Mediterranean Sea. The samples spanned the mesotrophic and eutrophic chlorophyll *a* concentration ranges from about 0.05–2.2 mg m<sup>-3</sup> (Hooker et al. 2000). Because there is a greater variation in chlorophyll levels in the Benguela system, it was desirable to collect samples for a second experiment to cover a more diverse range of high biomass (eutrophic) levels, i.e., 1–25 mg m<sup>-3</sup>. The number of laboratories participating in the second experiment was also expanded to include eight HPLC methods.

The *in situ* sampling of the BENCAL cruise was designed to address the following objectives:

- Conduct a diversity of bio-optical measurements using above- and in-water optical instruments to vicariously calibrate the satellite sensors;
- Interrelate diverse measurements of AOPs at satellite sensor wavelengths with IOPs and bio-optically active constituents of seawater (particles, pigments, and dissolved compounds);
- Determine the interrelationships between the optical properties, phytoplankton pigment composition, photosynthetic rates, and primary productivity; and
- Collect samples for a second pigment round robin (SeaHARRE-2).

The emphasis, in terms of optical measurements for the BENCAL cruise, was on measuring the AOPs of seawater, primarily with vertical profiles of the water column, while characterizing the IOPs and biogeochemical properties of the deployment sites.

The large diversity of ocean color missions currently in operation means a large number of different wavelengths are needed for ground truth measurements. Some of the *in situ* instruments used on the cruise were specifically configured with specific fixed wavelengths to support individual satellites, while others used hyperspectral sensors that could measure all the needed visible wavelengths. Consequently, the AOP instruments were a mixture of hyperspectral and

† NASA funding was provided by the SeaWiFS Project and the SIMBIOS Project.

fixed wavelength sensors and a combination of near-surface and water column measurement systems:

1. A TriOS† hyperspectral, above-water surface sampling system;
2. A Hyperspectral-Tethered Surface Radiometer Buoy (H-TSRB), serial number (S/N) 018;
3. The LI-COR hyperspectral radiometer and the Profiling Natural Fluorescence (PNF) radiometer;
4. The Three-Headed Optical Recorder (THOR) version of the Low-Cost NASA Environmental Sampling System (LoCNESS), S/N 011;
5. Two versions of the micro NASA Environmental Sampling System (microNESS), S/N 001 and 016; and
6. The micro Profiler (microPRO), S/N 030, which is a variant of the microNESS profiler.

The first is an above-water system, the second is a near-surface, in-water buoy, and the latter four are in-water profiling systems.

The H-TSRB and TriOS instruments were deployed with strictly experimental objectives, whereas the other instruments were all deployed to explicitly collect data for vicarious calibration (satellite matchups) and algorithm validation (maintenance and refinement) activities. The primary objective for the H-TSRB deployments was to demonstrate its capabilities for monitoring harmful algal blooms in the Benguela area. The TriOS system was deployed to a) compare it to the H-TSRB, and b) use the radiometers with an autonomous data logging system to assess their potential use in long-term deployments (for this objective, it is not necessary to calculate absolute water-leaving radiances).

## 2. CRUISE SYNOPSIS

The FRS *Africana* departed Cape Town at 1000 local time, or 0800 Greenwich Mean Time (GMT), on Friday, 4 October 2002, in heavy weather (3–5 m swell) following a few days of persistently strong southerly winds (8–14 m s<sup>-1</sup>). Because of the unfamiliarity of the officers and crew with the operations of so many new instruments, no station measurements were conducted on the first day, but mobilization and planning continued. The vessel made passage north to St. Helena Bay for a planned start of operations in sheltered and shallow waters on Saturday, 5 October. Operations at station 1 (5 October) proceeded cautiously as training continued. The cruise track is shown in Fig. 1, and details of the station locations in relation to the bathymetry are illustrated in Fig. 2. A number of stations were in close proximity to each other each day,

† Identification of commercial products to adequately specify or document the experimental problem does not imply recommendation or endorsement, nor does it imply that the equipment is necessarily the best available.

because the locations were selected according to prevailing sea, sky, weather, and trophic conditions. A summary of the Scientific Bridge Log is presented in Appendix B.

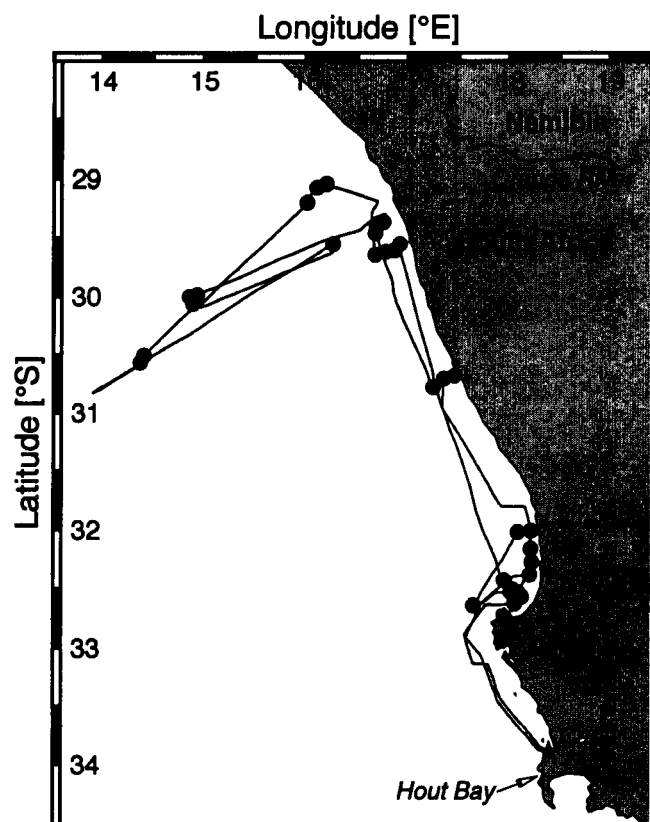


Fig. 1. The BENCAL cruise track (the solid circles are the individual stations).

Generally, the deployment of the scientific instruments during each station proceeded in a standard order. The first station each morning started with a conductivity, temperature, and depth (CTD) cast (0630–0700 GMT) to near bottom depth, with water samples for productivity, pigments, and other water constituents at 4–6 depths through the euphotic zone. The CTD was deployed amidships, starboard, and when possible, depending on wind and sea conditions, with the sun on the starboard beam to eliminate ship shadow of the photosynthetically available radiation (PAR) sensor. The CTD data of temperature, salinity, chlorophyll fluorescence, oxygen, and PAR provided information of the physical structure (mixed layer depth), biomass structure, and 1% light depth for production and other aspects.

Depending on illumination conditions (cloudiness), the station continued with the deployments of the internally self-logging instruments from the crane near the starboard quarter (outboard reach 4–7 m) using Kevlar™† nonconductor cable: first the FRRF instrument (PML), second

† Kevlar is a registered trademark of E.I. du Pont de Nemours and Company (Wilmington, Delaware).

BENCAL Cruise Report

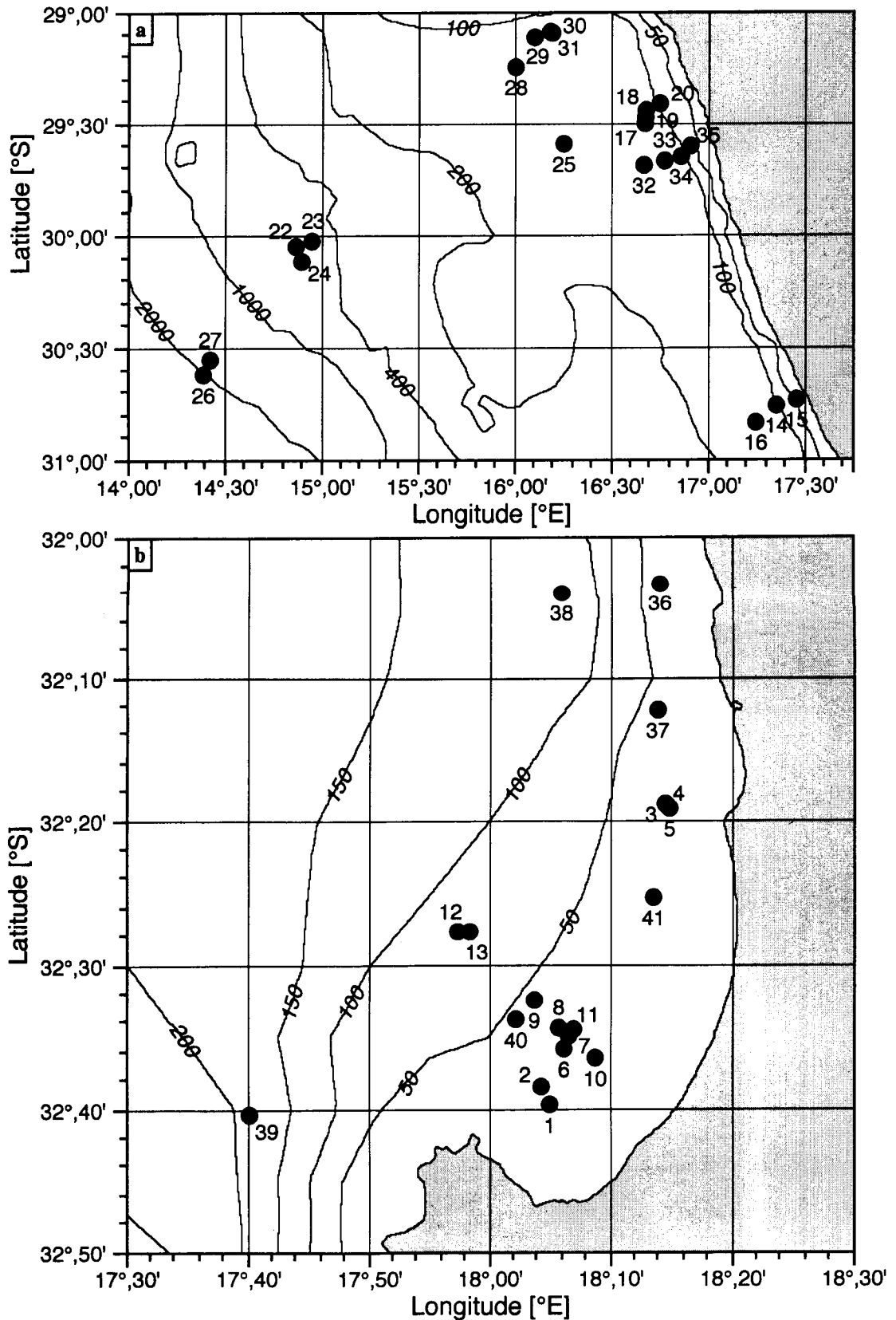


**Fig. 2.** BENCAL station locations and bathymetry in the a) Orange River, and b) St. Helena Bay regions. The numbers indicate the actual station number, and the water depth is in meters.

the AC-9 (MCM) and BB-6 (PML) combination rig, and third the LI-COR plus PNF radiometers (LOV). At later stations, with the sun at a high elevation, the LI-COR (with PNF) was usually the first instrument system deployed. Again for the crane operations, the vessel was positioned with the sun on the starboard beam or starboard quarter. These orientation requirements were attained for nearly all stations, even in difficult wind and sea conditions, thanks to the excellent seamanship of the officers and crew.

The PML microPRO and NASA microNESS free-fall profilers (known more generally during the cruise as the *rockets*) were deployed from the stern on each quarter, usually prior to the start of the crane operations, with the vessel going ahead at 0.5–1.0 kts, so that the instruments drifted astern relative to the vessel. Depending on the effect of wind and sea on the wire angle of the crane instrumentation, the rocket casts were limited to *sorties* of 3–5 successive profiles, as they tended to drift too close to the stern of the vessel as forward speed was lost. For the LI-COR and PNF radiometers, a vertical wire was a critical requirement and the rocket sorties were often short (2–3 profiles). For the FRRF and IOP instruments (independent of solar illumination), a wire angle of 10–15° was tolerated, subject to safety considerations, and often the rocket sorties extended up to 11 profiles.

For subsequent stations, the vessel was repositioned each day in higher or lower chlorophyll waters (guided by the most recent satellite imagery and the evolving understanding of the chlorophyll *a* concentration from the spectrophotometric analyses) and the deployment order was revised. The LI-COR and PNF package was usually deployed first, followed by the FRRF, IOP instruments, and finally the CTD cast. The rockets were deployed opportunistically, in 10–20 min sorties (3–11 profiles per sortie) throughout the station. The University of Cape Town (UCT) hyperspectral data buoy was deployed astern, usually at least once per day, during the crane operations. During each H-TSRB deployment, simultaneous rocket deployments were conducted, so intercomparison analyses could be made (approximately 11 rocket casts were executed). Three stations were occupied for most days with good illumination conditions (0600–1400 GMT), and when sky conditions were appropriate (no clouds on the western horizon), a fourth so-called *Q*-factor station (defined later) was occupied, involving double rocket casts (microNESS or microPRO, plus THOR) every 10 min to just before sunset (about 1630 GMT).

Work continued in the St. Helena Bay region until Tuesday 8 October, and the vessel then sailed north overnight to a new locality at approximately 17.25°E, 30.75°S. This location was occupied for three stations on 9 October, which was again followed by an overnight transit to the north. Station work continued for a few days in variable pigment concentrations just south and west of the Orange River outflow (9–11 October). FRS *Africana* then sailed

westwards into low concentration, offshore waters (2,000 m depth, 12–13 October), with a return to the inshore Orange River area over 14–15 October. The vessel finally sailed southwards for the last few days to Lamberts Bay, Cape Columbine, and a return to St. Helena Bay. FRS *Africana* docked in Cape Town at 1000 local time (0800 GMT) on Friday 18 October 2002. A summary of all the stations and the profiling instruments deployed at each one is presented in Table 1.

At the conclusion of the *in situ* sampling onboard FRS *Africana*, a smaller team of scientists deployed for small-boat operations on the *Ecklonia*. The purpose of this follow-on activity was to make coastal AOP observations in the vicinity of Hout Bay (Fig. 1), and to collect water samples for pigment analyses, so the data could be used for satellite match-up analyses. Unfortunately, an unanticipated algal bloom in Lambert's Bay prompted a re-assignment of personnel and equipment, so the Hout Bay deployments were suspended. Nonetheless, some data were collected near Hout Bay on 22 October and are included in the documentation presented below.

### 3. REMOTE SENSING

A primary objective of the BENCAL field campaign was to collect appropriate optical data in support of the calibration and validation of the presently operating ocean color sensors. Four sensors were in flight during the period of the cruise, namely MERIS, MODIS-A, MODIS-T, and SeaWiFS.

Vicarious calibration of the spaceborne sensor essentially deals with radiometric determinations, measured in water or above water, which allow the water-leaving radiance to be assessed (or derived) with the objective of comparing this radiance to the one which is retrieved from the satellite signal, at the end of the atmospheric correction process. A full set of radiometric instruments were used for this purpose (Sect. 5.1). Calibration may also include atmospheric measurements in order to reconstruct the signal at the top of the atmosphere and to compare the result to the signal as recorded by the sensor. This second aspect was not a BENCAL objective, because of a lack of suitable instrumentation in the science team.

Validation of the geophysical quantities (or *products*) derived from space observation, requires that the same quantities are measured in the field. Both the radiometric calibration and the specific algorithms (used to derive the products) are involved in this operation. Such an activity, besides its initial goal, is also essential for algorithm development. The main geophysical quantities commonly produced from ocean color observations are the chlorophyll *a* concentration, the suspended particulate matter (SPM) content, the amount of colored dissolved organic material (CDOM), and the chlorophyll fluorescence emission.

Some newly developed algorithms provide estimates of the absorption coefficient (*a*), as well as the backscattering coefficient (*b<sub>b</sub>*). These quantities must, therefore, be

BENCAL Cruise Report

**Table 1.** A summary of the instrument casts during BENCAL stations. The LI-COR (LC) entries include the PNF instrument, and the Hyper-TSRB (HT) entries, which are the number of minutes for the deployments, include the TriOS sensors. Whenever the LI-COR and PNF system was deployed, the cast number was assigned based on the station number. The microNESS profilers are given by  $\mu$ N, LoCNESS by LN, and the microPRO by  $\mu$ P. The station time periods are given in GMT.

Station Time and Position				Winch and Crane Systems				Free-Fall Profilers				
No.	SDY (Greg.)	Periods	Longitude	Latitude	CTD	FRRF	AC-9	LC	HT	$\mu$ N	LN	$\mu$ P
1†	278 (05Oct02)	0739-1216	18.0760	-32.6590	1	1a-b	1a-b	1		1-4		1
2	278 (05Oct02)	1218-1430	18.0708	-32.6483	2	2a-b	2a-b	2		5-12		2-7
3	279 (06Oct02)	0743-1000	18.2370	-32.3140	3			3		13-22		8-14
4	279 (06Oct02)	1055-1244	18.2428	-32.3163	4	3	3	4		23-26		15-23
5†	279 (06Oct02)	1317-1549	18.2433	-32.3138	5	4	4			27-42		24-38
6	280 (07Oct02)	0635-0836	18.0990	-32.5975	6	5	5	6		43-69		39-58
7	280 (07Oct02)	0840-1130	18.1050	-32.5815	7	6	6	7	38	70-132		59-90
8†	280 (07Oct02)	1140-1300	18.0877	-32.5733	8	7	7	8		133-171		91-130
9	280 (07Oct02)	1415-1635	18.0023	-32.0225		8-9	8-10				3-17	131-144
10	281 (08Oct02)	0700-0855	18.1408	-32.6082	9	10	11	10	16	172-207		145-167
11†	281 (08Oct02)	0948-1145	18.1080	-32.5672	10	11	12	11	24	208-232		168-182
12	281 (08Oct02)	1215-1359	17.9522	-32.4600	11	12	13	12	34	233-253		183-203
13	281 (08Oct02)	1405-1640	17.9692	-32.4580		13-15	14-16				18-33	204-218
14†	282 (09Oct02)	0607-0800	17.3507	-30.7550	12	16	17	14		254-258		
15	282 (09Oct02)	0907-1040	17.4537	-30.7320	14	17	18-19	15		259-269		219-227
16	282 (09Oct02)	1100-1550	17.2467	-30.8325	15	18-19	20-21	16	34	270-286	34-38	228-232
17†	283 (10Oct02)	0606-0725	16.6710	-29.4997	16	20	22-23					
18	283 (10Oct02)	0808-0946	16.6733	-29.4355	17	21	24	18	23	287-307	39-43	233-255
19	283 (10Oct02)	1037-1226	16.6718	-29.5040	18	22	25	19	30	308-324	44-48	256-277
20	283 (10Oct02)	1322-1453	16.7402	-29.4062		23	26	20	30	325-339	49-53	278
21	283 (10Oct02)	1504-1638	16.7477	-29.4092		24-25	27-28				54-63	
22	284 (11Oct02)	0645-0934	14.8610	-30.0435	19	26	29	22	52	340-358	64-71	279-283
23	284 (11Oct02)	1042-1100	14.9411	-30.0262				23		359-362		284-286
24†	284 (11Oct02)	1214-1427	14.8943	-30.1135	20	27-28	30-31			363-364		
25†	285 (12Oct02)	0607-0805	16.0837	-29.5893	22	29-30	32			365-368		287-290
26	286 (13Oct02)	0638-0955	14.3798	-30.6107	24	31	33	26	59	369-388	73-78	291-301
27†	286 (13Oct02)	1042-1513	14.4175	-30.5505	25	32-33	34-35	27		389-394		302-306
28	287 (14Oct02)	0613-0737	15.9980	-29.2387	27	34	36			395-399		307-311
29	287 (14Oct02)	0842-1156	16.1008	-29.1083	28	35	37	29		400-415		312-327
30†	287 (14Oct02)	1243-1443	16.1900	-29.0738	29	36	38			416-423		328-330
31	287 (14Oct02)	1457-1637	16.1964	-29.0877						424-434	82-92	
32	288 (15Oct02)	0612-0825	16.6692	-29.6827	30	37	39	32		435-444		331-339
33	288 (15Oct02)	0901-1110	16.7740	-29.5743	31	38	40	33	90	445-459	93-96	340-344
34†	288 (15Oct02)	1156-1427	16.8550	-29.6497	32	39-40	41	34	43	460-473	97-102	345-347
35	288 (15Oct02)	1503-1637	16.9086	-29.5957		41	42			474-483	103-112	
36	289 (16Oct02)	0717-0805	18.2292	-30.0550	33	42	43			484-492		348-356
37	289 (16Oct02)	1119-1325	18.2125	-32.0817	34	43	44	37	86	493-507		357-368
38	289 (16Oct02)	1408-1528	18.0936	-32.0668		44	45	38	16	508-523	114-124	
39†	290 (17Oct02)	0617-0849	17.6647	-32.6728	37	45-46	46		39	524-527	125-127	369-374
40	290 (17Oct02)	1111-1231	18.0305	-32.5652	38		47	40		528-541		375-378
41	290 (17Oct02)	1347-1514	18.2210	-32.4217	39	47	48	41	30	542-555		379-380
42	295 (22Oct02)	0945-0955	18.2629	-34.1283						556-558		
43	295 (22Oct02)	1107-1118	18.2497	-34.1344						559-561		

† Indicates a SeaHARRE-2 sample station.

measured, although a more extended set of properties is highly desirable to understand the respective role of the various bio-optically significant constituents, and finally to improve the algorithms. Several techniques and instruments were employed to satisfy this objective (Sects. 5.3 and 5.4).

The constraints on any attempt to calibrate and validate the performance of a particular sensor are straightforward:

1. Match the wavelengths (or spectral bands) of the field measurements with those of the spaceborne instrument;
2. Use field instruments and methods with a combined accuracy for the *in situ* (or *sea-truth*) radiometric measurements that is at least equal to, or preferably better than, that expected for the remote sensor; and
3. Acquire a complete set of *in situ* measurements within as short a time difference as possible (within 1 h, for instance) around the time of satellite overpass.

The first requirement was met, because the submersible instruments were explicitly configured with this in mind (Sect. 5.1), or are hyperspectral. The second one is the subject of permanent efforts inside the community and of precise protocols (Mueller 2003), which were followed during the data acquisition and subsequent processing. With respect to the time schedule, the guide was the ephemeris table for the four satellites produced (by the SIMBIOS Project) prior to the cruise. Unfortunately, the ephemeris for MERIS was wrong, which has not resulted in loss of quasi-concomitant sea-truth measurements, because the data acquisition rhythm (Sect. 7) was such that temporal coincidences were nevertheless achieved.

The satellite coverage during the BENCAL cruise is detailed in Sect. 7 (MERIS ephemeris corrected). During the cruise itself (4–18 October 2002), because of the differing orbit repeat cycles and swath widths of the four sensors, the average possible number of matchups were 9, 14, 15, and 17 for MERIS, MODIS-A, MODIS-T, and SeaWiFS, respectively. Between the possible number and the actual number of successfully realized matchups, the difference comes from the weather conditions and from the presence of sun glint in the satellite image, never from a lack of field measurements. The weather conditions were generally very favorable, predominantly cloudless skies (Table 2); however, frequent morning haze affected the general area (of cold water), so that the early satellites (MODIS-T and MERIS) could not capture the scene, whereas after the solar heating and the dissipation of the haze, the sky was clear.

SeaWiFS imagery (which was electronically transmitted to the ship from a shore facility) was of great help for choosing the ship's course, and selecting the sites within the zones experiencing intense mesoscale activity and complex distributions of biomass.

## 4. HYDROGRAPHIC DATA

The objectives of the hydrographic sampling executed during the cruise were to provide a description of the physical and chemical properties of the water column, and to capture water from a variety of depths for additional bio-optically significant analyses. Three types of water sampling procedures were used during the cruise to satisfy the latter:

- Niskin bottles (8L) for collecting water at various depths during CTD profiles,
- A pump for collecting surface water, particularly in simultaneity with the optical measurements, and
- Alternatively, a bucket was also used for the same purpose.

In addition to standard CTD-related analyses (salinity, oxygen, and nutrients), the discrete analyses were also concerned with the determination of pigment concentration (Sect. 5.2), IOPs (Sect. 5.3), plus the concentration, size distribution, and composition of the particle population (Sect. 5.4).

### 4.1 CTD Profiles

Hydrographic profiling was conducted on station with a Sea-Bird Electronics (SBE) 911 plus CTD. Other sensors and instruments fitted to the CTD included an SBE-43 oxygen sensor, an OBS-3 turbidity sensor (D & A Instruments Co.), an AquaTracka fluorometer (Chelsea Instruments, Ltd), and a spherical PAR sensor (Biospherical Instruments, Inc.). Underway near-surface measurements of temperature, salinity, and chlorophyll fluorescence were recorded with an SBE thermosalinograph and a flow-through laboratory fluorometer (Turner Designs, Inc.), using water from the uncontaminated seawater supply, which is pumped from a hull-mounted probe 4 m below the sea surface. A summary of the CTD log is presented in Appendix C.

Temperatures in the St. Helena Bay region (Fig. 2b) varied between 14.7–16.0°C in the surface layer during the first few days of the cruise (4–5 October), decreasing with depth to 10.0°C at 50 m and 7.4°C at 90 m. Salinities (practical salinity scale) were  $S = 34.91$ – $34.95$  near the surface, declining to 34.80 at 50 m and 34.56 at 90 m. Oxygen concentrations ranged from 5.95–6.65 mL L<sup>-1</sup> at the surface and decreased with depth to yield low concentrations of 1–2 mL L<sup>-1</sup> (50 m) at most stations. Very low oxygen levels of 0.27–0.33 mL L<sup>-1</sup>, however, were recorded near the bottom (40–50 m) at three stations.

Upon the return to the St. Helena Bay area at the end of the cruise (16–17 October), temperatures of 16.1–16.8°C were measured near the surface, 8.9–9.2°C at 90–100 m, while surface salinities were  $S = 34.89$ – $35.04$ . Oxygen levels were 6.00–8.16 mL L<sup>-1</sup> at the surface, and 0.78–1.79 mL L<sup>-1</sup> near the bottom (50–80 m).

## BENCAL Cruise Report

**Table 2.** A summary of the deployment time periods of the AOP instruments for each station presented with average values for the primary environmental parameters: wind speed,  $W$ ; wave height,  $H$ ; the chlorophyll  $a$  concentration,  $C_a^S$ , determined with the spectrophotometric method; and the cloud cover,  $CC$ . The start and end times correspond to whichever data acquisition system for the AOP instrument systems was started first and ended last, respectively. The station entries include the sequential day of the year (SDY) and the equivalent Gregorian date. The average wind speed, wave height, and cloud cover for the optical stations was  $5.4 \text{ ms}^{-1}$ ,  $0.9 \text{ m}$ , and  $2/8$ , respectively. No AOP data were collected during station 17, and stations 42 and 43 were executed after the sampling on the FRS *Africana* on board the small boat *Ecklonia*.

No.	Station		Time [GMT]		$W$ [ $\text{m s}^{-1}$ ]	$H$ [m]	$C_a^S$ [ $\text{mg m}^{-3}$ ]	$CC$ [eighths]	Sky Conditions Around the Sun
	SDY (Greg.)		Start	End					
1	278	(05Oct02)	0852	1150	5.8	0.5	5.1	1/8	Clear with haze.
2	278	(05Oct02)	1219	1317	4.5	0.5	1.8	1/8	Clear with haze.
3	279	(06Oct02)	0751	0923	2.6	3.5	3.6	1/8	Clear with some haze.
4	279	(06Oct02)	1055	1218	8.9	3.5	2.3	0/8	Clear with some haze.
5	279	(06Oct02)	1328	1549	12.2	3.5	1.8	0/8	Clear with some haze.
6	280	(07Oct02)	0707	0825	4.2	0.5	8.1	0/8	Clear with some haze.
7	280	(07Oct02)	0845	1115	5.0	0.5	4.3	1/8	Clear with some haze.
8	280	(07Oct02)	1141	1217	9.1	1.0	5.0	0/8	Clear with some haze.
9	280	(07Oct02)	1417	1637	8.4	1.0		0/8	Clear with some haze.
10	281	(08Oct02)	0730	0853	2.1	0.5	6.2	0/8	Clear with some haze.
11	281	(08Oct02)	0919	1043	3.3	0.5	2.5	0/8	Clear with some haze.
12	281	(08Oct02)	1212	1337	8.8	1.0	4.3	0/8	Clear with some haze.
13	281	(08Oct02)	1407	1637	8.0	0.5		0/8	Clear with some haze.
14	282	(09Oct02)	0659	1030	9.5	2.0	4.4	8/8	Overcast.
15	282	(09Oct02)	0951	1113	7.8	2.0		4/8	Clear with some haze and thin cirrus.
16	282	(09Oct02)	1100	1521	7.5	2.5	3.2	8/8	Overcast.
18	283	(10Oct02)	0808	0936	4.0	0.5	22.0	2/8	Clear with some haze.
19	283	(10Oct02)	1037	1214	3.3	1.0	9.5	1/8	Clear with some haze.
20	283	(10Oct02)	1320	1454	3.9	0.5	22.8	2/8	Clear with some haze.
21	283	(10Oct02)	1504	1636	3.9	0.5	0.2	1/8	Clear with some haze.
22	284	(11Oct02)	0721	0937	2.0	0.5		1/8	Clear with some haze.
23	284	(11Oct02)	1042	1125	1.1	0.5		2/8	Clear with some haze.
24	284	(11Oct02)	1405	1419	2.8	0.5	0.4	7/8	Clear with mostly clouds.
25	285	(12Oct02)	0703	0718	3.9	0.5		4/8	Clear with some haze and thin cirrus.
26	286	(13Oct02)	0711	0955	1.7	0.5	0.2	3/8	Clear with little haze.
27	286	(13Oct02)	1042	1350	3.0	0.5	0.2	3/8	Clear with little haze.
28	287	(14Oct02)	0647	0706	9.6	0.5		3/8	Clear with some haze.
29	287	(14Oct02)	0842	1030	9.7	0.5	0.9	3/8	Clear with little haze.
30	287	(14Oct02)	1243	1339	13.3	2.0	0.9	2/8	Clear with little haze.
31	287	(14Oct02)	1457	1637	13.3	2.0	0.9	2/8	Clear with little haze.
32	288	(15Oct02)	0706	0825	3.4	0.5	2.9	0/8	Clear with little haze.
33	288	(15Oct02)	0924	1114	1.0	1.5	7.0	0/8	Clear with little haze.
34	288	(15Oct02)	1156	1331	4.1	0.5	15.3	0/8	Clear with little haze.
35	288	(15Oct02)	1503	1637	4.2	0.5		0/8	Clear with little haze.
36	289	(16Oct02)	0738	0800	2.8	0.5	10.6	2/8	Clear with little haze.
37	289	(16Oct02)	1119	1257	2.8	0.5	1.8	1/8	Clear with little haze.
38	289	(16Oct02)	1408	1531	0.2	0.5		0/8	Clear with little haze.
39	290	(17Oct02)	0718	0817	5.8	2.0	3.2	8/8	Overcast.
40	290	(17Oct02)	1111	1144	5.6	0.5	3.2	4/8	Clear with little haze.
41	290	(17Oct02)	1347	1458	2.8	2.0	5.7	2/8	Clear with little haze.
42	295	(22Oct02)	0945	0955		1.5		1/8	Clear with little haze.
43	295	(22Oct02)	1107	1118		1.5		2/8	Clear with little haze.

Within the inshore environment near the Orange River (Fig. 2a), surface temperatures ranged from 13.6–16.7°C, with salinities being  $S = 34.86$ – $35.23$ . Oxygen concentrations of 5.18–8.18 mL L<sup>-1</sup> were recorded in the surface layers, with levels of 1.64–2.86 mL L<sup>-1</sup> at depths of 150–200 m. At offshore stations located between 14–15°E and 30–31°S, surface temperatures varied between 16.5–17.3°C, salinities were  $S = 35.50$ – $35.60$ , and surface oxygen concentrations were estimated to be 5.64–5.69 mL L<sup>-1</sup>.

## 4.2 Seawater Sampling and Analysis

The CTD package also included a rosette bottle sampling system fitted with twelve 8 L Niskin bottles for collecting seawater. The sampling depths were selected according to the chlorophyll fluorescence profile in the upper 200 m (Appendix C). Water was collected for measuring salinity, oxygen, inorganic nutrients, pigments, particulate absorption, particulate organic carbon (POC), SPM, and primary production. Random samples from 1–5 depths from various CTD casts were taken for discrete analysis of salinity and oxygen to check the calibration of the CTD sensors. Salinity was measured with a Guildline Autosol™ precision salinometer, standardized with the International Association for the Physical Sciences of the Ocean (IAPSO) standard seawater.

Oxygen was analyzed by means of Winkler titrations (Strickland and Parsons 1972). Samples were fixed with manganous chloride and alkaline potassium iodide, the precipitate allowed to settle, and then acidified with concentrated hydrochloric acid. The solution was titrated with sodium thiosulphate which had been standardized against potassium iodate.

Nutrient samples matched the depths for pigment samples and were stored frozen at -35°C. Nutrients were analyzed ashore for concentrations of nitrate, nitrite, phosphate, and silicate using a Technicon Autoanalyser according to Grasshoff et al. (1983) and Kirkwood (1994).

The sampling and analysis procedures for pigments, particulate absorption, POC, SPM, and primary production are detailed in the relevant sections below.

## 5. BIO-OPTICAL DATA

In line with the objectives and plans discussed in Sect. 3, the optical, bio-optical, and biogeochemical studies were composed of:

1. The determination of the AOPs, from above the surface, within the upper layer (that is viewed by the satellite sensor), and then inside the water column (several instruments and techniques were deployed, as described below);
2. The determination of the chlorophyll concentration, and the detailed and quantitative analysis of the pigment composition (this regular activity also included an intercomparison exercise between several laboratories);

3. The determination of IOPs, either as continuous vertical profiles of these quantities, or as measurements on discrete samples; and
4. Mainly associated with the sampling of the IOPs at each station, several parameters of optical significance and biogeochemical implications were also captured for further interpretations, and algorithm development.

These four kinds of experiments are successively presented in what follows.

## 5.1 Above- and In-Water AOPs

For the collection of the AOPs at each station, the environmental conditions encountered during the cruise were excellent (Table 2): the average wind speed on station was 5.4 m s<sup>-1</sup>, the average wave height was 0.9 m, and over 80% of the stations were in predominantly clear skies (cloud cover less than 4/8). Note the range in chlorophyll *a* concentration, as estimated during the cruise using a spectrophotometric technique, spans two orders of magnitude: 0.2–22.8 mg m<sup>-3</sup>.

THOR, microNESS, and microPRO are all free-fall systems deployed from the stern quarters of the vessel. A schematic of all the AOP instruments deployed during the BENCAL cruise is shown in Fig. 3 (the number of spectral channels for each sensor is given by  $\lambda_i$ , where  $i$  is the number of channels, and the hyperspectral instruments are denoted by  $\lambda_h$ ). Table 3 presents a comparison of the spectral overlap between the (fixed wavelength) free-fall profilers and the satellite sensors.

**Table 3.** The spectral overlap between the free-fall profilers and the satellite sensors. The profiler codes are as follows:  $\mu$ N is microNESS,  $\mu$ P is the microPRO, and LN is LoCNESS in the THOR configuration.

Profilers(s)		SeaWiFS	MODIS	MERIS
$\mu$ N	$\mu$ P	412	412	412.5
$\mu$ N	$\mu$ P LN	443	443	442.5
$\mu$ N	$\mu$ P LN	490	488	490
$\mu$ N	$\mu$ P LN	510		510
			531	
$\mu$ N	LN	555	551	
$\mu$ N†	$\mu$ P LN			560
	$\mu$ P			620
$\mu$ N‡	$\mu$ P LN		667	665
	$\mu$ P LN	670		
			678	681
				709
			748	
		765		
$\mu$ N		865	870	870

† S/N 1 microNESS only. ‡ S/N 16 microNESS only.

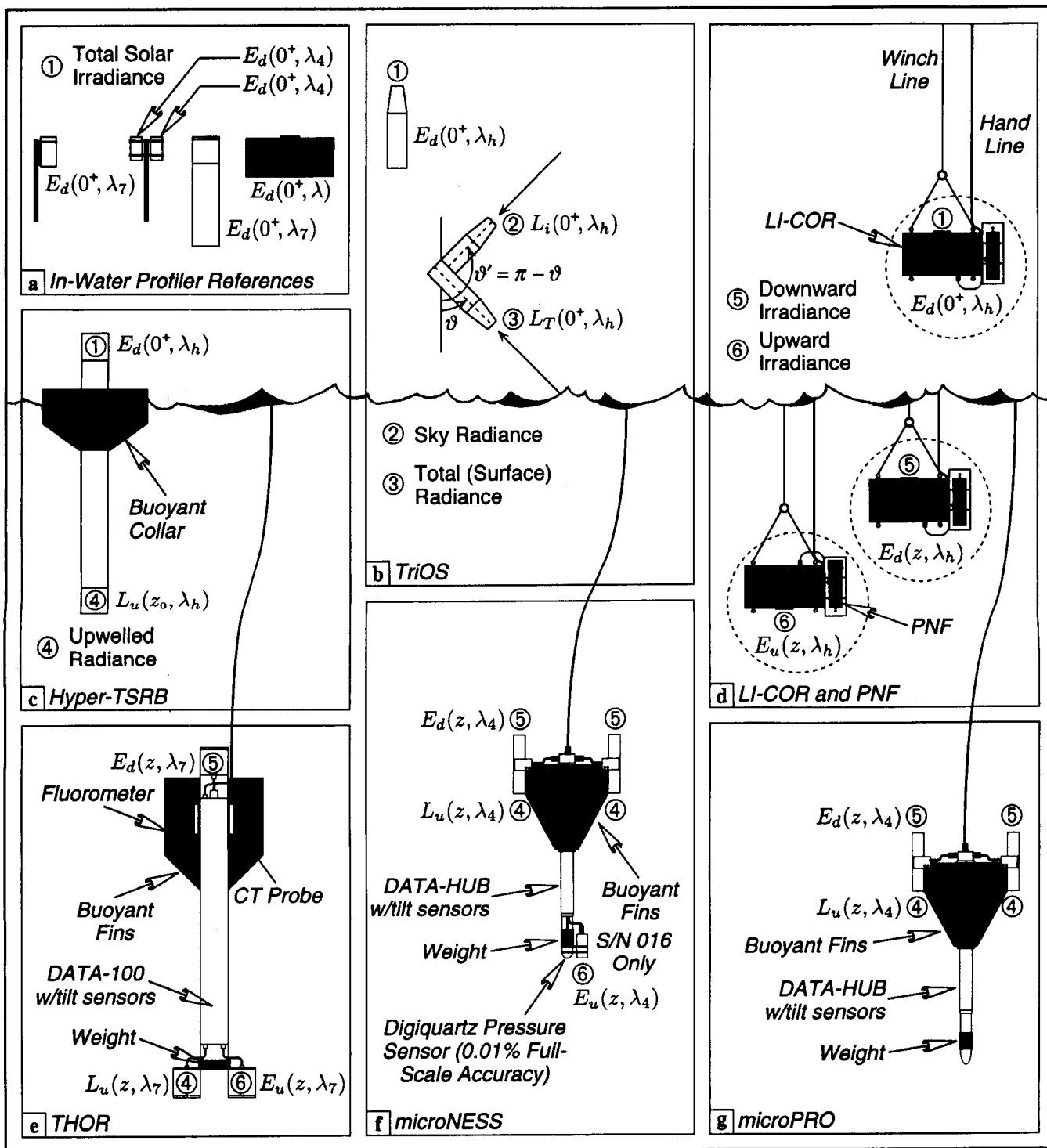


Fig. 3. The AOP instruments deployed during the BENCAL cruise: a) the solar references for the profiling systems, b) the Saturn above-water TriOS radiometers, c) the UCT H-TSRB, d) the LOV LI-COR and PNF radiometers, e) the NASA THOR, f) the NASA microNESS profiler(s), and g) the PML microPRO. The references, from left to right in panel a, correspond to microNESS, microPRO, THOR, and the LI-COR and PNF instruments. The in-water instruments for the latter are shown in the three configurations (dashed circles) used during data collection: incident solar irradiance (top), downward irradiance (middle), and upward irradiance (bottom). Note, the PNF-300 only acquires radiance data during downward irradiance casts (the sensor is covered during upward irradiance casts). Although not shown explicitly, the microNESS and microPRO profilers had external probes to measure seawater temperature.

Whenever possible, two free-fall instrument systems were deployed simultaneously (Table 4), so any anomalies in the data processing results from one instrument can be resolved by comparing the output to the other instrument. This cast-by-cast comparison is also a simple and effective way of demonstrating the *in situ* stability of the instruments over the duration of the cruise (this is especially effective for the BENCAL cruise, because it was almost entirely executed in Case-1 waters).

Deployment of the free-fall profilers began with the ship maintaining a headway speed of approximately 0.5–1.0 kts. The profilers were carefully lowered into the water, and then repeatedly released and hauled to the surface until they had drifted clear of any possible shadowing effect (while they were sinking, the boat was moving away from them, so only a few release-and-recover cycles were needed to achieve a reasonable deployment distance). In some wave and current conditions, a short burst from the propeller was used to create enough *prop wash* to push the profilers away from the stern.

When the profilers reached the desired distance from the stern (30 m minimum) and were far enough apart to prevent any likely entanglement during the cast, they were simultaneously released (radios were used to synchronize the release and the start of data acquisition). A concerted effort was made to prevent the telemetry cables from ever coming under tension; even brief periods of tension on the cable can adversely affect the vertical orientation (tilt) and velocity of the profiler. To ensure this did not occur, the operators always left one or more coils of cable at the surface. Care was taken not to leave too much free cable in the water, so it could not move under the ship and become entangled in the propeller (or prevent a rapid recovery of the profiler in shallow water).

The optical data for THOR and microNESS were logged on a Macintosh PowerBook G4 using software developed at the University of Miami Rosenstiel School for Marine and Atmospheric Science (RSMAS) and the SeaWiFS Project. The software, called Combined Operations (C-OPS), is written in LabVIEW™† and is used to control both the in-air and in-water data streams.

The primary task of C-OPS is to integrate the serial output from the optical instruments and to control the logging and display of these data streams as a function of the data collection activity being undertaken. All of the telemetry channels are displayed in real time and the operator can select from a variety of plotting options to visualize the data being collected. Several parameters are calculated during profiler descent, for example, the diffuse attenuation coefficient,  $K_d$ . One of the most important real-time diagnostic parameters is the 1% light level. Assuming sufficient water depth, all casts were executed to at least the 1% light level (and frequently to the 0.1% light level).

† LabVIEW is a registered trademark of National Instruments (Austin, Texas).

### 5.1.1 Water Column AOPs

For the fixed wavelength AOP sensors, the spectral configuration of the sensors were necessarily tied to the remote sensors (Table 3) and the bio-optical algorithms used in ocean color investigations, which are most frequently composed of blue–green band ratios of the remote sensing reflectance (O'Reilly et al. 2000). Whether for ground truth observations, algorithm validation, or the aforementioned *in situ* stability analyses, it is desirable that the center wavelengths and bandwidths for the individual channels agree as closely as possible. A detailed comparison of the individual wavelengths for the free-fall profilers is presented in Table 5.

Although the calibration and validation activities for the remote sensing objectives can be restricted primarily to the near-surface layer of the water column, generalized inquiries into the biogeochemical properties of the ocean require water column sampling throughout the euphotic depth (i.e., to as deep as the 1% light level). The optical profiling systems deployed during BENCAL all contributed to extensive sampling of the euphotic layer.

#### 5.1.1.1 THOR

The LoCNESS profiler was designed to be built from the modular, low-cost components used with winch and crane sampling systems (Robins et al. 1996): a DATA-100 with 16 bit analog-to-digital (A/D) converters for power and telemetry, plus 7-channel Ocean Color Radiance and Irradiance Series 200 sensors, OCR-200 and OCI-200, respectively. All of this equipment was manufactured by Satlantic, Inc. (Halifax, Canada). The principal reason for configuring it into a free-fall system was to remove any chance of ship contamination during data collection (which is very hard to prevent with winch and crane systems, because the crane always has a limited reach).

In the THOR configuration (Fig. 3e), an adapter plate is used on the nose to permit the measurement of spectral upwelled radiance and irradiance plus downwelled irradiance as a function of depth,  $L_u(z, \lambda)$ ,  $E_u(z, \lambda)$ , and  $E_d(z, \lambda)$ , respectively. The former two measurements permit the computation of the  $Q$ -factor:  $Q(\lambda) = E_u(\lambda)/L_u(\lambda)$ . Internal tilt sensors quantify the vertical orientation ( $\varphi$ ) during descent through the water column; the addition of a conductivity and temperature (CT) probe, plus a miniature fluorometer, provide a comprehensive characterization of water properties. The two nose sensors do not disturb the stability of the profiler during descent. In fact, THOR has small and stable tilts (less than  $2^\circ$ ), because of its length and the large surface area of the fins. This stability, and the fact that three components of the light field are measured, makes it a very versatile profiler.

An in-air irradiance sensor measured the incident solar irradiance just above the sea surface,  $E_d(0^+, \lambda)$ . The irradiance sensor was packaged with a DATA-100 module

BENCAL Cruise Report

**Table 4.** The deployment numbers and times for the AOP instruments used during the BENCAL cruise. The THOR cast numbers are not completely continuous, because of specialized acquisition sequences with the solar reference which are not recounted here. The time periods for the TRIOS sensors corresponds to those given for the H-TSRB instrument, and the time periods for the PNF sensors corresponds to those given for the LI-COR instrument. Note stations 42 and 43 were from the small-boat operations on *Ecklonia*.

Station No.	SDY (Greg.)	Free-Fall Casts			Free-Fall Times			Hyperspectral	
		microNESS	microPRO	THOR	microNESS	microPRO	THOR	LI-COR	H-TSRB
1	278 (05Oct02)	1- 4†		1	1134-1150	1005-1015		0852-1017	
2	278 (05Oct02)	5- 12†		2- 7	1219-1252	1300-1317		1220-1252	
3	279 (06Oct02)	13- 22†		8- 14	0751-0910	0854-0909		0851-0923	
4	279 (06Oct02)	23- 26		15- 23	1141-1150	1100-1218		1055-1128	
5	279 (06Oct02)	27- 42		24- 39	1328-1549	1338-1548			
6	280 (07Oct02)	43- 69		40- 59	0707-0825	0635-0822		0708-0748	
7	280 (07Oct02)	70-132		60- 91	0845-1115	0840-1115		0847-0920	0935-1013
8	280 (07Oct02)	133-171		92-131	1141-1259	1140-1300		1144-1217	
9	280 (07Oct02)			132-145		1512-1613	1417-1637		
10	281 (08Oct02)	172-207		146-168	0733-0852	0730-0851		0730-0801	0837-0853
11	281 (08Oct02)	208-232		169-183	0928-1041	0948-1041		0919-1004	1019-1043
12	281 (08Oct02)	233-253		184-204	1215-1335	1215-1235		1212-1251	1303-1337
13	281 (08Oct02)			205-219		1407-1630	1407-1637		
14	282 (09Oct02)	254-258			0659-0728	0958-1030		0833-0849	
15	282 (09Oct02)	259-269		220-228	0951-1037	0958-1030		1039-1113	
16	282 (09Oct02)	270-286		229-233	1322-1517	1100-1218	1425-1433	1350-1420	1447-1521
18	283 (10Oct02)	287-307		234-256	0808-0934	0808-0930	0850-0901	0811-0844	0913-0936
19	283 (10Oct02)	308-324		257-278	1037-1211	1037-1210	1122-1134	1040-1113	1144-1214
20	283 (10Oct02)	325-339		279	1322-1453	1322-1324	1408-1414	1320-1353	1424-1454
21	283 (10Oct02)						1504-1636		
22	284 (11Oct02)	340-358		280-284	0721-0934	0721-0759	0827-0929	0723-0816	0845-0937
23	284 (11Oct02)	359-362		285-287	1042-1100	1042-1056		1113-1125	
24	284 (11Oct02)	363-364			1405-1419				
25	285 (12Oct02)	365-368		288-291	0703-0718	0703-0716			
26	286 (13Oct02)	369-388		292-302	0711-0955	0807-0907	0927-0955	0705-0802	0835-0934
27	286 (13Oct02)	389-394		303-307	1042-1350	1042-1340		1046-1132	
28	287 (14Oct02)	395-399		308-312	0647-0706	0647-0705			
29	287 (14Oct02)	400-415		313-328	0842-1030	0842-1030		0900-0930	
30	287 (14Oct02)	416-423		329-331	1243-1339	1243-1317	1331-1339		
31	287 (14Oct02)	424-434			1457-1637		1457-1637		
32	288 (15Oct02)	435-444		332-340	0706-0825	0709-0825		0730-0810	
33	288 (15Oct02)	445-459		341-345	0924-1110	0924-0945	1053-1110	1005-1040	0944-1114
34	288 (15Oct02)	460-473		346-348	1156-1327	1156-1202	1300-1325	1200-1236	1248-1331
35	288 (15Oct02)	474-483			1503-1637		1503-1637		
36	289 (16Oct02)	484-492		349-357	0738-0800	0738-0800			
37	289 (16Oct02)	493-507		358-369	1119-1255	1119-1205		1200-1240	1131-1257
38	289 (16Oct02)	508-523			1408-1528		1454-1528	1400-1445	1515-1531
39	290 (17Oct02)	524-537		370-375	0718-0817	0718-0745	0759-0817		0714-0753
40	290 (17Oct02)	538-541		376-378	1114-1122	1111-1119		1111-1144	
41	290 (17Oct02)	542-555		379-380	1347-1453	1347-1350		1411-1422	1428-1458
42	295 (22Oct02)	556-558			0945-0955				
43	295 (22Oct02)	559-561			1107-1118				
<i>Totals</i>		561	380	124				28	644 min

† Casts 1-22 were executed with microNESS S/N 016; all other microNESS casts were done with microNESS S/N 001.

**Table 5.** Channel numbers and center wavelengths (in nanometers) for the radiometers used with the fixed-wavelength AOP sampling systems (10 nm bandwidths). The sensors for each system are given with their individual sensor codes, which are formed from a three-digit model or serial number (S/N), preceded by a one-letter designator for the type of sensor: R and S, in-water radiance; I and K, in-water irradiance; and M and O, above-water irradiance. The microNESS S/N 016 profiler used references O001 and M030 (the latter was needed for the 665 nm channel). For the microNESS profilers, the four channels for K001, S001, K039, and S039 are shown as channels 1–4; the four channels for K002, S002, K040, and S040 are shown as channels 5–8.

Ch. No.	microNESS S/N 001			microNESS S/N 016			microPRO S/N 030			THOR S/N 011			
	K001,2	S001,2	O001	K039,40	K041	S039,40	K003,4	S003,4	O042,43	I050	I048	R036	M030
1	412.2	412.4	412.2	411.8	412.2	412.0	412.3	412.5	412.3	560.1	559.4	560.2	560.0
2	490.9	490.0	443.8	491.0	490.7	491.0	442.8	442.8	442.8	442.5	442.7	442.7	443.0
3	509.4	509.2	490.7	510.5	554.8	510.8	490.4	490.7	490.4	489.3	490.0	489.9	490.6
4	554.6	554.0	509.3	554.3	665.4	555.0	509.9	509.7	509.9	510.1	509.3	510.3	511.0
5	412.4	412.3	554.5	412.0		411.9	559.8	560.1	560.0	554.8	554.3	554.2	555.5
6	442.9	443.0	560.1	442.3		442.3	619.6	620.7	620.8	666.0	665.9	665.3	665.2
7	560.1	560.0	865.1	665.4		665.3	664.3	664.8	664.3	682.9	682.4	683.8	683.7
8	865.2	865.5		865.2		864.6	683.5	682.6	683.5				

that converted the analog output of the OCI-200 radiometer to RS-485 serial communications. The sensor package was mounted on a mast on the starboard trawl post. The height and location of the mast ensured none of the ship's superstructure shadowed the sensor under almost all illumination conditions.

#### 5.1.1.2 microNESS

The LoCNESS profiler was an extremely capable unit (Hooker and Maritorea 2000), but it was difficult to use in small boat operations or in the shallow water normally associated with coastal (nominally Case-2) conditions; the overall length was 1.8 m, the diameter of the individual system components was approximately 9 cm, the weight in air was 23 kg, and the primary light sensors ( $E_d$  and  $L_u$ ) were not mounted on the same horizontal plane—they were separated by the length of the profiler.

A smaller version of LoCNESS, called miniNESS, was built to determine whether or not light sensors could be mounted on the fins (in the same horizontal plane) in a more compact configuration without degrading the light-field measurements. Intercomparisons of miniNESS with traditional profilers established the efficacy of the new concept during open ocean cruises, and then subsequently during coastal campaigns in the northern Adriatic Sea (Hooker et al. 1999). The success of miniNESS led to a new design effort, called microNESS (Fig. 3f), to further decrease the overall size and weight of the profiling package.

Another microNESS design objective was to replace the analog cabling used with traditional profilers with digital interfaces. The new digital light sensors are referred to as the OCR-507-R series. This objective was particularly important, because when it was combined with the desired size reduction, it would help ensure, with respect to the original equipment: a) a lowering of power requirements; b) a smaller, lighter profiler (a 1.0 m length and an in-air

weight of 4 kg); c) a reduction in the perturbation caused by the instrument to the *in situ* light field (the main-body diameter was reduced to 4.6 cm); and d) a profiling system that could be easily deployed from a small boat.

THOR has a descent speed of approximately  $90 \text{ cm s}^{-1}$ , whereas microNESS has a descent speed of  $25\text{--}30 \text{ cm s}^{-1}$ . A low descent speed means a higher vertical sampling resolution, so microNESS produces about three times as much data within each meter of water sampled. This is a significant advantage in waters with shallow mixed layers or in vertically complex waters (which are often encountered in the coastal environment).

#### 5.1.1.3 microPRO

The microPRO profiler is the commercial version of the microNESS profiler and is available from Satlantic, Inc. The instrument used (S/N O30) was fitted with the new OCR-507-R digital optical sensors. Figure 3g shows the configuration of the profiler with four-channel downward irradiance and upwelling radiance sensors mounted on each side of the buoyant fins. Table 5 indicates the wavelengths for each of the eight optical channels, and also includes the two four-channel irradiance sensors used to measure the total solar irradiance. The sensors are very well matched to the optical channels of the MERIS satellite sensor (Table 3), and have four overlapping channels with SeaWiFS and five with MODIS.

The microPRO depth sensor was an Entran pressure sensor, which has 0.25% (full scale) accuracy and a 150 m depth range. The deepest cast completed was 100 m at an offshore station; shallow casts of about 25 m were carried out at the inshore stations. A total of 380 casts were completed during the cruise with this instrument, and under most conditions where water depth was not a limiting factor, cast depths were determined by the 1% light level

(as determined by the microNESS data acquisition software). The fall rate of the instrument was approximately  $30\text{--}50\text{ cm s}^{-1}$ , ideal for the high chlorophyll Case-1 waters experienced during this cruise. Ancillary data taken included pitch and roll measured with a tilt sensor of  $0.20^\circ$  accuracy, and a thermal probe provided information on the temperature structure.

#### 5.1.1.4 LI-COR and PNF

Two optical instruments, the PNF-300, built by Biospherical Instruments, Inc. (San Diego, California), and the LI-1800 UW, built by LI-COR (Lincoln, Nebraska), were attached together and simultaneously immersed using a (Kevlar) rope. The PNF-300 is equipped with a pressure gauge, so the immersion depth of the whole package was known with an accuracy of about 10 cm. The package was deployed near the starboard quarter, from a crane operated with its maximal extension (about 7 m) toward the sun direction. The ship was oriented in such a way that the sun was abeam on starboard (about  $120\text{--}140^\circ$  from the ship's heading).

The PNF-300 is a submersible instrument with two sensors aligned in the vertical axis, but at opposite ends of the pressure housing. The first nadir-pointing sensor measures the upwelling radiance within a spectral domain encompassing the chlorophyll *a* fluorescence band (approximately 665–740 nm). The second zenith-pointing sensor uses a spherical collector designed for the spectral PAR domain (the 400–700 nm band) to measure the scalar irradiance. The former radiance is denoted  $L_u(683)$ , and the latter irradiance is denoted  $E_0^{\text{PAR}}$ . Both signals† are recorded in a continuous way, and vertical profiles for  $L_u(683)$  and  $E_0^{\text{PAR}}$  are obtained as the instrument is winched through the water column. A separate (in-air) PAR sensor mounted on the ship's superstructure monitors the incident solar irradiation during the entire experiment. With this information, the underwater determinations can be corrected for any shifts in incident irradiance.

The hyperspectral LI-COR instrument is a submersible spectroradiometer. It measures plane irradiance (cosine collector) between 300–800 nm, with a resolution ranging from 5 nm (in the ultraviolet domain) to 8 nm (in the near infrared). The immersion factors were provided by the manufacturer. Downward and upward irradiances,  $E_d(\lambda)$  and  $E_u(\lambda)$ , respectively, were measured during two separate casts. These two casts were performed in rapid succession (a few minutes apart); one with the collector facing upward and receiving the downward flux, the other one after having turned the instrument upside down in such a way that it received the upward flux. The data were recorded every 2.5 nm. The dynamic range exceeds

five decades, and the noise for spectral irradiance ranges from  $3 \times 10^{-4}\text{ W m}^{-2}\text{ nm}^{-1}$  near 300 nm, to as low as  $1 \times 10^{-5}\text{ W m}^{-2}\text{ nm}^{-1}$  beyond 700 nm.

The recorded data were also corrected for changes in incident irradiance, by using the same PAR sensor as mentioned above. All  $E_d(\lambda)$  and  $E_u(\lambda)$  recorded at various depths and different times were, therefore, normalized to the same incident flux. During the BENCAL cruise, measurements were generally carried out in excellent sky conditions (cloudless skies, or extended *blue holes* and distant clouds, or on one occasion, an entirely overcast sky), so that effecting the normalization of all radiometric data to a constant above-surface irradiance was easily and accurately achieved. The duration of an entire experiment (consisting of the two casts) was on the average 30 min.

The PNF sensor performs measurements in a continuous manner and provides vertical profiles, whereas the LI-COR instrument must be stopped at discrete depths for the spectral irradiance determinations (scanning the spectrum lasts about 30 s). The normal protocol was to lower the package (without stopping) to a maximal depth (from 30–60 m, depending on the expected water properties, and if upward or downward flux were to be measured), and then during the ascent to stop at selected levels to operate the spectroradiometer.

Fluctuations caused by surface waves and so-called *lens effects* prevent the accurate measurement of  $E_d(\lambda)$  close to the surface. Noise-free spectra were successfully recorded only when the depth exceeded 5–7 m in green waters, and even 15 m in blue waters. The values just below the surface (at  $0^-$ ) were derived from those above the surface (at  $0^+$ ) through

$$E_d(0^-, \lambda) = E_d(0^+, \lambda) \frac{1 - \rho_a}{1 - \rho_w R}, \quad (1)$$

where  $\rho_a$  is the global (sun plus sky) air–water Fresnel reflectance,  $1 - \rho_a$  is the transmittance (typically 0.96),  $\rho_w$  represents the water–air Fresnel reflectance (about 0.48), and  $R$  is the irradiance reflectance, defined as  $E_u/E_d$  (typically a few percent or less). For solar elevations above  $30^\circ$ , and for low-to-moderate wind speeds, (1) can be safely approximated, with an accuracy better than 1%, by

$$E_d(0^-, \lambda) = 0.97 E_d(0^+, \lambda). \quad (2)$$

In contrast, the  $E_u(\lambda)$  determinations are not noisy even when made very close to the surface and in the presence of waves. The practical limitations, however, to carry out measurements at exactly  $0^-$  obviously result from the ship's movements and from the crossing waves. Maintaining (for the duration of the scan) the collector under water, required a minimal depth of about 0.5 m when weather conditions were very good, and a greater depth when they were difficult (several measurements were always carried out as close as possible to the air–sea interface).

† The units for  $L_u(683)$  are expressed as photons per square meter per second per steradian, and the units for  $E_0^{\text{PAR}}$  are given as photons per square meter per second.

The extrapolation toward the ideal  $0^-$  level is, in principle, possible from the series of measurements made deeper. Practically, it remains uncertain because the exact (average) depth where measurements have been performed near the surface can never be accurately known. Consequently, for the dark-green waters observed during the BENCAL cruise, the  $E_u(\lambda)$  spectra, as well as the irradiance reflectance spectra may be slightly degraded, particularly in the red part of the spectrum.

Note that the uncertainties resulting from any imperfect radiometric calibration of the instrument completely disappears when producing quantities like  $R(\lambda)$ , or the diffuse attenuation coefficients for downward and upward irradiance,  $K_d(\lambda)$  and  $K_u(\lambda)$ , respectively, because such quantities are obtained as ratios of irradiance spectra (from the same instrument), and thus are independent of the calibration.

### 5.1.2 Near-Surface AOPs

The primary use of the H-TSRB instrument during the BENCAL cruise was to evaluate its use for coastal monitoring, specifically to develop bio-optical methods for the real-time monitoring of harmful algal blooms. The sampling for the H-TSRB instrument was conducted with two objectives:

1. The development of in-water reflectance algorithms to estimate algal IOPs, which will provide algal biomass and assemblage descriptors; and
2. An assessment of the ability of surface measurements alone (measured with the H-TSRB) to return the absolute measurements of water-leaving radiance required for satellite calibration and validation purposes.

The H-TSRB deployments were made concurrent with both discrete and profiled IOP measurements where possible. For monitoring purposes, the uncertainties associated with the instrument configuration, as discussed below, are expected to have a minimal impact, because absolute water-leaving radiance values are not required.

In terms of the remote sensing calibration and validation objective, however, the configuration of the instrument as an in-water buoy has specific sources of uncertainties which need to be considered. The most important uncertainty sources are: a) the measurement of upwelling radiance at a single depth (nominally 66 cm) means the measured values must be propagated to the surface using a radiative transfer processing scheme, e.g., Morel (1988) or Mueller and Trees (1997); and b) both the in-water radiance and the above-water irradiance measurements are subject to high-frequency perturbations caused by the physical effects of wind effects, surface roughness, and wave motion, as well as the optical effects of wave focusing on the upwelling light field in the near-surface layer (Zaneveld et al. 2001).

#### 5.1.2.1 H-TSRB

The H-TSRB (Fig. 3c) is manufactured by Satlantic, Inc., and is designed to measure both the upwelled near-surface spectral radiance,  $L_u(z_0, \lambda)$ , and the downward solar irradiance,  $E_d(0^+, \lambda)$ . The instrument can be floated away from the vessel and free of any perturbations to the submarine light field. Upwelling radiance is measured at a nominal depth of 66 cm. The instrument consists of two 256-channel spectrographs linked by fiber optic bundles to a) an upward-viewing (cosine-corrected) irradiance sensor, and b) a downward-viewing  $8.5^\circ$  (half-angle) field of view baffled Gershun tube radiance sensor.

Data acquisition, at a nominal frame rate of 1 Hz, is provided by an 18 bit A/D converter. Adaptive gain allows a variable integration time to be chosen independently for each sensor based on the ambient light field. Real time dark current measurements are provided by an optical shutter operating every sixth frame. Actual acquisition rates are, therefore, variable and dependent upon instrument response to the light field. Typical rates range from 0.7–1.6 Hz. The 256 channel spectrographs provide a spectral range of 400–800 nm, at a spectral resolution of 3.3 nm and an accuracy of 0.3 nm.

The H-TSRB was deployed concurrently with a variety of the free-fall AOP profiling systems available on the BENCAL cruise: THOR, microNESS, and microPRO. The multisensor data set will permit an evaluation of the variability associated with the various frequency dependent perturbations in the H-TSRB measurements, and the propagation schemes necessary to derive water-leaving radiance values from near-surface upwelling radiance measurements.

The H-TSRB was deployed off the stern quarter of the vessel, typically with 0.5–1.0 kt forward way to assist in moving the instrument away from the vessel as soon as possible. Two deployment patterns were used: stationary deployment where the buoy was left at a fixed cable distance from the vessel (50–70 m), and an in-out deployment corresponding to the free-fall instrument up and down casts. In the latter case, the buoy was given excess slack cable on down casts and hauled in on up casts, in an attempt to minimize surface roughness and wave effects during the targeted down cast periods. Total logging times were typically about 30 min.

#### 5.1.2.2 TriOS

The Ocean-i system is composed of an Ocean-i data unit manufactured by Saturn Solutions, Ltd. (Southampton, United Kingdom) interfaced with TriOS Radiation Measurement Sensor with Enhanced Spectral Resolution (RAMSES) instruments made by TriOS, GmbH for the hyperspectral measurement of above-water surface radiance.

The Ocean-i data unit was initially developed for the Volvo Ocean Adventure (as part of the Volvo Ocean Race 2001–02) in which the system was required to interface

with TriOS RAMSES radiometers and autonomously control the sampling regime, and store and transmit data. The unit initiates data acquisition from the radiometers according to a user-programmed sampling regime. This data is stored on an internal memory card along with the position, heading, and time of the acquisition from the integral Global Positioning System (GPS) unit.

The TriOS RAMSES sensors are hyperspectral sensors that sample 190 usable channels between 320–950 nm. The channels are approximately 3.3 nm apart. The RAMSES instruments are available as Advanced Radiance Collector (ARC) and Advanced Cosine Collector (ACC) sensors. The RAMSES-ARC (radiance) sensor has a 7° full-angle field of view in air; the RAMSES-ACC (irradiance) sensor is fitted with a cosine collector. Integration time is automatically determined by the sensor with a range from 4 ms to 8 s. Typical integration times are 128–512 ms for  $E_d(0^+)$  (the solar reference), 16–64 ms for the sky radiance ( $L_i$ ), and 256–512 ms for the total sea radiance ( $L_T$ ).

For the purposes of the BENCAL cruise, the sensors were mounted near the bow of the ship in a configuration with one irradiance sensor, measuring the incident solar irradiance, and two radiance sensors: one measuring sky radiance, and the other measuring total surface radiance. The position of the sensors was fixed, and it was not possible to orient them with respect to sun plane, so the position of the sensors with respect to the sun plane was determined by the position of the ship on station.

The nadir viewing angles were set to  $\vartheta = 40^\circ$  for the sea-viewing radiance sensor and  $\vartheta' = 140^\circ$  for the sky-viewing sensor (Fig. 3b). Because of limitations in mounting the irradiance sensor, some contamination or shadowing by the ship's superstructure is expected in the data. The Ocean-i data unit controlling the data collection was mounted near the sensors. Data were collected when on station at a sampling frequency of 15 s to be coincident with data from the H-TSRB.

## 5.2 Pigment Concentration

One of the goals of ocean color investigations is to explore the distribution patterns and seasonal variability of phytoplankton in various ecosystems. A combination of *in situ* measurements and satellite observation is very useful in these studies, as well as validating remotely-sensed pigment data. The main role of pigments in phytoplankton is to absorb light for photosynthesis (Kirk 1994). Chlorophylls *a*, *b*, and *c* absorb in the blue and red regions of the visible spectrum, while photosynthetic carotenoids absorb in the blue and green bands. A range of photoprotective carotenoids serve to protect microalgal cells from damage due to excess light, particularly at the surface, and they absorb at blue and green wavelengths. As the composition of phytoplankton pigments changes, the relationship between ocean color and pigment concentrations change, and it is necessary to investigate the spatial and temporal variations in pigment distribution.

A diverse range of pigments has evolved in the phytoplankton and, thus, in addition to their characteristic optical properties, pigments are also very useful signatures or indicators of the chemotaxonomic composition of phytoplankton communities (Jeffrey et al. 1997). Fucoxanthin, for example, is a biomarker of diatoms, and peridinin is related to dinoflagellates. Furthermore, 19'-hexanoyloxyfucoxanthin, chlorophyll *b*, 19'-butanoyloxyfucoxanthin, alloxanthin, and zeaxanthin indicate the presence of various nano- and picoflagellates (such as, prymnesiophytes, pelagophytes, cryptophytes, green flagellates, and cyanobacteria, respectively).

HPLC is the most suitable technique for analyzing the range of chlorophyll and carotenoid pigments in phytoplankton, and provides accurate chlorophyll *a* concentrations for ocean color calibration and validation activities. During research cruises, onboard spectrophotometric analysis of chlorophyll *a* is also useful for providing information on phytoplankton biomass as an aid in the location of stations and sampling strategies.

Two laboratories (MCM and LOV) took part in the sampling and analysis of water column pigments over 3–6 depths during CTD profiling. The MCM sampled most of the CTD casts for both spectrophotometric and HPLC analysis, while the LOV sampled one vertical profile per day, completed by a number of surface layer samples at each station. The latter were collected in coincidence with satellite overpass or with the deployment of different optical instruments.

### 5.2.1 MCM Pigment Determination

Seawater was collected from 3–6 depths during CTD profiling and the phytoplankton were harvested by filtering 0.5–2.0 L through 25 mm GF/F filters. Samples for HPLC analysis were immediately frozen and stored in liquid nitrogen for subsequent analysis ashore.

Samples for spectrophotometric analysis were rapidly analyzed on board. They were placed in 20 mL glass vials, 10 mL of 90% acetone was added, and the pigments were extracted by soaking over 24 h in a  $-20^\circ\text{C}$  freezer. The extracts were warmed to laboratory temperature and measured at 750, 664, 647, and 630 nm in a Unicam Helios spectrophotometer. The 664, 647, and 630 nm absorbances were corrected for any turbidity effects by subtracting the 750 nm reading.

The chlorophyll *a* concentration,  $C_a$ , was estimated using the Jeffrey and Humphrey (1975) simultaneous trichromatic equation:

$$C_a = \frac{11.85A(664) - 1.54A(647) - 0.08A(630)V_e}{V_f P_l}, \quad (3)$$

where  $A(\lambda)$  is the spectral absorbance ( $\lambda$  is the wavelength in nanometers),  $V_e$  is the volume of the extract (in milliliters),  $V_f$  is the volume of the filtered seawater (in

liters), and  $P_l$  is the path length of the cuvette (in centimeters).

Samples for HPLC analysis were extracted in acetone, with the aid of ultrasonication, and clarified by centrifugation. The analysis of pigment concentrations followed a reversed-phase HPLC procedure (Barlow et al. 1997) using a 3  $\mu\text{m}$  Hypersil MOS2  $\text{C}_8$  column (100 $\times$ 4.6 mm), a Varian ProStar tertiary pump, a Thermo Separations AS3000 autosampler, a Thermo Separations UV6000 diode array absorbance detector, and the ChromQuest chromatography software. The autosampler was capable of cooling samples to 2°C and maintaining the column temperature at 25°C.

Acetone extracts were vortex mixed with 1 M ammonium acetate (1:1, v/v) in the autosampler just prior to injection, and the pigments separated at a flow rate of 1 mL min<sup>-1</sup> by a linear step gradient programmed as follows (in minutes for the percentage of solvent A and solvent B, respectively):

- 0 75% and 25%,
- 1 50% and 50%,
- 20 30% and 70%,
- 25 0% and 100%, and
- 30 0% and 100%.

Solvent A consisted of 70:30 (v/v) methanol:1 M ammonium acetate, and solvent B was 100% methanol.

Pigments were detected at 440 and 665 nm, identified by retention time and diode array spectra (400–700 nm), and quantified with respect to the *trans*- $\beta$ -apo-8'-carotenal internal standard via relative response factors. *Trans*- $\beta$ -apo-8'-carotenal (Fluka) and chlorophyll *a* standards were both purchased from Sigma-Aldrich, Ltd., and all other standards were obtained from the DHI Institute for Water and Environment (Hørsholm, Denmark).

The CTD pigment sampling log and water column chlorophyll *a* concentrations estimated by spectrophotometry are presented in Table 6. The chlorophyll *a* concentrations ranged from 0.18–28.58 mg m<sup>-3</sup>, exhibiting a good spread through oligotrophic, mesotrophic, and eutrophic water masses. The selection of stations, therefore, appeared to be near optimal for optical deployments related to ocean color calibration and validation activities.

## 5.2.2 LOV Pigment Determination

The extraction and analysis of pigment concentrations were performed in January 2003, about three months after collection. The filters were extracted in 3 mL of methanol, according to the procedure described by Vidussi et al. (1996). The HPLC system is composed of the following equipment:

- A Hewlett Packard (HP) Chemstation for liquid chromatography software (version A.06.03),
- A Thermoquest Autosampler (AS 3000),
- An HP 1100 degasser,

- An HP 1100 binary pump, and
- An HP 1100 diode array detector.

The diode array detector made measurements at 440 nm for carotenoids and chlorophylls, and at 667 nm for phaeopigments.

The analytical method, based on a gradient between a methanol and ammonium acetate mixture (70:30) and a 100% methanol solution (solvent A and solvent B respectively), is similar to that described by Vidussi et al. (1996). Modifications were made to this method in order to separate certain peaks and increase sensitivity:

1. The flow rate was 0.5 mL min<sup>-1</sup>;
2. A 10 cm reversed phase chromatographic column (RP-C<sub>8</sub>), with a 3  $\mu\text{m}$  internal diameter (Hypersil MOS 3  $\mu\text{m}$ ), was used; and
3. The gradient in minutes for the percentage of solvent A and solvent B, respectively, was
  - 0 80% and 20%,
  - 4 50% and 50%,
  - 18 0% and 100%, and
  - 22 0% and 100%.

The use of an internal standard (*trans*- $\beta$ -apo-8'-carotenal) allowed the pigment concentrations to be corrected relative to internal standard variations.

All the filters collected for HPLC analysis, first underwent a particulate absorption measurement (Sect. 5.3.2.1) before being stored in liquid nitrogen for shipment back to shore. Once the samples were received at the shore laboratory, they were transferred to a -80°C freezer until further analysis was undertaken. A calibration of the measurement equipment was performed in January 2003, providing HPLC response factors for 19'-butanoyloxyfucoxanthin, fucoxanthin, 19'-hexanoyloxyfucoxanthin, alloxanthin, peridinin, zeaxanthin, chlorophyll *b*, and chlorophyll *a*. The standards for these pigments were purchased from DHI. The extraction and HPLC analysis were performed in February 2003.

The response factors for divinyl chlorophyll *a* and divinyl chlorophyll *b* were computed a) using the specific extinction coefficients of chlorophyll *a* or chlorophyll *b*, respectively, b) knowing the respective absorption of chlorophyll *a* and divinyl chlorophyll *a* (or chlorophyll *b* and divinyl chlorophyll *b*) at 440 nm when the spectra of both pigments are normalized at their red maxima, and c) considering that both pigments have the same molar absorption coefficient at this red maximum. For the remaining pigments, their specific extinction coefficients were either derived from previous calibrations or from the scientific literature (Jeffrey et al. 1997).

## 5.2.3 Pigment Intercomparison

Whether for biogeochemical studies or ocean color validation activities, HPLC is an established reference technique for the analysis of chlorophyll *a* and associated phytoplankton pigments. The emphasis of the HPLC method

BENCAL Cruise Report

**Table 6.** The CTD pigment and discrete IOP sampling log including the spectrophotometric chlorophyll *a* concentration,  $C_a^S$  (in units of milligrams per cubic meter), determined on board the ship during the cruise. Up to six depths were sampled,  $Z_1$ - $Z_6$  (in units of meters), for each CTD cast, and all times are in GMT. The geolocation (longitude and latitude) for each CTD cast is presented in Table 1. The last two stations are from the *Ecklonia* small-boat operations.

Station No.	Station		CTD Cast	Niskin Bottle Sample					
	SDY	Time		$Z_1 (C_a^S)$	$Z_2 (C_a^S)$	$Z_3 (C_a^S)$	$Z_4 (C_a^S)$	$Z_5 (C_a^S)$	$Z_6 (C_a^S)$
1§	278	0817	1[2]	2.2 ( 5.06)	2.3 (11.29)	3.2 ( 9.76)	14.1 (10.25)		
2	278	1405	2[1]	3.3† ( 1.83)	10.3† ( 2.04)	25.2† ( 8.79)			
3	279	0817	3[2]	2.3 ( 3.53)	2.3† ( 3.60)	6.0† ( 3.60)	12.8† ( 4.34)	18.3 ( 3.36)	21.8† ( 2.30)
4	279	1228	4[1]	3.5 ( 1.63)	3.5† ( 2.27)	10.9† ( 2.75)	16.5† ( 3.19)	32.7† ( 1.59)	48.2 ( 1.36)
5§	279	1418	5[1]	2.9 ( 0.92)	2.9† ( 1.80)	10.2† ( 2.24)	20.7† ( 3.39)	25.9† ( 1.36)	41.2 ( 1.21)
6	280	0635	6[2]	2.7 ( 6.79)	2.7† ( 8.12)	10.5† ( 8.32)	20.7† ( 8.56)	28.1† ( 5.43)	33.4 ( 1.59)
7	280	1119	7[3]	3.9† ( 4.31)	10.9† ( 7.50)	15.5† ( 5.97)	22.8† ( 6.34)	44.1 ( 2.07)	
8§	280	1309	8[1]	3.3† ( 5.02)	7.8† ( 8.59)	15.3† ( 8.86)	20.9† ( 7.94)	45.2 ( 3.16)	
9	280	1645	[1]						
10	281	0701	9[2]	2.2† ( 6.25)	2.2 ( 6.78)	7.2† ( 8.97)	13.4† ( 7.44)	17.9† ( 5.37)	26.3 ( 6.28)
11§	281	1053	10[1]	2.2† ( 2.51)	9.9† ( 4.72)	13.4† ( 5.64)	19.5† ( 4.55)	39.8 ( 0.85)	
12	281	1346	11[1]	2.6† ( 4.31)	12.0† ( 4.99)	17.2† ( 3.63)	22.5† ( 2.27)	30.2† ( 0.47)	
13	281	1505	[1]						
14§	282	0607	12[1]	2.6† ( 4.45)	11.8† ( 6.96)	19.4† ( 7.22)	26.1† ( 2.82)		
15	282	0907	14[1]	2.8† ( 3.22)	9.3† ( 2.51)	17.8†	30.4† ( 1.36)	50.3† ( 0.58)	
16	282	1535	15	3.0† ( 2.27)	10.3† ( 2.25)	18.3† ( 2.04)	27.7† ( 1.59)	40.8† ( 0.34)	
17§	283	0606	16	2.3 (22.34)	2.3†(21.96)	4.7 (23.56)	5.7†(22.64)	17.2†(19.72)	28.1† ( 1.48)
18	283	0933	17[2]	3.0† ( 9.47)	10.9†(11.10)	20.5†(10.45)	31.4† ( 7.27)	40.2† ( 1.92)	
19	283	1205	18[1]	3.3†(22.81)	7.9†(28.58)	14.5†(16.80)	20.4† ( 4.78)	30.9† ( 0.58)	
20	283	1350	[1]						
21	283	1800	[1]						
22	284	0645	19[2]	2.1 ( 0.66)	2.1† ( 0.24)	9.5† ( 0.36)	24.3† ( 0.59)	50.0† ( 0.24)	75.5† ( 0.21)
23	284	1137	[1]						
24§	284	1214	20	2.8† ( 0.36)	18.2† ( 0.58)	35.8† ( 0.24)	60.0†		
25§	285	0607	22	1.9† ( 0.46)	13.7† ( 0.68)	22.9† ( 1.14)	40.1† ( 0.58)	60.0† ( 0.46)	
26	286	0638	24[3]	1.7† ( 0.18)	19.8† ( 0.25)	40.0† ( 0.34)	60.8† ( 0.30)	80.3† ( 0.34)	
27§	286	1250	25[2]	2.0† ( 0.24)	10.6† ( 0.24)	29.9† ( 0.24)	49.8† ( 0.35)	80.8† ( 0.23)	
28	287	0613	27[1]	3.0 ( 0.90)	3.0† ( 0.84)	16.6† ( 1.70)	25.0† ( 2.23)	40.8† ( 1.58)	69.6† ( 0.24)
29	287	1132	28[2]	2.5† ( 0.88)	11.7† ( 0.81)	23.0† ( 2.38)	29.0† ( 2.16)	42.1† ( 2.14)	51.1† ( 0.75)
30§	287	1427	29[2]	3.8† ( 0.92)	9.4† ( 0.90)	19.7† ( 2.36)	26.9† ( 1.46)	39.2† ( 0.22)	
31	287	1554	[1]						
32	288	0612	30[2]	1.9 ( 5.20)	1.9† ( 5.81)	4.0† ( 5.58)	10.5† ( 5.61)	21.7† ( 6.08)	31.7† ( 0.56)
33	288	0901	31[2]	2.3 (12.44)	2.3†(13.96)	7.5†(14.11)	14.7†(14.97)	21.2†(16.60)	28.2† ( 1.68)
34§	288	1411	32[2]	2.9 (17.24)	2.9†(15.27)	8.1†(18.02)	16.4†(22.23)	30.4† ( 7.64)	40.3† ( 0.80)
35	288	1800	[1]						
36	289	0717	33[1]	2.2 (12.25)	2.2†(10.56)	10.5†(10.83)	20.3† ( 5.43)	30.7† ( 0.55)	
37	289	1307	34[4]	2.8† ( 1.77)	6.6† ( 1.73)	11.5† ( 5.16)	20.6† ( 1.29)	30.4† ( 0.66)	
38	289	1436	[2]						
39§	290	0830	37[1]	3.4† ( 3.17)	7.5† ( 2.62)	15.8† ( 5.24)	24.3† ( 4.89)	35.1† ( 0.73)	
40	290	1219	38[2]	3.1† ( 3.16)	9.8† ( 7.20)	13.1†(17.42)	15.5† ( 3.19)	20.2† ( 0.89)	
41	290	1503	39[1]	3.4† ( 5.67)	6.7† ( 5.02)	12.0† ( 3.40)	20.8† ( 0.80)		
42	295	1005		0.0†					
43	295	1130		0.0†					

§ Indicates a SeaHARRE-2 sample station (round-robin sampling details are presented in Sect. 5.2.3 and Table 7).

□ The boxed value indicates the number of LOV surface samples for HPLC pigment and discrete IOP analyses.

† Indicates the pigment concentration will be determined by HPLC as part of the MCM analyses.

‡ Indicates an MCM HPLC pigment sample plus an LOV HPLC pigment and discrete IOP sample.

in marine studies has also been promoted, because the international Joint Global Ocean Flux Study (JGOFS) program recommended the use of HPLC techniques in the determination of chlorophyll *a* (JGOFS 1994), and, more precisely, from 1991, to use the protocol of Wright et al. (1991).

As part of the PROSOPE JGOFS-France cruise, which occurred from 4 September to 4 October 1999, four laboratories, using four different HPLC methods, participated in an intercomparison exercise based solely on natural (field) samples (Hooker et al. 2000). This exercise was called SeaHARRE-1, and the samples were collected over a large gradient of trophic conditions ranging from the high productivity (upwelling) regime off the northwestern coast of Africa ( $2.2 \text{ mg m}^{-3}$ ) to the highly oligotrophic conditions of the Ionian Sea ( $0.045 \text{ mg m}^{-3}$ ).

Despite the diversity in trophic conditions and HPLC methodologies, the agreement between laboratories during SeaHARRE-1 was approximately 7.0% for total chlorophyll *a*, which is well within the 35% accuracy objective for remote sensing validation purposes (Hooker and Esaias 1993). For other pigments (mainly chemotaxonomic carotenoids), the agreement between methods was 21% on average (ranging from 11.5% for fucoxanthin to 32.5% for peridinin), and inversely depended on pigment concentration (with large disagreements for pigments whose concentrations were close to the methodological detection limits). Although every effort was made to make SeaHARRE-1 as complete as possible (e.g., all analyses were based on replicates), there were deficiencies in the work plan, and a follow-on activity which could investigate the deficiencies, was agreed to.

The BENCAL cruise was selected as an opportunity to collect additional field samples and to address the following recommendations from the first round robin: a) a more concerted effort to sample oligotrophic and eutrophic regimes (from a remote sensing perspective, data from these two concentration levels are also where the most new data is needed), and b) the inclusion of standard pigment samples, so a control data set is available for analysis. The use of standard pigment samples was deemed particularly important, because several sources of uncertainty are best quantified if the concentration of the samples are independently known.

Eight international laboratories, three of which participated in the first round robin, agreed to participate in SeaHARRE-2:

1. The American Horn Point Laboratory (HPL),
2. The French LOV,
3. The South African MCM,
4. The British PML,
5. The Danish DHI,
6. The Canadian Bedford Institute of Oceanography (BIO),

7. The Australian Commonwealth Scientific and Industrial Research Organisation (CSIRO), and
8. The American Center for Hydro-Optics and Remote Sensing (CHORS).

Of these laboratories, only HPL, LOV, and MCM participated in the first round robin.

The initial plan was for each laboratory to analyze 12 samples, with each sample provided in triplicate. Consequently, 24 replicate samples were collected from various depths at 12 different stations over a large range of phytoplankton biomass levels. Seawater was obtained from several CTD bottles, or from the surface using an *in situ* pump or a bucket. The water was transferred into one or two 20 L carbuoys and thoroughly mixed in order to preserve the homogeneity between the 24 replicate samples. Volumes ranging from 0.25–2.8 L were filtered through 25 mm GF/F filters, such that a visually similar amount of phytoplankton was retained on each filter. The filters were placed in cryovials or in aluminum foil jackets and immediately frozen and stored in liquid nitrogen. Details of the sampling conducted for SeaHARRE-2 are presented in Table 7.

**Table 7.** The sampling log for SeaHARRE-2. The complete identification (ID) number for each of the 24 samples collected at each station was constructed as RR2-*nnn*1, where *nnn* was the number from the first column of the table and 1 was a sequential letter of the alphabet (a–x). The station number entry includes the SDY in parentheses. The volume of water filtered is given by  $V_f$ .

ID No.	Station No. (SDY)	Time [GMT]	Sample Type	Depth [m]	$V_f$ [L]
1†	1 (278)	0817	CTD 1	2.0	0.50
2	5 (279)	1405	CTD 5	2.9	0.50
3‡	8 (280)	1309	CTD 8	3.3	0.50
4	11 (281)	1053	Bucket	0.0	0.50
5	14 (282)	0800	CTD 13	3.0	0.50
6	17 (283)	0715	Pump	0.0	0.25
7	24 (284)	1336	CTD 21	10.0	2.00
§	24 (284)	1735	Pump	0.0	2.00
8	25 (285)	0757	CTD 23	30.0	1.00
9	27 (286)	1447	CTD 26	40.0	2.80
10	30 (287)	1435	Pump	0.0	1.00
11	34 (288)	1245	Pump	0.0	0.50
§	35 (288)	1540	Pump	0.0	0.50
12	39 (290)	0617	CTD 36	3.2	1.00
§	(290)	1603	Pump	0.0	1.00

†RR2-001m Complete filtration took a very long time.

‡RR2-003x  $V_f = 0.44 \text{ L}$  (loss of 60 mL).

§ A residence time sample.

A total of 288 samples were distributed between the eight participating laboratories, with each laboratory receiving three replicates from each station. Despite being carefully monitored over a two-week period to ensure the

functionality of the dry shippers (by weighing them), several defrosted during transport, resulting in the degradation (to an unknown degree) of three complete sets of replicate batches (108 filters). Samples were then redistributed between laboratories such that each laboratory received two frozen replicates instead of the original set of triplicates (with the exception of MCM which retained a set of triplicates).

Most of the laboratories were also sent a batch of unknown standard samples from HPL (7 extracts) and DHI (6, 7, and 20 extracts). The standard samples were to be analyzed with the *in situ* samples and were the only samples with known concentrations for the constituent pigments.

Three sets of so-called *residence time* samples were also collected, but these were transported in one of the dewars that arrived defrosted. Consequently, two larger sets of replacement samples were provided by LOV and MCM after the cruise in mesotrophic (Mediterranean Sea) and eutrophic (Benguela Current) waters, so the specialized experiments associated with these samples could still be conducted.

### 5.3 Continuous and Discrete IOPs

Although the primary BENCAL objective of validating existing ocean color algorithms is focused on maintaining and refining the empirical relationships between water-leaving radiances and algal intracellular chlorophyll concentrations, a broader understanding of the causes of variability in the light leaving the ocean surface requires knowledge of marine IOPs. The characterization of absorbing and scattering processes in the ocean with regard to algal biomass, pigmentation, carbon content, assemblage structure, and physiological state greatly enhances the effectiveness of ocean color measurements.

The productive upwelling system of the Benguela and adjacent southern Atlantic waters provide Case-1 water types ranging from oligotrophic to eutrophic, accessible to a single research cruise. Corresponding changes in algal biomass and assemblage structure, ranging from low biomass offshore waters (dominated by nano- and picoplankton) to high biomass inshore waters (typically dominated by larger diatom and dinoflagellate cells), result in a wide range of IOP environments.

The determination and characterization of IOPS are also necessary for the validation, development, and operational implementation of analytical and semi-analytical ocean color reflectance algorithms that typically solve for absorption and backscattering coefficients (Carder et al. 1999, Morel and Antoine 2000, and Garver and Siegel 1997). Standard empirical (Aiken et al. 1995, and Morel and Antoine 2000) and experimental semi-analytical ocean color products (Schiller and Doerffer 1999) require IOP measurements in coastal waters to determine if the presence of particulate or dissolved constituents noncovariant

with algal pigment concentrations are indicative of Case-2 water types.

The following instruments were used for IOP determinations on the BENCAL cruise (continuous deployment indicates *in situ* measurements were made by lowering and raising the instrument through the water column, and discrete deployment indicates bench-top analyses made on discrete water samples obtained from the surface pump, a bucket lowered over the side of the ship, or Niskin bottles from the CTD rosette):

1. Two AC-9 (plus models) instruments, manufactured by Western Environmental Technology Laboratories (WETLabs), Inc. (Philomath, Oregon), for continuous and discrete sampling of a) total absorption,  $a_T$ ; b) total attenuation,  $c_T$ ; and c) total scattering,  $b_T$  (MCM and LOV).
2. One HydroSCAT-6 instrument (also referred to as a BB-6), built by Hydro-Optics, Biology, and Instrumentation (HOBI) Laboratories, Inc. (Tucson, Arizona), for continuous sampling of total backscattering,  $b_{bT}$  (PML).
3. One LI-1800 UW (with an integrating sphere) instrument, manufactured by LI-COR (Lincoln, Nebraska), for the discrete analysis of a) particulate absorption,  $a_p$ ; b) phytoplankton absorption,  $a_\phi$ ; and c) detrital absorption,  $a_d$  (LOV).
4. One Shimadzu UV-2501 spectrophotometer, manufactured by the Shimadzu Corp. (Kyoto, Japan), for discrete measurements of yellow substance (*gelbstoff*) absorption,  $a_y$  (UCT).

A summary of the deployment times and positions for the combined discrete IOP and HPLC sampling log is given in Table 8.

#### 5.3.1 Continuous IOPs

IOP profiles were collected with the MCM AC-9 (plus) instrument along with the PML HydroSCAT-6. The two instruments were mounted in a vertical configuration on the same support frame. Such a setup provided concurrent measurements of absorption, attenuation, and backscattering, and permitted the use of the attenuation data from the AC-9 in the correction schemes used to process the HydroSCAT-6 backscatter data (HOBI Labs 2002). A consistent flow rate upwards through the AC-9 flow tubes was provided by an SBE water pump.

The IOP instrument package was deployed off the starboard aft deck, frequently concurrent with the free-fall AOP instrument deployments. The package was initially taken to a depth of 2 m for 5 min, to permit both instruments to reach ambient temperature and allow the AC-9 flow tubes to flush. The package was then brought to the surface and profiled through the water column at approximately  $1 \text{ m s}^{-1}$  to a variable depth of 30–300 m.

**Table 8.** A summary of the deployment times and positions for the combined discrete IOP and HPLC sampling log. One sample was collected for each indicated checkmark (✓). The bottle depths are given by the  $Z_n$  entries, where  $n$  indicates the bottle. The spectral absorption analyses are indicated in the  $a(\lambda)$  column.

Station			Position		Sample Depths					Analyses				
No.	SDY (Greg.)	Time	Longitude	Latitude	$Z_1$	$Z_2$	$Z_3$	$Z_4$	$Z_5$	HPLC	$a(\lambda)$	POC	SPM	AC-9
1	278 (05Oct02)	0837	18.0760	-32.6500	2.0					✓†				
1	278 (05Oct02)	1155	18.0700	-32.6417	0.0					✓		✓	✓	✓
1	278 (05Oct02)				0.0					✓	✓			
2	278 (05Oct02)	1305	18.0698	-32.6508	0.0					✓	✓	✓	✓	✓
2	278 (05Oct02)	1405	18.0698	-32.6508	2.6					✓	✓	✓	✓	✓
2	278 (05Oct02)					10.4	25.5			✓	✓	✓	✓	
3	279 (06Oct02)	0820	18.2375	-32.3145	0.0					✓	✓			
3	279 (06Oct02)	0920	18.2383	-32.3188	0.0					✓	✓	✓	✓	✓
4	279 (06Oct02)	1140	18.2495	-32.3265	0.0					✓	✓	✓	✓	✓
4	279 (06Oct02)	1245	18.2578	-32.3300	2.0					✓	✓	✓	✓	✓
4	279 (06Oct02)					10.0	16.2	30.0		✓	✓	✓	✓	
5	279 (06Oct02)	1340	18.2458	-32.3155	0.0					✓	✓			
5	279 (06Oct02)	1432	18.2477	-32.3168	2.9					✓†				
6	280 (07Oct02)	0730	18.1005	-32.5880	0.0					✓	✓	✓	✓	✓
6	280 (07Oct02)	0825	18.1027	-32.5845	0.0					✓				
7	280 (07Oct02)	0905	18.1068	-32.5790	0.0					✓	✓	✓	✓	✓
7	280 (07Oct02)	0935	18.1068	-32.5790	0.0					✓	✓			
7	280 (07Oct02)	1040	18.0907	-32.5767	0.0					✓	✓			
7	280 (07Oct02)	1130	18.0902	-32.5748	2.5					✓	✓	✓	✓	✓
7	280 (07Oct02)					10.3	15.2	23.7		✓	✓	✓	✓	
8	280 (07Oct02)	1215	18.0927	-32.5765	0.0					✓	✓			✓
8	280 (07Oct02)	1322	18.0893	-32.5770	2.9					✓†				
9	280 (07Oct02)	1645	18.0515	-32.5472	0.0					✓	✓	✓	✓	✓
10	281 (08Oct02)	0750	18.1350	-32.6058	0.0					✓	✓	✓	✓	✓
10	281 (08Oct02)	0850	18.1347	-32.6027	0.0					✓	✓			✓
11	281 (08Oct02)	0935	18.1097	-32.5727	0.0					✓	✓	✓	✓	✓
11	281 (08Oct02)	1100	18.1102	-32.5663	0.0					✓†				
11	281 (08Oct02)	1105	18.1102	-32.5663	2.2					✓	✓	✓	✓	✓
11	281 (08Oct02)					9.8	13.2	19.0		✓	✓	✓	✓	✓
12	281 (08Oct02)	1213	17.9592	-32.4600	0.0					✓	✓	✓	✓	✓
13	281 (08Oct02)	1505	17.9668	-32.4737	0.0					✓	✓	✓	✓	✓
14	282 (09Oct02)	1505	17.4517	-30.7300	2.0					✓	✓			
14	282 (09Oct02)	0900			2.0					✓†				
15	282 (09Oct02)	0930	17.4542	-30.7338	2.0					✓	✓	✓	✓	
16	282 (09Oct02)	1541	17.2308	-30.8063	2.5					✓	✓	✓	✓	✓
16	282 (09Oct02)					18.3	27.4	40.8		✓	✓	✓	✓	
17	283 (10Oct02)	0715	16.6700	-29.4983	0.0					✓†				
18	283 (10Oct02)	0825	16.6755	-29.4350	0.0					✓	✓	✓	✓	✓
18	283 (10Oct02)	0933	16.6780	-29.4337	0.0					✓	✓			✓
19	283 (10Oct02)	1100	16.6862	-29.4980	0.0					✓	✓	✓	✓	✓
19	283 (10Oct02)	1226	16.6862	-29.4957	2.0					✓	✓	✓	✓	✓
19	283 (10Oct02)					8.2	15.1			✓	✓	✓	✓	
19	283 (10Oct02)							20.6	30.6	✓	✓	✓	✓	
20	283 (10Oct02)	1350	16.7432	-29.4033	0.0					✓	✓	✓	✓	✓
21	283 (10Oct02)	1800	14.7488	-29.4152	0.0					✓	✓			
22	284 (11Oct02)	0838	14.8615	-30.0282	0.0					✓	✓	✓	✓	✓
22	284 (11Oct02)	0950	14.8553	-30.0278	0.0					✓	✓			
23	284 (11Oct02)	1137	14.9060	-30.0285	0.0					✓	✓	✓	✓	✓

† Indicates a SeaHARRE-2 sample.

BENCAL Cruise Report

Table 8. (cont.) A summary of the combined discrete IOP and HPLC sampling log.

No.	Station		Position		Sample Depths					Analyses				
	SDY (Greg.)	Time	Longitude	Latitude	Z <sub>1</sub>	Z <sub>2</sub>	Z <sub>3</sub>	Z <sub>4</sub>	Z <sub>5</sub>	HPLC	a(λ)	POC	SPM	AC-9
24	284 (11Oct02)	1236	14.8933	-30.1083	2.2					✓	✓	✓		✓
24	284 (11Oct02)					18.0	35.0	60.4		✓	✓			
24	284 (11Oct02)	1342	14.8998	-30.1247	10.0					✓†				
24	284 (11Oct02)	1735			0.0					✓‡				
25	285 (12Oct02)	0805	16.2512	-29.5900	2.0					✓	✓	✓	✓	✓
25	285 (12Oct02)					25.0				✓†				
26	286 (13Oct02)	0805	14.3768	-30.5882	0.0					✓	✓	✓	✓	✓
26	286 (13Oct02)	0835	14.3703	-30.5788	0.0					✓	✓			
26	286 (13Oct02)	0950	14.3527	-30.5635	0.0					✓				
27	286 (13Oct02)	1123	14.4188	-30.5470	0.0					✓	✓	✓	✓	✓
27	286 (13Oct02)	1230	14.4155	-30.5413	0.0					✓	✓			
27	286 (13Oct02)	1513	14.4260	-30.5365		40.0				✓†				
28	287 (14Oct02)	0735	15.9752	-29.2243	0.0					✓	✓	✓	✓	✓
29	287 (14Oct02)	0908	16.0972	-29.1028	0.0					✓	✓	✓	✓	✓
29	287 (14Oct02)	1027	16.0913	-29.0822	0.0					✓	✓			
29	287 (14Oct02)	1156	16.0993	-29.0642	1.5					✓	✓	✓	✓	✓
29	287 (14Oct02)				12.2	21.8	29.6	42.0	50.9	✓	✓	✓	✓	
30	287 (14Oct02)	1323	16.0300	-29.0970	0.0					✓	✓			
30	287 (14Oct02)	1422	16.0307	-29.0910	0.0					✓	✓	✓	✓	✓
30	287 (14Oct02)	1435	16.0307	-29.0910	0.0					✓†				
31	287 (14Oct02)	1554	16.0342	-29.0983	0.0					✓				
32	288 (15Oct02)	0810	16.6788	-29.6643	0.0					✓	✓	✓	✓	✓
32	288 (15Oct02)	0825	16.6788	-29.6643	0.0					✓	✓			
33	288 (15Oct02)	0930	16.7750	-29.6543	0.0					✓	✓			
33	288 (15Oct02)	1032	16.7655	-29.6473	0.0					✓	✓	✓	✓	✓
34	288 (15Oct02)	1205	16.8535	-29.6497	0.0					✓	✓			
34	288 (15Oct02)	1231	16.8540	-29.6448	0.0					✓	✓	✓✓✓	✓✓✓	✓
34	288 (15Oct02)	1245	16.8450	-29.6448	0.0					✓†				
34	288 (15Oct02)	1427	16.0283	-29.1297	2.2					✓		✓	✓	✓
34	288 (15Oct02)					8.1	16.0	30.4		✓		✓	✓	
34	288 (15Oct02)							40.6		✓	✓	✓	✓	
35	288 (15Oct02)	1540	16.9225	-29.6448	0.0					✓‡				
35	288 (15Oct02)	1800	16.9220	-29.5958	0.0					✓	✓			
36	289 (16Oct02)	0755	18.2283	-32.0548	0.0					✓	✓			
37	289 (16Oct02)	0905	18.2283	-32.2040	0.0					✓	✓	✓	✓	✓
37	289 (16Oct02)	1010	18.2192	-32.2210	0.0					✓	✓			
37	289 (16Oct02)	1200	18.1995	-32.0738	0.0					✓	✓	✓	✓	✓
37	289 (16Oct02)	1240	18.1957	-32.0738	0.0					✓	✓			
37	289 (16Oct02)	1325	18.1912	-32.0695	1.9					✓	✓	✓	✓	✓
37	289 (16Oct02)					6.2	11.0	20.1	30.0	✓	✓	✓	✓	
37	289 (16Oct02)						11.0			✓		✓	✓	
38	289 (16Oct02)	1436	18.0955	-32.0673	0.0					✓	✓	✓	✓	✓
38	289 (16Oct02)	1531	18.1003	-32.0742	0.0					✓	✓			
39	290 (17Oct02)	0630	17.6647	-32.6728	3.2					✓†				
39	290 (17Oct02)	0820	17.6512	-32.7008	0.0					✓	✓	✓	✓	✓
40	290 (17Oct02)	1115	18.0305	-32.5658	0.0					✓	✓			
40	290 (17Oct02)	1140	18.0337	-32.5697	0.0					✓	✓	✓	✓	✓
40	290 (17Oct02)	1231	18.0358	-32.5707	3.2	9.4	12.4	16.2	20.2	✓	✓	✓	✓	✓
41	290 (17Oct02)	1400	18.2208	-32.4222	0.0					✓	✓	✓	✓	✓
	290 (17Oct02)	1603	18.0763	-32.4298	0.0					✓‡				

† Indicates a SeaHARRE-2 sample.

‡ Indicates a SeaHARRE-2 residence time sample.

### 5.3.1.1 AC-9

The WETLabs AC-9 (plus) consists of two optically distinct flow tubes, using a tungsten light source in combination with interference filters to directly obtain absorption and attenuation, and derive scattering measurements, at nine different wavelengths (Moore et al. 1992). An internally reflecting quartz-lined tube with a diffuser plate is used for absorption measurements, and a  $0.7^\circ$  acceptance angle nonreflecting tube is used for attenuation measurements, both with a path length of 25 cm. Center wavelengths of both instruments were 412, 440, 488, 510, 532, 555, 676, and 715 nm, with a bandwidth of 10 nm.

The instrument has a sampling rate of 6 Hz, and in profiling mode was set to depth bin every 10 samples. The profiled measurements, summarized in Table 9, were recorded using the internal logging system and subsequently downloaded. The discrete measurements were recorded directly using software provided by the manufacturer (WETView v5.0a). The instruments were cleaned and their stability monitored on a daily basis using an air-tracking procedure (WETLabs 2000).

The AC-9 and HydroSCAT-6 data were processed concurrently to permit the AC-9 data to be used for attenuation corrections in the HydroSCAT-6 processing schemes. Briefly, the raw AC-9 data were first binned to a 1 m interval, and corrected for daily measured air-tracking offsets, which had maximal values at 412 nm of approximately  $0.01 \text{ m}^{-1}$  for absorption and about  $0.025 \text{ m}^{-1}$  for attenuation. Data were then median filtered to remove spiking, and the up and down casts were merged.

The temperature and salinity corrections of Pegau et al. (1997) were applied, using temperature and salinity data from the equivalently-binned CTD cast executed closest in time. Scattering corrections were made according to Zaneveld et al. (1994), as per the protocols supplied for the instrument by the manufacturer (WETLabs 2000). Pure water absorption and scattering values at the nine relevant wavelengths (Pope and Fry 1997, Kou et al. 1993, and Buiteveld et al. 1994, as cited in WETLabs 2000) were then added to the final water-referenced absorption and attenuation values to produce the total absorption and scattering values needed for HydroSCAT-6 data processing.

### 5.3.1.2 HydroSCAT-6

The HydroSCAT-6 instrument is used to calculate the total backscattering coefficient at six discrete wavelengths by measuring the angular scattering centered at an angle of  $140^\circ$  (Maffione and Dana 1997). The instrument is a self-contained logging system suitable only for *in situ* measurements (Table 9), and has center wavelengths of 442, 488, 550, 620, 671, and 852 nm, with a bandwidth of 10 nm.

The HydroSCAT-6 data were processed using the same binning, median filtering, plus up and down cast merging schemes described earlier for the AC-9. The correction

terms needed to account for attenuation effects within the HydroSCAT-6 measurement geometry (HOBI Labs 2002) were made using measured absorption and scattering values from the AC-9, as described above (Sect. 5.3.1.1).

It should be noted that the AC-9 and HydroSCAT-6 spectral bands are not perfectly matched, although in all cases, except for the HydroSCAT-6 620 nm band, there is a maximum discrepancy at visible wavelengths of no more than 5 nm. Absorption and scattering values at 620 nm were, therefore, calculated for initial processing purposes using a linear interpolation between the 555 and 650 nm AC-9 bands. This procedure must be considered approximate and was only implemented to provide preliminary results.

### 5.3.2 Discrete IOPs

Volumes ranging from 0.25–2.8 L were used for discrete analyses. The selected volume depended upon the expected concentration of particles and pigments, in such a way that similar amounts of material were retained on the filters, whatever the trophic state of the investigated water.

The analytical volumes were filtered in parallel through GF/F filters, for the following four determinations: particle absorption spectrum, and by using the same filter, pigment composition and concentration, plus the mass concentration of SPM, and the POC content of this material. The GF/F filters were conditioned according to their analytical use. For the first and second determinations, nothing special was necessary, and the filters were used as they were provided by the manufacturer. For the SPM determination, the filters were preweighed in well-controlled conditions (temperature and humidity) and numbered. For the POC determination, they were precleaned with a solvent to eliminate any traces of organic carbon.

In addition, the determination of the absorption and attenuation coefficients ( $a$  and  $c$ ) of total material (dissolved and particulate) was made on discrete samples by using an AC-9 profiler as a bench-top instrument.

#### 5.3.2.1 Filter Pad Particulate Absorption

The LI-1800 UW is a modular spectroradiometer, with a central optical system consisting of a grating monochromator, an order sorting filter wheel, and a silicon detector. For filter pad absorption measurements, input optics are provided by an 1800-12 external integrating sphere, allowing a wavelength range of 370–750 nm.

At each depth, a predetermined volume of seawater was filtered through a Whatman GF/F glass-fiber filter. The optical densities of the particles were promptly measured using the LI-1800 UW spectroradiometer equipped with an integrating sphere. Properly hydrated GF/F filters were measured as blanks with every set of samples. The spectral absorption coefficient of particulate matter,  $a_p(\lambda)$ , was recorded from 370–750 nm (in 0.2 nm increments). The

BENCAL Cruise Report

**Table 9.** The FRRF, HydroSCAT-6 (BB-6), and AC-9 combined sampling log (all times in GMT). The last column indicates whether or not the AC-9 was deployed.

Station	SDY (Greg.)	Longitude	Latitude	FRRF	Begin	End	BB-6	Begin	End	AC-9
1	278 (05Oct02)	18.0760	-32.6590	F01ab	1003	1015	B01	1003	1015	✓
2	278 (05Oct02)	18.0708	-32.6483	F02ab	1300	1316	B02	1300	1316	✓
4	279 (06Oct02)	18.2428	-32.3163	F03	1138	1155	B03	1205	1215	✓
5	279 (06Oct02)	18.2433	-32.3138	F04	1326	1335	B04	1355	1402	✓
6	280 (07Oct02)	18.0990	-32.5975	F05	0757	0811	B05	0825	0836	✓
7	280 (07Oct02)	18.1050	-32.5815	F06	1029	1043	B06	1056	1109	✓
8	280 (07Oct02)	18.0877	-32.5733	F07	1224	1236	B07	1248	1300	✓
9	280 (07Oct02)	18.0023	-32.0225	F08	1514	1524	B08	1439	1448	✓
9	280 (07Oct02)			F09ab	1554	1513	B09	1536	1545	✓
9	280 (07Oct02)						B10	1625	1636	✓
10	281 (08Oct02)	18.1408	-32.6082	F10	0809	0825	B11	0828	0842	✓
11	281 (08Oct02)	18.1080	-32.5672	F11	1009	1021	B12	1033	1044	✓
12	281 (08Oct02)	17.9522	-32.4600	F12	1301	1312	B13	1324	1333	✓
13	281 (08Oct02)	17.9692	-32.4580	F13	1418	1427	B14ab	1438	1458	✓
13	281 (08Oct02)			F14ab	1505	1525	B15	1536	1545	✓
13	281 (08Oct02)			F15	1551	1600	B16	1610	1618	✓
14	282 (09Oct02)	17.3507	-30.7550	F16	0604	0613	B17	0624	0630	✓
15	282 (09Oct02)	17.4537	-30.7320				B18	0952	1001	✓
15	282 (09Oct02)			F17	0931	0940	B19	1012	1023	✓
16	282 (09Oct02)	17.2467	-30.8325	F18ab	1258	1320	B20	1331	1345	✓
16	282 (09Oct02)			F19	1611	1618	B21	1600	1608	✓
17	283 (10Oct02)	16.6710	-29.4997	F20	0642	0652	B22	0705	0714	✓
17	283 (10Oct02)						B23	0715	0725	✓
18	283 (10Oct02)	16.6733	-29.4355	F21	0855	0903	B24	0912	0923	✓
19	283 (10Oct02)	16.6718	-29.5040	F22	1123	1134	B25	1144	1151	✓
20	283 (10Oct02)	16.7402	-29.4062	F23	1358	1407	B26	1417	1427	✓
21	283 (10Oct02)	16.7477	-29.4092	F24	1506	1516	B27	1524	1533	✓
21	283 (10Oct02)			F25	1538	1547	B28	1555	1601	✓
22	284 (11Oct02)	14.8610	-30.0435	F26	0821	0837	B29	0846	0905	✓
24	284 (11Oct02)	14.8943	-30.1135	F27	1243	1258	B30	1307	1327	✓
24	284 (11Oct02)			F28	1347	1403	B31	1412	1427	✓
25	285 (12Oct02)	16.0837	-29.5893	F29	0640	0651	B32	0707	0724	✓
25	285 (12Oct02)			F30	0730	0746				
26	286 (13Oct02)	14.3798	-30.6107	F31	0812	0842	B33	0912	0959	✓
27	286 (13Oct02)	14.4175	-30.5505	F32	1141	1203	B34	1216	1238	✓
27	286 (13Oct02)			F33	1323	1345	B35	1412	1432	✓
28	287 (14Oct02)	15.9980	-29.2387	F34	0657	0707	B36	0722	0737	✓
29	287 (14Oct02)	16.1008	-29.1083	F35	1046	1100	B37	1111	1122	✓
30	287 (14Oct02)	16.1900	-29.0738	F36	1347	1357	B38	1407	1418	✓
32	288 (15Oct02)	16.6692	-29.6827	F37	0648	0659	B39	0708	0722	✓
33	288 (15Oct02)	16.7740	-29.5743	F38	0928	0940	B40	0953	1003	✓
34	288 (15Oct02)	16.8550	-29.6497	F39	1245	1255	B41	1305	1317	✓
34	288 (15Oct02)			F40	1322	1333				
35	288 (15Oct02)	16.9086	-29.5957	F41	1505	1518	B42	1527	1539	✓
36	289 (16Oct02)	18.2292	-30.0550	F42	0738	0750	B43	0757	0805	✓
37	289 (16Oct02)	18.2125	-32.0817	F43	1120	1130	B44	1140	1152	✓
38	289 (16Oct02)	18.0936	-32.0668	F44	1454	1505	B45	1514	1525	✓
39	290 (17Oct02)	17.6647	-32.6728	F45	0650	0701	B46	0715	0726	✓
39	290 (17Oct02)			F46	0800	0820				
40	290 (17Oct02)	18.0305	-32.5652				B47	1203	1211	✓
41	290 (17Oct02)	18.2210	-32.4217	F47	1427	1435	B48	1443	1451	✓

value of  $a_p(750)$  should be zero, so the remaining  $a_p$  values were shifted at all wavelengths so  $a_p(750) = 0$ . The path length amplification due to multiple scattering inside the filter was corrected using a parameterization given by Mitchell and Kiefer (1988).

Duplicate filtrations were carried out, in a nonsystematic manner, and one of the filters was soaked (in MeOH) to depigment the sample (Kishino et al. 1985) and, thus, to determine the absorption spectrum of bleached cells and detritus. When the bleaching protocol is not applied, the deconvolution of the  $a_p$  spectrum into its algal and detrital components ( $a_{\phi}$ , and  $a_d$ , respectively) can be carried out according to Bricaud and Stramski (1990).

After the absorption determination was made, the filters were immediately frozen in liquid nitrogen, and then stored at  $-80^{\circ}\text{C}$ , for subsequent laboratory analysis of the (HPLC) pigment composition (Sect. 5.2.2). Preliminary experiments have demonstrated that the exposition to the light beam of the radiometer does not affect the pigment composition and content of the filter pad.

### 5.3.2.2 Absorption, Attenuation, and Scattering

The LOV AC-9 was used for discrete absorption, attenuation, and scattering measurements. The instrument included nine spectral bands at 412, 440, 488, 510, 532, 555, 650, 676, and 715 nm, all with a bandwidth of 10 nm. The signals were recorded as recommended in the user's manual. The instrument was factory calibrated prior to the cruise, and operated as a bench-top instrument in a fixed tilted position ( $45^{\circ}$ ). The flow tubes of the instrument were filled from below using a tank positioned above the AC-9 and containing about 4 L of water. This arrangement avoided bubble formation and allowed the measurement chambers to be abundantly rinsed.

In addition to daily air-tracking procedures, an ultrapure water calibration was carried out every third day using Milli-Q™† purity water. Only surface samples were measured in this fashion, with the exception of a single 400 m sample taken in very low biomass (oligotrophic) waters for the purposes of assessing the performance of the instrument.

Bench-top AC-9 data were processed following the procedures for the profile data, with the exception that salinity data came from bottled salinometer determinations, and the analysis temperature was calculated using a constant  $1^{\circ}\text{C h}^{-1}$  time-dependent offset based on the length of time samples stood between sampling and analysis.

### 5.3.2.3 Yellow Substance Absorption

The Shimadzu UV-2501 is a double-beam (chopped) spectrophotometer with dual monochromators, each configured with 5 nm slit widths. A wavelength range of 250–800 nm, at a 1 nm resolution, was used for dissolved organic

measurements. Measurement baselines were set in air, and 10 cm path length-matched quartz cuvettes were used during the analyses.

Samples were prepared by filtering discrete water samples through GF/F filter papers under less than 10 mm mercury pressure, using stainless steel filter frits. Absorbance measurements were then made using BDH Lichrosolv HPLC-grade water as a pure water reference. Absorption coefficients were calculated following Mueller and Austin (1995), with a null absorption point set to 800 nm. Data were then fit to the following expression (Bricaud et al. 1981):

$$a_y(\lambda) = a_y(400)e^{-s(\lambda-400)}, \quad (4)$$

where  $a_y(400)$  is the yellow substance absorption at the reference wavelength ( $\lambda = 400$  nm), and  $s$  is the exponential slope. Note that the formulation in (4) allows the yellow substance absorption curve to be described by only two parameters.

In approximately 30% of the samples measured, yellow substance absorption at visible wavelengths was below the detection limit of the spectrophotometer (which was approximately 0.001 absorbance units or an absorption of  $0.023 \text{ m}^{-1}$ ). In these detection-limited cases, data from the ultraviolet part of the spectrum were used to obtain a fit to (4).

## 5.4 Bio-Optically Significant Parameters

A thorough understanding of particulate absorption and scattering in the ocean requires a knowledge of the concentration, size distribution, and composition of the particle population. Bulk particle measurements, in combination with microscopic phytoplankton and bacterial counts, provide fundamental taxonomic and microbial community structure information. Such data allow detailed analyses of the optical properties of the marine algal community, which typically is widely polydispersed in the natural state, on the level of equivalent single particles (Bricaud et al. 1988).

Algal taxonomic and cell volume data can also be used to estimate planktonic carbon concentrations, which are needed for primary production calculations. Additionally, particle measurements are necessary for a better understanding of the role of nonalgal particulates with regard to backscattering—specifically to explain the discrepancy between observed and predicted oceanic backscatter (Morel and Ahn 1991). A summary of the particle samples collected for Coulter, phytoplankton, and bacteria counting is presented in Table 10.

### 5.4.1 Bulk Particle Counts

Bulk particle size measurements were made using a 128-channel Coulter Multisizer II (UCT) with a  $140 \mu\text{m}$  aperture (range  $3.4\text{--}70 \mu\text{m}$ ) in manometer mode, using freshly prepared  $0.2 \mu\text{m}$  filtered seawater as both the blank and

† Milli-Q is a registered trademark of the Millipore Corporation (Bedford, Massachusetts).

## BENCAL Cruise Report

**Table 10.** A summary of the *in situ* samples collected for particle analyses during the BENCAL cruise. The depth of the sample is given by  $Z_D$  (in units of meters), and the type of counting is given by the  $N_C$ ,  $N_P$ , and  $N_B$  symbols which correspond to Coulter, phytoplankton, and bacteria, respectively.

Station			Sample Source	$Z_D$	Counts			Station			Sample Source	$Z_D$	Counts		
No.	SDY (Greg.)	Time			$N_C$	$N_P$	$N_B$	No.	SDY (Greg.)	Time			$N_C$	$N_P$	$N_B$
1	278 (05Oct02)	0817	CTD	2	✓	✓	✓	17	283 (10Oct02)	0715	Pump	0	✓	✓	✓
2	278 (05Oct02)	1405	CTD	2	✓	✓	✓	18	283 (10Oct02)	0825	Pump	0	✓	✓	✓
2	278 (05Oct02)	1405	CTD	10	✓			18	283 (10Oct02)	0933	Pump	0	✓		
2	278 (05Oct02)	1405	CTD	25	✓			19	283 (10Oct02)	1100	Pump	0	✓	✓	✓
2	278 (05Oct02)	1305	Pump	0	✓	✓	✓	20	283 (10Oct02)	1350	Pump	0	✓	✓	✓
3	279 (06Oct02)	0920	Pump	0	✓	✓	✓	22	284 (11Oct02)	0838	Pump	0	✓	✓	✓
4	279 (06Oct02)	1140	Bucket	0	✓	✓	✓	23	284 (11Oct02)	1137	Pump	0	✓	✓	✓
4	279 (06Oct02)	1245	CTD	2	✓			24	284 (11Oct02)	1236	CTD	2	✓	✓	✓
4	279 (06Oct02)	1245	CTD	10	✓			24	284 (11Oct02)	1236	CTD	18	✓		
4	279 (06Oct02)	1245	CTD	16	✓			24	284 (11Oct02)	1236	CTD	35	✓		
4	279 (06Oct02)	1245	CTD	30	✓			24	284 (11Oct02)	1236	CTD	60	✓		
6	280 (07Oct02)	0730	Bucket	0	✓	✓	✓	25	285 (12Oct02)	0805	CTD	2	✓	✓	✓
7	280 (07Oct02)	1040	Bucket	0	✓	✓	✓	26	286 (13Oct02)	0835	Pump	0	✓	✓	✓
7	280 (07Oct02)	1130	CTD	2	✓			27	286 (13Oct02)	1123	Pump	0	✓	✓	✓
7	280 (07Oct02)	1130	CTD	10	✓			27	286 (13Oct02)	1513	CTD	400	✓		✓
7	280 (07Oct02)	1130	CTD	15	✓			28	287 (14Oct02)	0735	Pump	0	✓	✓	✓
7	280 (07Oct02)	1130	CTD	24	✓			29	287 (14Oct02)	1156	CTD	2	✓	✓	✓
8	280 (07Oct02)	1215	Bucket	0	✓	✓	✓	29	287 (14Oct02)	1156	CTD	12	✓		
9	280 (07Oct02)	1645	Bucket	0	✓	✓	✓	29	287 (14Oct02)	1156	CTD	22	✓		
10	281 (08Oct02)	0750	Bucket	0	✓	✓	✓	29	287 (14Oct02)	1156	CTD	30	✓		
10	281 (08Oct02)	0850	Bucket	0	✓	✓	✓	30	287 (14Oct02)	1422	Pump	0	✓	✓	✓
11	281 (08Oct02)	0935	Bucket	0	✓	✓	✓	32	288 (15Oct02)	0810	Pump	0	✓	✓	✓
11	281 (08Oct02)	1105	CTD	2	✓			33	288 (15Oct02)	1032	Pump	0	✓	✓	✓
11	281 (08Oct02)	1105	CTD	10	✓			34	288 (15Oct02)	1231	Pump	0	✓	✓	✓
11	281 (08Oct02)	1105	CTD	13	✓			34	288 (15Oct02)	1245	Pump	0	✓	✓	✓
11	281 (08Oct02)	1105	CTD	19	✓			34	288 (15Oct02)	1427	CTD	2	✓		
12	281 (08Oct02)	1213	Bucket	0	✓	✓	✓	36	289 (16Oct02)	0905	Pump	0	✓	✓	✓
14	282 (09Oct02)	0900	CTD	2	✓	✓	✓	37	289 (16Oct02)	1200	Pump	0	✓	✓	✓
15	282 (09Oct02)	0930	CTD	2	✓	✓	✓	37	289 (16Oct02)	1325	CTD	2	✓		
16	282 (09Oct02)	1541	CTD	2	✓	✓	✓	38	289 (16Oct02)	1436	Pump	0	✓	✓	✓
16	282 (09Oct02)	1541	CTD	18	✓			39	290 (17Oct02)	0820	Pump	0	✓	✓	✓
16	282 (09Oct02)	1541	CTD	27	✓			40	290 (17Oct02)	1140	Pump	0	✓	✓	✓
16	282 (09Oct02)	1541	CTD	41	✓			40	290 (17Oct02)	1231	CTD	2	✓		
								41	290 (17Oct02)	1400	Pump	0	✓	✓	✓

electrolyte. Unscreened samples were diluted to keep coincidence levels below 10%, and 20 mL of sample were counted, with typical count times of approximately 250 s. It should be noted that the Coulter technique is based on volume equivalence and calculates particle diameter based on an equivalent volume sphere. Coincidence-corrected particle counts in cells per liter were median filtered to remove electronic spiking, and left in their original log-spaced size bins.

A further description of the particle size distribution (PSD) functions was supplied by calculating the effective radius  $r_{\text{eff}}$ , and effective variance  $v_{\text{eff}}$  (Hansen and Travis 1974) for each size distribution. These parameters are de-

defined as follows:

$$r_{\text{eff}} = \frac{\int_{r_1}^{r_2} r \pi r^2 F(r) dr}{\int_{r_1}^{r_2} \pi r^2 F(r) dr} \quad (5)$$

$$= \frac{1}{G} \int_{r_1}^{r_2} r \pi r^2 F(r) dr$$

and

$$v_{\text{eff}} = \frac{1}{G r_{\text{eff}}^2} \int_{r_1}^{r_2} (r - r_{\text{eff}})^2 \pi r^2 F(r) dr, \quad (6)$$

where  $F(r)$  is the number of particles of radius  $r$  in the radius interval  $dr$  ( $r_1$  and  $r_2$  are the minimum and maxi-

imum interval values, respectively), and  $G$  is the geometrical cross-sectional area of particles per unit volume. Because particles scatter light proportional to  $\pi r^2$ , the effective radius and variance reflect the mean size and width of the size distribution (Hansen and Travis 1974).

#### 5.4.2 Phytoplankton Counts

Discrete 200 mL water samples were collected for phytoplankton counts. The samples were fixed with a 2% buffered formalin solution and counted ashore using the  $\ddot{U}$ termohl technique as modified by Smayda (1978). Taxa were identified to a genus level.

#### 5.4.3 Bacterial Counts

Unfiltered, discrete water samples were fixed with 25% glutaraldehyde, which produced a final fixative concentration of 1.25%. The samples were stored at 4°C until they were counted using the Hobbie et al. (1977) methods.

#### 5.4.4 Particle Mass Concentration

The 25 mm GF/F filters were weighed (23°C, 38% humidity) at least twice before the cruise and individually stored in numbered Petri slides. The initial weight was around 37.5 mg, and was determined within an accuracy of  $\pm 0.001$  mg, and a repeatability of  $\pm 0.002$  over several days. The filtered volumes were adjusted in such a way that the mass retained on the filter was in the 0.5–1.0 mg range, leading to a theoretical accuracy better than 1% in terms of mass determination. The filters (including their annular periphery) were rinsed several times with a minimal amount of distilled water and gentle filtration to eliminate the salts embedded within the glass fibers. The slides were then stored at  $-25^\circ\text{C}$ .

The filters were dried at room temperature in a clean laboratory over the course of several days. Once dry, the filters were weighed and reweighed until a constant weight was observed (at 22°C and 35% humidity). The final accuracy, which involves all operations (sampling, filtration, rinsing, and weighing), was assessed through duplicates and triplicates, and was better than  $\pm 3\%$ . The values for the surface water range from  $121 \text{ mg m}^{-3}$  (station 25, far offshore) to  $2,494 \text{ mg m}^{-3}$  (station 41, inshore turbid water). Among the 79 determinations, 68 were successful; small mechanical damage of the filters, which may occur during the manipulations and are visually detectable, explain the failures.

#### 5.4.5 Particulate Organic Carbon

The volumes to be filtered for this determination were the same as for the mass determination, but the GF/F filters were prepared differently. They were previously washed with dichloromethane within a Soxhlet apparatus.

This procedure produces blanks as good as precombustion at high temperature (400°C), without altering the filter porosity. After filtering and rinsing with filtered seawater, the filters were also kept at  $-25^\circ\text{C}$ . The samples will be processed with a LECO-900 carbon analyzer, using ethylenediaminetetracetic acid as a standard.

## 6. OCEANIC PRODUCTIVITY

Understanding primary productivity along with the corresponding distributions of phytoplankton biomass is important in biological oceanography, because the survival of organisms at higher trophic levels depends on the supply of energy from primary producers (Kuring et al. 1990). To understand the distribution and variability of phytoplankton biomass, and to compute primary production, information from *in situ* and satellite sensors are combined.

The use of remotely-sensed ocean color data has significantly improved the understanding of biological variability, because it has proven the viability of using satellite observations for estimating primary production (Platt et al. 1991). Knowing the intensity and dynamics of primary productivity within short and long time scales has been particularly helpful for understanding highly dynamic pelagic ecosystems, such as the Benguela. One of the objectives of the *in situ* sampling conducted during the BEN-CAL cruise was to examine the inshore-offshore variability of primary productivity along the west coast of South Africa during the austral spring.

Primary production, and the resulting high biomass (eutrophication) in upwelling waters, are attributed to the fresh supplies of inorganic macronutrients ( $\text{NO}_3$ ,  $\text{PO}_4$ , and  $\text{SiO}_4$ ) which are brought to the surface by the episodically, wind-driven upwelled bottom water. The physical processes and their episodic nature, provide large fluctuations of the nutrient supply, which coupled with the high rates of photosynthesis, lead to an extreme heterogeneity of primary production and biomass. Upwelling zones are characterized by *streamers* of phytoplankton-rich water, transported offshore for up to 200 km. The sequence of nutrient resupply, utilization, and transport can mean the streamers can be rich in biomass for some time after the nutrients have been consumed and the rates of photosynthesis have declined.

Recent research has focused on the links between measurements of phytoplankton photosynthesis, primary production, pigment composition, and optical properties. The inquiries have been facilitated by the rapid, nondestructive measurements provided by *in situ* instrumentation, specifically, the FRRF measurements of photosynthetic quantum efficiency (PQE), the effective cross-section for photosystem 2 (PS2) absorption ( $\sigma_{\text{PS2}}$ ), photosynthesis turn-over times ( $\tau$ ), plus optical instruments for measuring spectral absorption and attenuation. These are compared with the conventional rates of primary production derived from radio-carbon incubations, simulated on deck or laboratory photosynthesis-irradiance relationships.

**Table 11.** The primary production sampling log. The station time periods are given in GMT. The sample depths (in meters) are given by  $Z_1$ – $Z_5$ .

Station	SDY (Greg.)	Time	Longitude	Latitude	$Z_1$	$Z_2$	$Z_3$	$Z_4$	$Z_5$
1	278 (05Oct02)	0817	18.0760	-32.6587	0.0	2.0	3.2	4.5	12.5
10	281 (08Oct02)	0701	18.1408	-32.6081	0.0	2.2	4.5	7.3	13.5
17	283 (10Oct02)	0606	16.6707	-29.4878	0.0	2.3	4.8	9.5	
28	287 (14Oct02)	0613	15.9935	-29.2370	0.0	3.0	7.2	22.0	
32	288 (15Oct02)	0612	16.6703	-29.6812	0.0	1.9	3.8	13.5	

## 6.1 FRRF Profiles

Since the late 1960s, chlorophyll *a* fluorescence measurements have been widely used to map and quantify the distribution of phytoplankton biomass in the marine environment (Aiken 2001). Chlorophyll *a* *in vivo* fluoresces with the emission of red light (at approximately 683 nm) when excited by blue light over a broad spectrum in the so-called *Soret* band (400–470 nm). The chlorophyll *a* *in vivo* fluorescence yield is highly variable: it is low in high light and in nutrient repleted conditions (when photosynthesis is high), and it is high at night or in nutrient depleted conditions (when photosynthesis is low). This makes the interpretations of measurements by simple filter fluorometers difficult and ambiguous (Falkowski and Kiefer 1985).

The causes of fluorescence variability are well known. At physiological temperatures, 683 nm fluorescence originates mostly from electron-hole recombination processes in PS2, i.e., delayed luminescence (Kolber and Falkowski 1993, and Barber et al. 1989). Bulk antenna chlorophyll contributes only a small fraction of the emission at 683 nm. The luminescence process has a high but variable efficiency, inversely related to photosynthetic rates, yet it still dominates stimulated fluorescence from antenna chlorophyll by a factor of 10 or more (efficiency is 1–4% compared to 0.1–0.4%).

The FRRF, as well as the Pump and Probe Fluorometer (PPF), were developed at the Brookhaven National Laboratory (Kolber and Falkowski 1993). These instruments exploit the variable fluorescence phenomenon to determine phytoplankton photosynthetic activity and parameter values. A description of the measurement principles of the PPF aids the understanding of the operation of the FRRF, so a brief summary is provided here.

When phytoplankton are pumped with a high-intensity, saturating flash of visible radiation, all the reaction centers of PS2 (PS2-traps) are closed, and the fluorescence yield, which is measured by a low-intensity probe pulse (less than 1% of the saturating level), is maximal ( $F_m$ ). A low-intensity (ambient light) probe pulse before the pump gives the fluorescence yield ( $F_o$ ) proportional to the fraction of open (inactive) PS2-traps. The variable fluorescence ( $F_v$ ) is equal to the difference between  $F_m$  and  $F_o$  ( $F_v = F_m - F_o$ ). The activity of PS2 is proportional to the fraction of closed PS2-traps ( $F_v/F_m$ ). The latter is

the PQE, which is proportional to phytoplankton productivity (a constant times the products of absorption, PQE, and light) with a minimum value of approximately 0.1 and a maximum value of about 0.65 for eukaryotic algae, but less for prokaryotes.

The FRRF was developed to measure other photosynthetic rates and parameters besides the PQE. The FRRF has a light chamber exposed to ambient light and a dark chamber† with a flush-time of 0.2–1.0 s, sufficient to inhibit the light reactions and photochemical quenching. The FRRF uses a rapid sequence of flashlets of subsaturating intensity (100 at 1 ms interval) to pump PS2 to saturation. Both  $F_mD$  and  $F_mL$  are derived from the fluorescence yield at saturation, and  $F_oD$  and  $F_oL$  are determined by extrapolation of the curve to the initial condition.

The size of the cross-section of PS2 ( $\sigma_{PS2}$ ) is proportional to the slope of the fluorescence-yield curve. After saturation, lowering the frequency of flashlets (10 ms interval) causes the saturation of PS2 to decay, with a rate proportional to the turnover time of PS2,  $\tau$ . Both  $\sigma_{PS2}$  and  $\tau$  are derived by fitting exponential functions to the data. A mechanistic model and the operational protocols for the FRRF are given in Kolber and Falkowski (1993) and Kolber et al. (1998).

## 6.2 Primary Production

Primary production was measured at five stations from the uptake of  $^{14}C$  at different depths in the euphotic layer in simulated *in situ* experiments. Water samples were collected from depths corresponding to 100, 45, 19, 8, and 1% of the surface light intensity (Table 11), estimated from light attenuation curves. For each sample, radioactive  $^{14}C$ , in the form of sodium bicarbonate ( $NaH^{14}CO_3$ ), was added to three light and one dark bottle. The bottles were then incubated for 24 h in deck incubators that simulated light conditions at the respective depths sampled.

At the end of the incubation period, the samples were filtered onto 25 mm GF/F filters that were air-dried and placed inside scintillation vials. Hydrochloric acid (0.5 mL

† In the following lexicon and symbology, light chamber measurements are denoted by the “L” suffix, and dark chamber measurements by the “D” suffix (e.g.,  $F_vD/F_mD$  and  $F_vL/F_mL$  are the PQE measurements in the dark and ambient light chambers, respectively).

1 N) was added to each vial to remove any remaining inorganic  $^{14}\text{C}$ . The vials were allowed to stand uncapped in a fume hood overnight. The following morning, scintillation fluor (Packard Ultima Gold LLT) was added to each vial. In addition, parallel samples from the 8% and 45% light depths were incubated for fractionation studies, and prescreened through  $10\ \mu\text{m}$  meshes before filtration and treatment as described above. The radioactivity was measured ashore using a Beckman LS 1800 liquid scintillation counter. In the calculation of production rates at each depth, the *dark* bottle values were subtracted from the *light* bottle values.

## 7. PRELIMINARY RESULTS

Although a complete match-up analysis is beyond the scope of the results presented here, it is one of the primary objectives of the BENCAL cruise, so it is instructive to consider the potential for matchups based on the *in situ* sampling times and the satellite overpass schedules. Table 12 summarizes the nominal satellite coverage during the BENCAL cruise as a function of the BENCAL stations. One of the most striking aspects of the summary is the effect of the three-day orbit repeat cycle for MERIS. The average possible number of SeaWiFS and MODIS matchups is about 18, whereas it is 9 for MERIS. Note that the amount of *in situ* sampling for each overpass time is frequently very high, i.e., more than 20 samples.

### 7.1 Apparent Optical Properties

After accounting for the immersion and calibration factors, the data from the hyperspectral LI-COR instrument are converted into absolute units, for either spectral downwelling irradiance,  $E_d(\lambda)$ , or upwelling irradiance,  $E_u(\lambda)$ . Examples for both kinds of irradiance are displayed in Figs. 4 and 5. They have been selected to illustrate two extreme conditions in terms of phytoplanktonic biomass (and optical properties in Case-1 waters). Indeed, the total chlorophyll concentration,  $[\text{TChl } a]$ , at station 19 ranges between approximately  $20\text{--}30\ \text{mg m}^{-3}$  within the 0–10 m upper layer. In contrast, at station 27, the concentration is about two orders of magnitude smaller:  $0.2\text{--}0.4\ \text{mg m}^{-3}$ , between 0–59 m. As expected for Case-1 waters with such a chlorophyll content, the  $E_d(\lambda)$  and  $E_u(\lambda)$  maxima (at all depths) are located at 575 nm in dark green waters (station 19), and at 480 nm in blue waters (station 27).

The reflectance spectra for the upper layer, presented in Fig. 6, are obtained by forming the ratio

$$R(z, \lambda) = \frac{E_u(z, \lambda)}{E_d(0^-, \lambda)}, \quad (7)$$

where  $z$  is one of the shallowest depths where data have been acquired (about 0.5–2 m), and  $0^-$  means *just beneath the sea surface*. The spectrum at  $0^-$  is actually derived from an above-surface measurement, corrected for

the transmission through the interface, as indicated above (2). Some extrapolations (not shown) must be made to obtain the subsurface reflectance spectrum that is needed for radiometric validation of ocean color sensors. Nevertheless the extrapolation does not change the main features observed in Fig. 6.

In green waters, the reflectance is maximal at 573 nm, and minimal around 440 nm; a secondary maximum appears in the ultraviolet domain at about 360 nm, whereas the sun-induced chlorophyll *a* fluorescence peak is located at 685 nm. In blue waters, the maximal reflectance is at 360 nm; a relative minimum occurs at 450 nm followed by a relative weak maximum at 490 nm. In spite of the small chlorophyll *a* concentration, the fluorescence peak is easily discernible. The patterns of these reflectance spectra confirm the predictions (Morel and Maritorena 2001).

### 7.2 Pigment Distribution

HPLC analysis of CTD samples yielded concentrations for 15 chlorophyll and carotenoid pigments. Data from three stations have been selected to illustrate the distribution of phytoplankton pigments. Diagnostic pigment (DP) indices were derived to assess the composition of phytoplankton communities (Vidussi et al. 2001), and were defined as the sum of seven selected biomarker pigments (Sect. 5.2) as given in Table 13.

$[\text{TChl } a]$ , estimated as the sum of monovinyl chlorophyll *a*, divinyl chlorophyll *a*, chlorophyllide *a*, and chlorophyll *a* allomers and epimers (Table 13), was used to indicate the biomass of phytoplankton. A linear regression between  $[\text{DP}]$  and  $[\text{TChl } a]$  involved 14 points ( $N = 14$ ) and exhibited a significant linear correlation coefficient ( $R^2 = 0.99$ ), which indicates  $[\text{DP}]$  is also a valid indication of biomass. The proportion of each phytoplankton group(s) contributing to the biomass was defined as given in Table 13.

Diatoms and dinoflagellates are greater than  $10\ \mu\text{m}$  in size, nanophytoplankton are  $2\text{--}10\ \mu\text{m}$ , and picophytoplankton are less than  $2\ \mu\text{m}$ . The ratios involving  $[\text{TPig}]$  were computed to assess the bio-optical role of the chlorophyll and carotenoid pigments. These included  $[\text{TChl } a]/[\text{TPig}]$ ,  $[\text{Chl } bc]/[\text{TPig}]$ ,  $[\text{PSC}]/[\text{TPig}]$  and  $[\text{PPC}]/[\text{TPig}]$ .

$[\text{TChl } a]$  values at inshore station 11 ( $18.11^\circ\text{E}, 32.57^\circ\text{S}$ ) were  $2.9\ \text{mg m}^{-3}$  at 2 m, increasing to  $6.4\ \text{mg m}^{-3}$  at 14 m (Fig. 7a). The  $[\text{Fuco}]/[\text{DP}]$  and  $[\text{Peri}]/[\text{DP}]$  ratios of 0.43 indicated the equal importance of diatoms and dinoflagellates at 2 m, but the increase in the  $[\text{Peri}]/[\text{DP}]$  ratio to 0.64–0.70 revealed the dominance of dinoflagellates at depth (Fig. 7b). The  $[\text{TChl } a]$  comprised 54% of the total pigments,  $[\text{PSC}]/[\text{TPig}]$  ratios were 0.22–0.25, while  $[\text{PPC}]/[\text{TPig}]$  ratios were low in the dinoflagellate community (Fig. 7c).

At inshore station 19 ( $16.68^\circ\text{E}, 29.49^\circ\text{S}$ ),  $[\text{TChl } a]$  values were very high in the upper 10 m ( $22\text{--}36\ \text{mg m}^{-3}$ ,

BENCAL Cruise Report

**Table 12.** The satellite coverage during the BENCAL cruise. The letter codes given with the (nominal) overpass times indicate the likelihood of a high quality matchup: S (s) indicates a good (bad) chance for a high quality SeaWiFS matchup; T (t) indicates a good (bad) chance for a high quality MODIS-T matchup; A (a) indicates a good (bad) chance for a high quality MODIS-A matchup; and M (m) indicates a good (bad) chance for a high quality MERIS matchup. The number of free-fall casts (microNESS, LoCNESS, plus microPRO) during each station is given by  $N_F$ , and the  $L$  and  $T$  codes indicate when LI-COR (plus PNF), and H-TSRB (plus TRIOS) data were collected, respectively.

Station		Overpass Times and Match-up Quality				Casts		Station and Sampling Notes
No.	SDY (Greg.)	SeaWiFS	MODIS-T	MODIS-A	MERIS	$N_F$	L T	
1	278 (05Oct02)	1045 S	0918 T	1154 a	0836 m	5		
2	278 (05Oct02)			1331 A		14	L	
3	279 (06Oct02)	0948 s	0823 t		0805 M	17	L	
4	279 (06Oct02)	1126 s		1236 A		13	L	
5	279 (06Oct02)			1236 A		32	L	
6	280 (07Oct02)					47		
7	280 (07Oct02)	1029 S	0905 T			95	L	
8	280 (07Oct02)			1319 a		79	L T	
9	280 (07Oct02)					29	L	Q-factor
10	281 (08Oct02)	0933 s	0810 t		0842 m	59		
11	281 (08Oct02)	1110 s	0948 t		0842 m	40	L	
12	281 (08Oct02)			1224 A		42	L	
13	281 (08Oct02)					31	L	Q-factor
14	282 (09Oct02)		0853 t		0810 m	5		Overcast
15	282 (09Oct02)	1054 S				20	L	SeaWiFS also at 1013
16	282 (09Oct02)			1307 a		27	L	Overcast
18	283 (10Oct02)		0935 T			49	L T	Very high $C_a$
19	283 (10Oct02)	1054 s		1213 a		44	L T	Very high $C_a$
20	283 (10Oct02)					21	L T	Very high $C_a$
21	283 (10Oct02)					10	L T	Q-factor, Low $C_a$
22	284 (11Oct02)	0957 s	0840 T		0847 m	32		Low $C_a$
23	284 (11Oct02)	1135 s		1255 A		7	L T	Low $C_a$
24	284 (11Oct02)					2	L	Low $C_a$
25	285 (12Oct02)	1038 S	0923 T	1201 a	0816 M	8		Very low $C_a$
26	286 (13Oct02)	0942 s	0828 t			37		Very low $C_a$
27	286 (13Oct02)	1119 S		1243 A		11	L T	Very low $C_a$
28	287 (14Oct02)					10	L	
29	287 (14Oct02)	1022 S	0911 T		0852 m	32		
30	287 (14Oct02)			1326 a		14	L	
31	287 (14Oct02)					22		Q-factor
32	288 (15Oct02)		0816 t		0821 M	20		
33	288 (15Oct02)	1103 S	0954 t			24	L	
34	288 (15Oct02)			1231 A		23	L T	
35	288 (15Oct02)					20	L T	Q-factor
36	289 (16Oct02)		0859 T			18		
37	289 (16Oct02)	1007 S		1313 A		27		Case-2?
38	289 (16Oct02)			1313 A		27	L T	
39	290 (17Oct02)		0942 t			23	L T	Overcast
40	290 (17Oct02)	1048 S		1218 A		7	T	
41	290 (17Oct02)					16	L	Case-2?
42	295 (22Oct02)	0920 s	0823 T		0803 M	3	L T	<i>Ecklonia</i> small boat
43	295 (22Oct02)	1058 S		1236 A		3		<i>Ecklonia</i> small boat

Note: the duplicate entries for MERIS on SDY 281 and MODIS-A on SDY 289 indicate the AOP sampling, for the two stations involved on each day, temporally overlap the given overpass times to within 1 h.

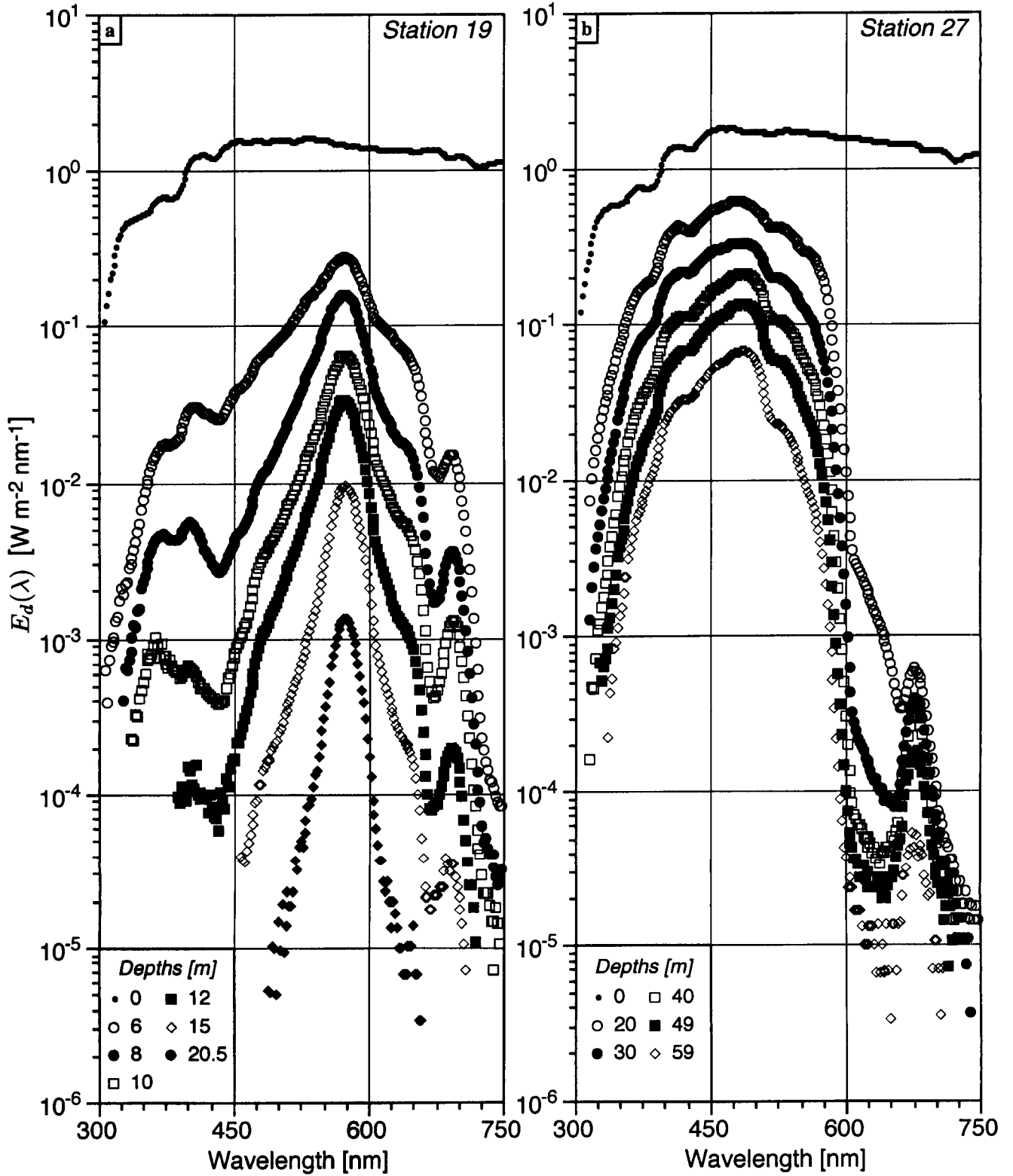


**Fig. 4.** Downwelling irradiance spectra,  $E_d(z, \lambda)$ , at several depths as indicated, for a) station 19 (high chlorophyll *a* concentration), and b) station 27 (low chlorophyll *a* concentration). The vertical scale is logarithmic.

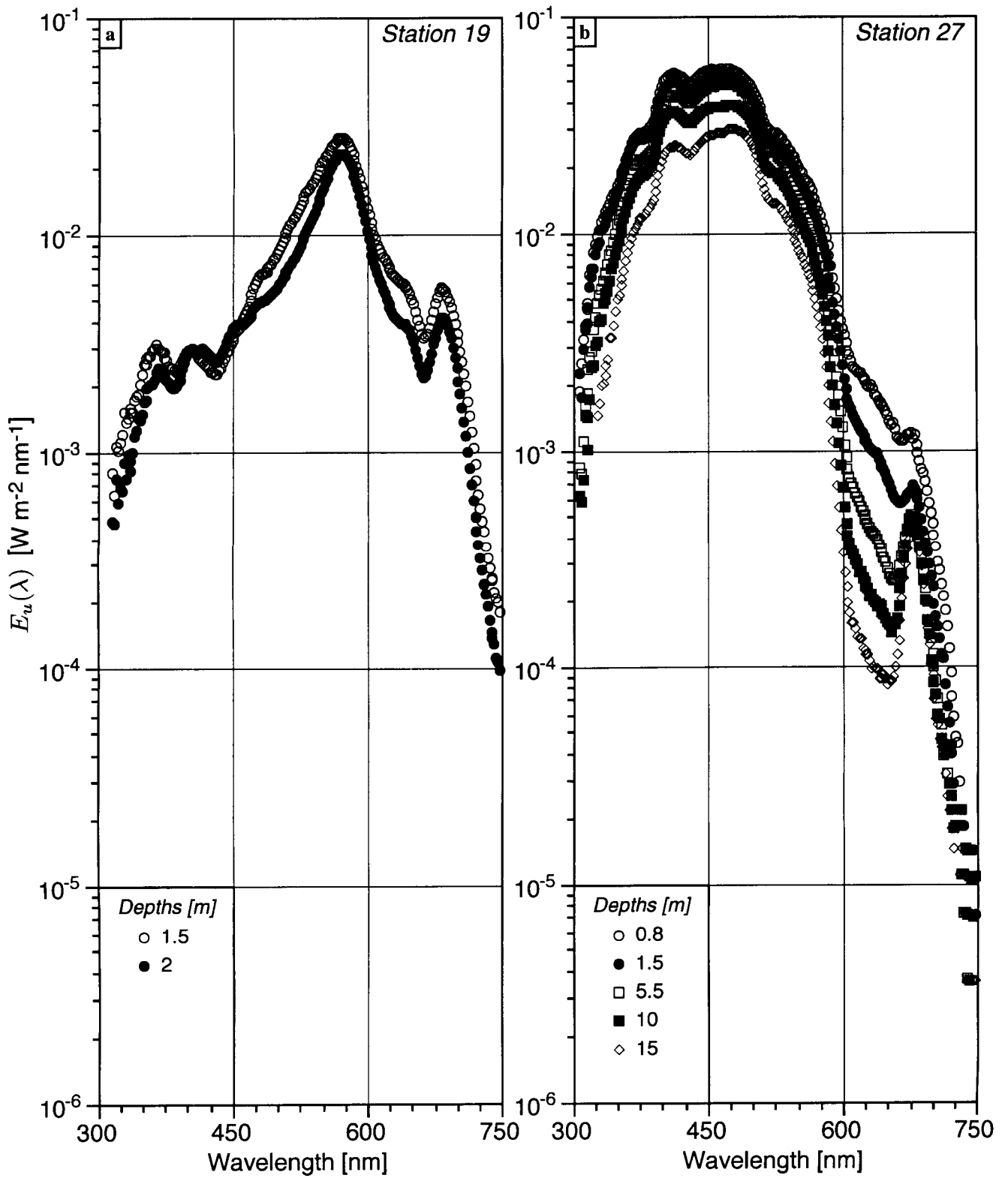


**Fig. 5.** As in Fig. 4, but for upwelling irradiance,  $E_u(z, \lambda)$ . Note, the logarithmic scales are not the same as in Fig. 4.

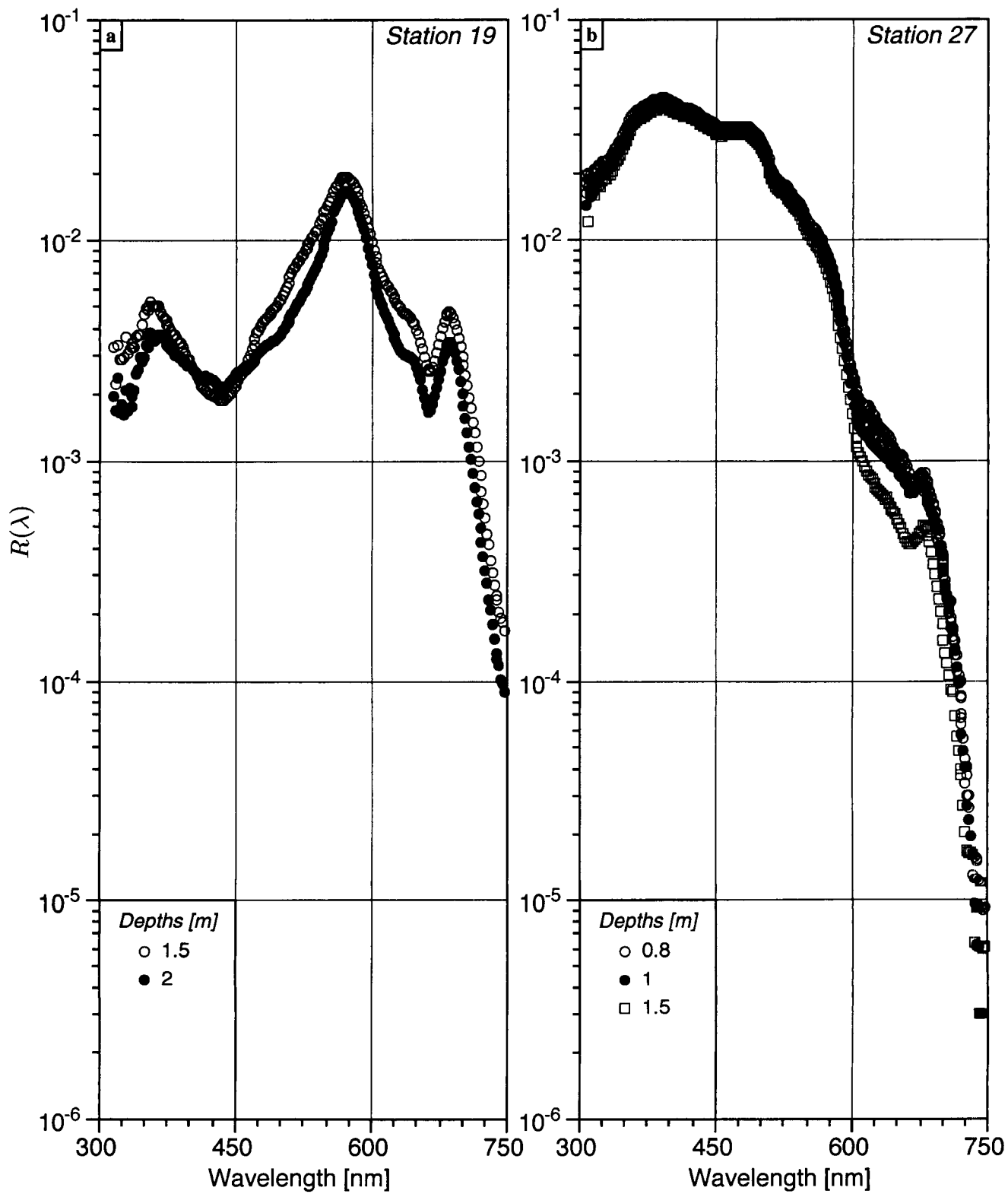


**Fig. 6.** Reflectance spectra (see text) for the upper layer for the same stations and data presented in Figs. 4 and 5.

**Table 13.** The chlorophyll, carotenoid, pigment sums, and pigment ratios shown with their symbols, names, and calculation formulae (if applicable). The pigment symbols, which are used to indicate the concentration of the pigment, are patterned after the nomenclature established by the Scientific Committee on Oceanographic Research (SCOR) Working Group 78 (Jeffrey et al. 1997). Abbreviated forms for the carotenoid names are shown in parentheses. Three plankton proportion factors are shown: the microplankton, nanoplankton, and picoplankton, which are indicated as [mPF], [nPF], and [pPF], respectively. The [mPF] is separated into diatoms, [Fuco]/[DP], and dinoflagellates, [Peri]/[DP]; these two groups need to be separated, because they are each independently important in the Benguela system. Some pigment sums and ratios are not discussed explicitly in the text, but are included here for completeness.

Symbol	Pigment	Calculation
[Chl a]	Chlorophyll a (plus allomers and epimers)	
[Chl b]	Chlorophyll b	
[Chl c <sub>1</sub> ]	Chlorophyll c <sub>1</sub>	
[Chl c <sub>2</sub> ]	Chlorophyll c <sub>2</sub>	
[Chl c <sub>3</sub> ]	Chlorophyll c <sub>3</sub>	
[Chlide a]	Chlorophyllide a	
[DVChl a]	Divinyl chlorophyll a	
[DVChl b]	Divinyl chlorophyll b	
[TChl a]	Total chlorophyll a	[Chlide a] + [DVChl a] + [Chl a]
[TChl b]	Total chlorophyll b	[DVChl b] + [Chl b]
[TChl c]	Total chlorophyll c	[Chl c <sub>1</sub> ] + [Chl c <sub>2</sub> ] + [Chl c <sub>3</sub> ]
[Allo]	Alloxanthin (Allo)	
[But]	19'-Butanoyloxyfucoxanthin (But-fuco)	
[Caro]	Carotenes	[ββ-car] + [βε-car]
[Diad]	Diadinoxanthin (Diadino)	
[Diato]	Diatoxanthin (Diato)	
[Fuco]	Fucoxanthin (Fuco)	
[Hex]	19'-Hexanoyloxyfucoxanthin (Hex-fuco)	
[Peri]	Peridinin (Perid)	
[Zea]	Zeaxanthin (Zea)	
[Chl bc]	The sum of chlorophylls b and c	[TChl b] + [TChl c]
[PPC]	Photoprotective carotenoids	[Allo] + [Diad] + [Diato] + [Zea] + [Caro]
[PSC]	Photosynthetic carotenoids	[But] + [Fuco] + [Hex] + [Peri]
[PSP]	Photosynthetic pigments	[PSC] + [TChl a] + [TChl b] + [TChl c]
[TAcc]	Total accessory pigments	[PPC] + [PSC] + [TChl b] + [TChl c]
[TPig]	Total pigments	[TAcc] + [TChl a]
[DP]	Total diagnostic pigments	[PSC] + [Allo] + [Zea] + [TChl b]
[TAcc]/[TChl a]	Total accessory pigments to total chlorophyll a	[TAcc]/[TChl a]
[TChl a]/[TPig]	Total chlorophyll a to total pigments	[TChl a]/[TPig]
[Chl bc]/[TPig]	Sum of chlorophylls b and c to total pigments	[Chl bc]/[TPig]
[PPC]/[TPig]	Photoprotective carotenoids to total pigments	[PPC]/[TPig]
[PSC]/[TPig]	Photosynthetic carotenoids to total pigments	[PSC]/[TPig]
[PSP]/[TPig]	Photosynthetic pigments to total pigments	[PSP]/[TPig]
[mPF]	Microplankton proportion factor†	([Fuco] + [Peri])/[DP]
[nPF]	Nanoplankton proportion factor†	([Hex] + [But] + [Allo])/[DP]
[pPF]	Picoplankton proportion factor†	([Zea] + [TChl b])/[DP]

† As a group, also considered as indices or macrovariables.

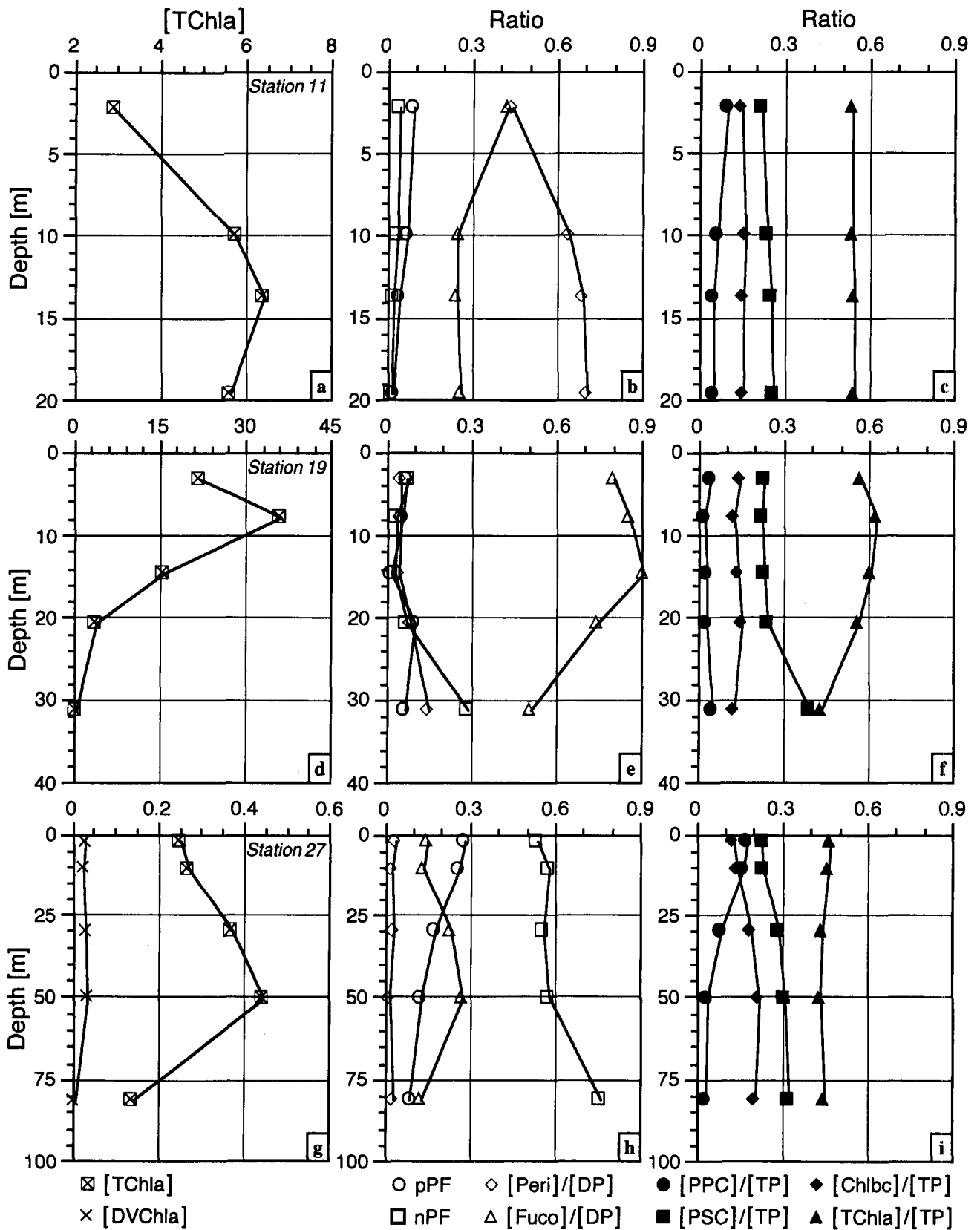


Fig. 7. [TChl *a*] and [DVChl *a*] (in units of milligrams per cubic meter), diagnostic ratios, and pigment ratios for station 11 (a–c, respectively), station 19 (d–f, respectively), station 27 (g–i, respectively). The water depths for the three stations were 38 m, 127 m, and 1,900 m, respectively.

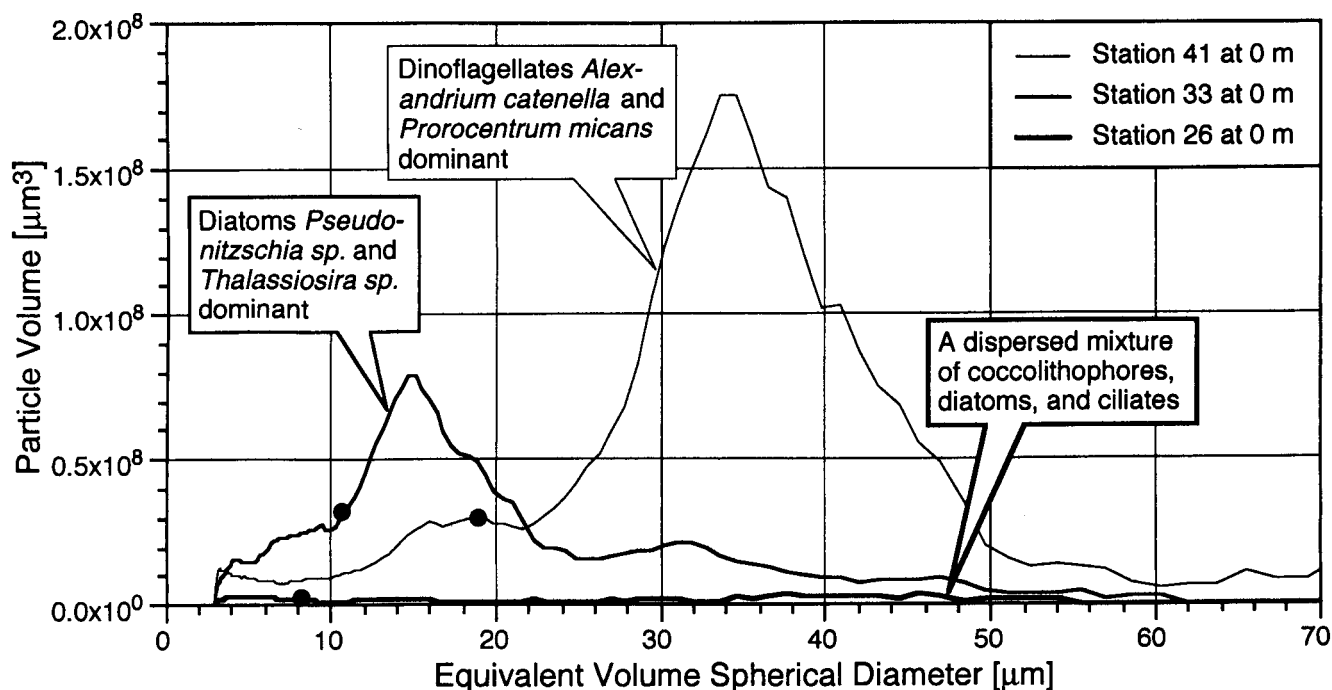


Fig. 8. A plot of the volume PSDs from three sample stations: oligotrophic offshore station 26, diatom-dominated inshore station 33, and dinoflagellate-dominated inshore station 41. Microscopic plankton count data and cell volume calculations are used to identify peaks in the Coulter-measured PSD. Closed circles indicate the effective diameter,  $2r_{\text{eff}}$ , as per (3).

Fig. 7d), with a sharp decline at depth to  $0.31 \text{ mg m}^{-3}$  at 31 m. Diatoms accounted for most of the phytoplankton biomass at this station,  $[\text{Fuco}]/[\text{DP}] = 0.8\text{--}0.9$ , with  $[\text{TChl } a]$  contributing 57–63% and  $[\text{PSC}]$  22–24% to the total pigment pool in the upper 20 m (Figs. 7e and 7f). At 31 m, the  $[\text{nPF}]$  ratio had increased to 0.28, with the  $[\text{PSC}]/[\text{TPig}]$  ratio increasing to 0.39 and the  $[\text{TChl } a]/[\text{TPig}]$  declining to 0.43 (Figs. 7e and 7f).  $[\text{PPC}]/[\text{TPig}]$  ratios at station 19 were very low at less than 0.05.

In contrast to the (comparatively shallow) inshore environment, the offshore stations in (deep) blue water had low values of phytoplankton biomass.  $[\text{TChl } a]$  values of  $0.25 \text{ mg m}^{-3}$  were measured at 2 m at offshore station 27 ( $14.42^\circ\text{E}, 30.54^\circ\text{S}$ ), with a subsurface  $[\text{TChl } a]$  value of approximately  $0.44 \text{ mg m}^{-3}$  at 50 m (Fig. 7g). Divinyl chlorophyll *a* was detected in low concentration at this station, indicating the presence of tiny prochlorophyte cells (note the negligible presence of divinyl chlorophyll *a* for stations 11 and 19.). Diagnostic pigment ratios confirmed that nanophytoplankton dominated the community, the  $[\text{nPF}]$  ratios ranged from 0.54–0.76, while the picophytoplankton were also prominent in the upper 10 m, the  $[\text{pPF}]$  ratios ranged from 0.26–0.28 (Fig. 7h). In this community, the  $[\text{TChl } a]/[\text{TPig}]$  ratios were about 0.45–0.47, the  $[\text{PSC}]/[\text{TPig}]$  ratios ranged from 0.23–0.32, while the proportion of  $[\text{PPC}]$  in the total pigment pool was 16–18% in the upper 10 m (Fig. 7i).

In summary, the preliminary pigment data indicated the occurrence of high phytoplankton biomass in the upper water column at inshore stations where diatoms or dinoflagellates (greater than  $10 \mu\text{m}$ ) were the dominant phytoplankton groups. In these populations, total chlorophyll *a* constituted a high proportion (up to 60%) of the total pigment pool. Offshore stations were characterized by low biomass and communities dominated by small (less than  $10 \mu\text{m}$ ) nano- and picoplankton cells. The proportion of total chlorophyll *a* in the total pigment pool was lower (45%), while photosynthetic carotenoids were significant in nanoplankton, and photoprotective pigments more prominent in the picoplankton.

### 7.3 Inherent Optical Properties

Three example stations, displaying notable differences in algal assemblage structure, are used to demonstrate preliminary data from all IOP instruments:

- 26 An offshore low biomass station with no dominant algal group (surface  $C_a = 0.18 \text{ mg m}^{-3}$ ),
- 33 An inshore high biomass station dominated by diatom species (surface  $C_a = 12.44 \text{ mg m}^{-3}$ ), and
- 41 An inshore intermediate biomass station dominated by dinoflagellates (surface  $C_a = 5.67 \text{ mg m}^{-3}$ ).

Figure 8 shows surface particle size distribution data for the three stations—peaks in the particle volume distri-

bution derived from the Coulter Multisizer have been identified as dominant algal groups using microscope counts. There is an increase in average particle size from the oligotrophic algal community (station 26), through the diatom-dominated community (station 33), to the dinoflagellate-dominated community (station 41). Note the disparity between chlorophyll *a* concentration and total particle volume for stations 33 and 41—the sample dominated by dinoflagellates has approximately twice the particle volume despite having less than half the chlorophyll *a* concentration.

Figure 9 presents the discrete surface measurements for total absorption  $a_T$ , total attenuation  $c_T$ , and total scattering  $b_T$  from the AC-9, in addition to spectrophotometric measurements of particulate absorption,  $a_p$ , and yellow substance absorption,  $a_y$ . A direct comparison can be made between total absorption as measured by the AC-9, and summed total absorption from spectrophotometrically measured  $a_p$  and  $a_y$ . Although the comparison is not good between the two  $a_T(440)$  measurements for low biomass station 26 (the  $a_T(440)$  value from AC-9 is more than 50% higher), the two higher biomass stations (33 and 41) show reasonable agreement between the three modes of measurement with maximal 10% difference across the spectrum. Discrepancies at low biomass between the modes of absorption measurement requires further investigation in the context of the whole data set.

The three stations exhibit marked variations in absorption and scattering properties, particularly with respect to biomass. Stations 33 (diatom dominated and surface  $C_a = 12.44 \text{ mg m}^{-3}$ ) and 41 (dinoflagellate dominated and surface  $C_a = 5.67 \text{ mg m}^{-3}$ ) display similar values of particulate absorption, despite station 33 having a chlorophyll *a* concentration more than twice as high. Station 41 also displays an attenuation coefficient approximately 50% higher than station 33 at 440 nm, despite having similar  $a_p(440)$  values, indicating the increased presence of non-chlorophyllous particles at station 41. Additionally, the yellow substance absorption at station 41 is about 3.5 times higher than at station 33, the effects of which are displayed in the shape of the AC-9 absorption spectra.

Figure 10 shows profiles of total absorption  $a_T(\lambda)$  and attenuation  $c_T(\lambda)$  (water corrected) derived from the AC-9, and total backscattering  $b_{b_T}(\lambda)$  (water included) derived from the HydroSCAT-6. Station 26 displays a broad subsurface maximum in absorption, attenuation, and backscattering at approximately 25 m. The total backscattering values below about 70 m appear to be approximately the same magnitude as those of seawater†, which indicates a paucity of scattering particles. Stations 33 and 41 both display enhanced surface backscattering values, concomitant with the increased surface biomass, absorption, and

attenuation values at these stations. The backscattering data at station 41, with significantly higher surface values ( $b_{b_w}(442) \approx 0.02 \text{ m}^{-1}$ ) than 33 despite a lower chlorophyll *a* concentration, provide further evidence of the presence of non-chlorophyllous particles at this location.

## 7.4 Particulate Absorption

By using the LI-1800 UW instrument implemented with an integrating sphere (Sects. 5.3 and 5.3.2), the absorption spectra of the total particulate retained on GF/F filters were determined in reference to a properly hydrated blank filter. The measured transmission was converted into the absorption coefficient,  $a_p(\lambda)$ , by accounting for the filtered volume and appropriate conversion factors (Mitchell et al. 2002). Often, but not systematically, duplicate samples were analyzed and one of the filters was then processed to remove its pigments (the other was kept for further HPLC analysis).

The Kishino bleaching technique (a 100% methanol extraction) was employed. The residual (detrital) absorption of the depigmented filter is measured as above, and provides  $a_d(\lambda)$ . By difference, the phytoplankton absorption is obtained as  $a_p(\lambda) = a_T(\lambda) - a_d(\lambda)$ . When the chemical bleaching technique has not been used, the (numerical) deconvolution technique (Bricaud and Stramski 1990) can be applied. The comparison of the two techniques generally demonstrates a good agreement.

All of the  $a_p(\lambda)$  spectra determined during the BEN-CAL cruise are displayed in Fig. 11, with the main intent of showing the extremely wide range of values observed in the various locations visited. Despite the large variety in sampling environments, the measurements were possible (and comparable in terms of accuracy), because the volumes of water filtered were varied (in a 1:12 ratio), according to the expected pigment content (via optical measurements, or visual observation, or spectrophotometric quick determinations).

Without entering into details, another preliminary remark is worth mentioning: in general, these spectra are strongly featured, with prominent peaks and a steep decrease toward the ultraviolet (UV) domain. Such patterns, similar to those that can be observed for pure cultures, demonstrate that the influence of detritus or other terrigenous particles was minimal, and thus that most of the stations were located in true Case-1 waters.

## 7.5 FRRF

The FRRF, which was used in the internally self-logging mode, was deployed from the stern crane near the starboard quarter (outboard reach 4–6 m) using a Kevlar non-conducting line. There were 47 FRRF profiles (Tables 1 and 9) executed at 37 of the 41 *Africana* stations. Generally, the instrument performed fault free, although  $F_m$

† The data presented here show  $b_{b_T}(442) \approx 0.0026 \text{ m}^{-1}$  and Table 3.8 in Mobley (1994) indicates  $b_{b_w}(440) \approx 0.0025 \text{ m}^{-1}$ , where the latter is the backscattering for seawater alone.

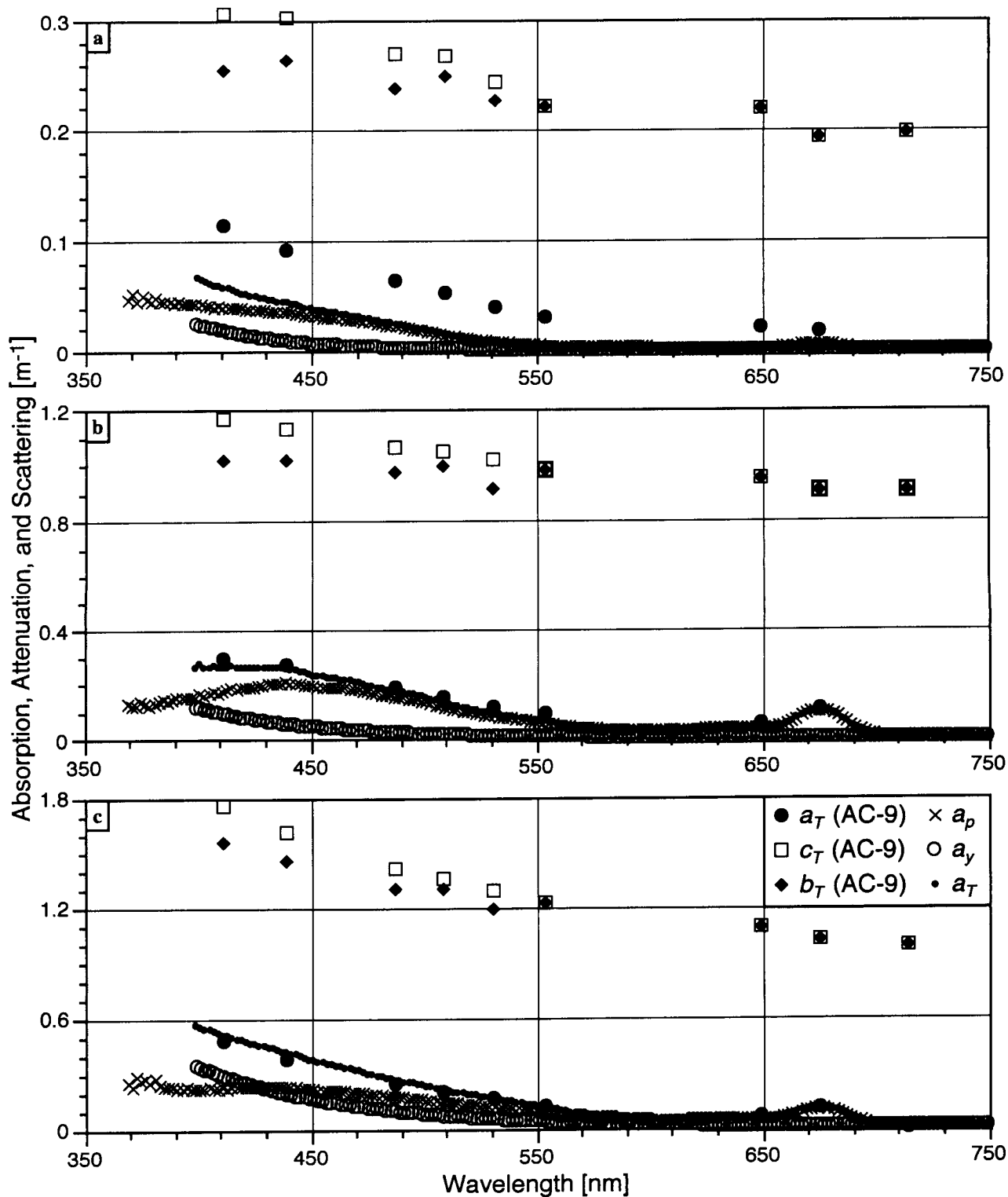


Fig. 9. Spectra of total absorption (large solid circles), attenuation (open squares), and scattering (solid diamonds) from bench-top AC-9 measurements, in addition to particulate absorption (crosses), yellow substance absorption (open circles), and the sum of these two parameters from bench-top spectrophotometric measurements (small solid circles). The analyses are from surface sampling for the following example stations: a) 26, b) 33, and c) 41.

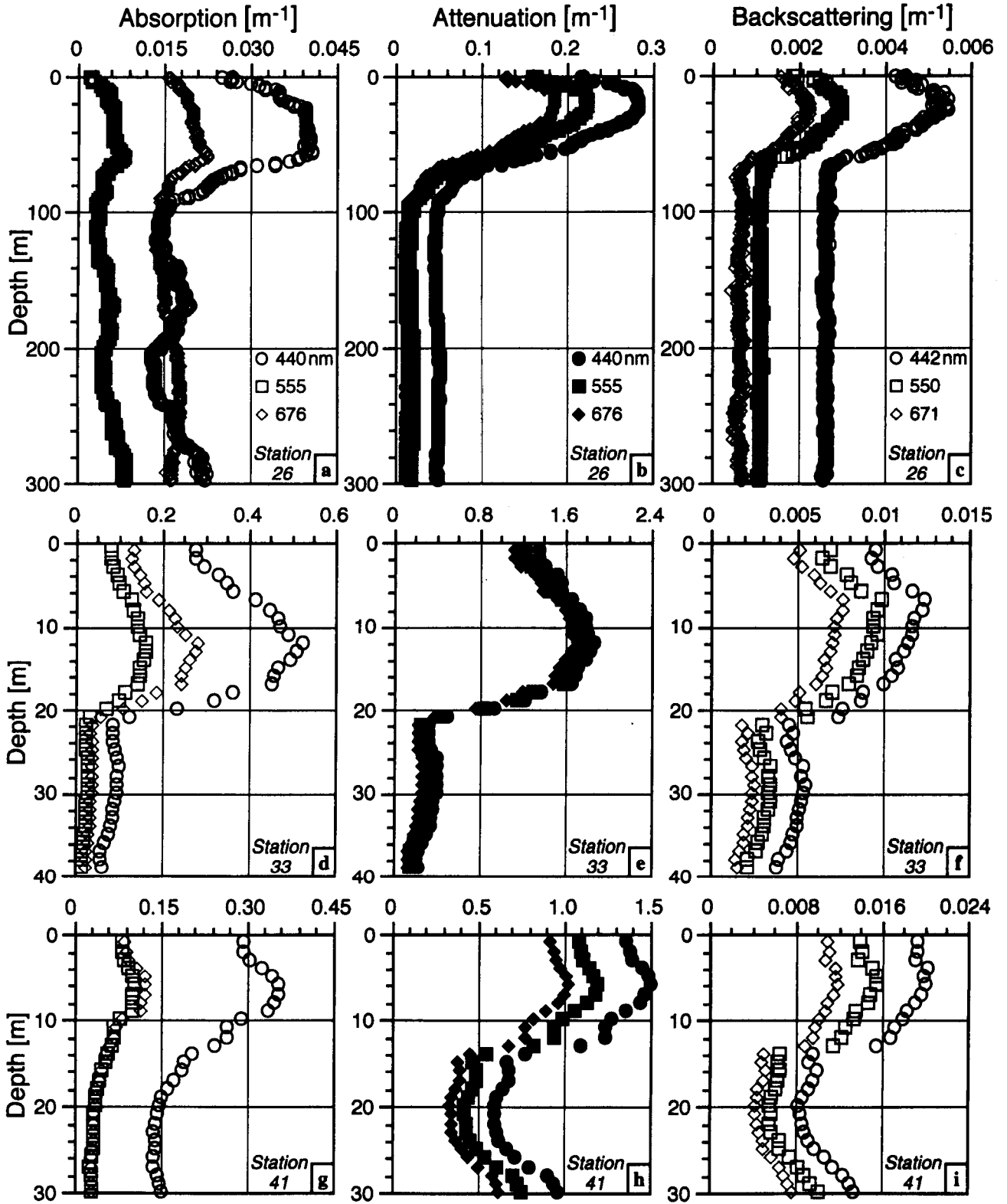


Fig. 10. Vertical profiles of  $a_T(\lambda)$ ,  $c_T(\lambda)$ ,  $b_{bT}(\lambda)$  for three different stations: 26 (a-c), 33 (d-f), and 41 (g-i), respectively.

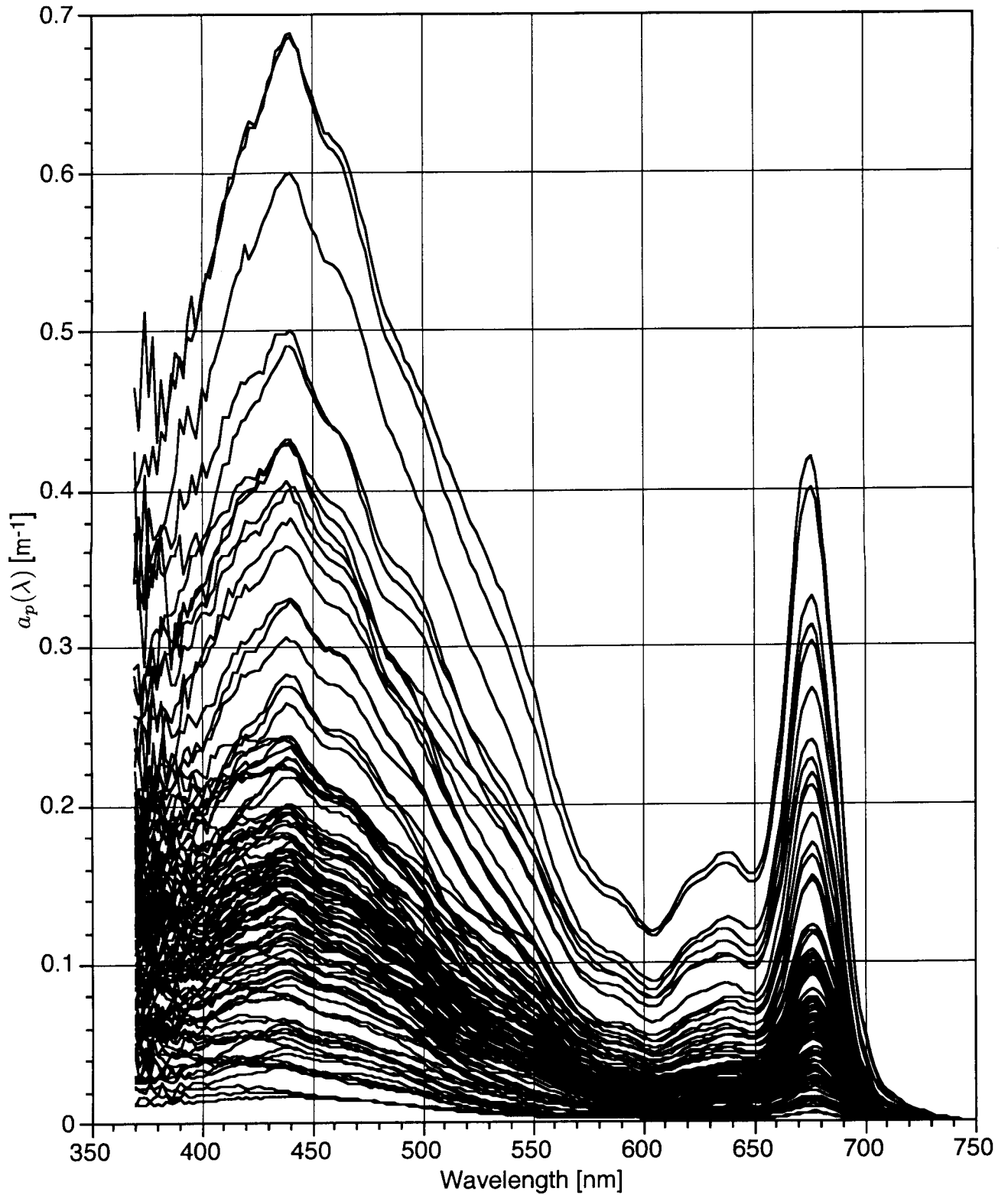


Fig. 11. The absorption coefficient of particulate matter,  $a_p(\lambda)$ , between 370–750 nm (in 2 nm increments). The value of  $a_p(750)$  is supposed to equal zero, so all other  $a_p(\lambda)$  values are shifted accordingly.

reached saturation values ( $F_m > 60$  arbitrary units) in waters with very high pigment (chlorophyll) concentrations, at stations 18–21 on 20 October and stations 33–35 on 15 October; in these cases, the values of  $F_v/F_m$  (PQE) were corrupted for the depth region (the surface layer) with saturated  $F_m$  values. Examples of FRRF profiles from three stations in different coupled physical and biological structures are presented in Figs. 12–14 (corresponding to stations 27, 30, and 32, respectively, which are geolocated in Fig. 2).

For station 27, the temperature structure (Fig. 12a) indicates a basically unstratified system, with a thermocline from the surface to 110 m, although there are several temperature discontinuities and a hint of a shallow surface layer above 7 m ( $T = 17.2^\circ\text{C}$ ). Chlorophyll fluorescence ( $F_mD$  and  $F_mL$ , Fig. 12b) show an  $F_m$  maximum at about 45 m ( $F_mD = 10$  arbitrary units) corresponding to the depth of one of the temperature discontinuities. The maximum (layer unquenched) values of  $F_vD/F_mD$  and  $F_vL/F_mL$  are very low in the surface phytoplankton layer to 45 m ( $F_vD/F_mD = 0.25$ ) and higher ( $F_vD/F_mD = 0.42$ ) in the deeper portion of the water column ( $z > 45$  m). Figure 12d shows the product of PAR ( $E^{\text{PAR}}$ ) and  $F_vL/F_mL$ , which represents the scaled productivity, has an incoherent structure corresponding to the multiple physical strata, each with phytoplankton assemblages of differing physiology and different light and nutrient adaptation.

The temperature profile for station 30 (Fig. 13a) shows a nearly constant temperature layer extending to about 7 m ( $T = 16.5^\circ\text{C}$ ), a slight decrease to 15 m ( $T = 16.4^\circ\text{C}$ ) and a sharp thermocline to 21 m ( $T = 15.3^\circ\text{C}$ ). There are two very high subsurface chlorophyll fluorescence maxima (Fig. 13b), at 20 m ( $F_mD = 25$ –30 arbitrary units) and at 24 m ( $F_mD = 45$  arbitrary units). The PQE profiles (Fig. 13c) have different values of maximum PQE (saturated) for each layer: 0.25 at 7 m; 0.39 at 15 m; 0.415 at 20 m; 0.45 at 25 m, and deeper. Again, because of the complex physical structure and differently-adapted phytoplankton physiology for each layer, the curve showing the product of  $E^{\text{PAR}}$  and  $F_vL/F_mL$  (Fig. 13d) is difficult to interpret with any certainty, but could be used to calculate integrated primary production.

The temperature structure for station 32 (Fig. 14a) shows the classical isothermal surface layer ( $T = 14.6^\circ\text{C}$ ) to 29 m and a sharp thermocline to approximately 35 m ( $T = 11.5^\circ\text{C}$ ). The surface layer chlorophyll fluorescence profile (Fig. 14b) shows the biomass maximum is in the surface layer and very high ( $F_m > 35$ ), although there is fluorescence quenching from the surface to 7–8 m. The PQE profiles (Fig. 14c) also show quenching in the surface layer to approximately 10 m and a maximum  $F_v/F_m$  value of 0.46 (only moderate value).

For all the stations, values of  $F_m$  range from 7 (arbitrary units) offshore to 60 (saturated) and maximum PQE (unquenched value) ranged from 0.25 (dimensionless,

range 0.2–0.7) in the oligotrophic surface waters offshore ( $C_a \approx 0.2 \text{ mg m}^{-3}$ ) to 0.57 in the inshore, nutrient-rich waters ( $C_a \approx 7.0 \text{ mg m}^{-3}$ ). The cross-section of photosystem 2 ( $\sigma\text{PS2}$ ) varied from 700 ( $10$ – $20 \text{ m}^2 \text{ quanta}^{-1}$ ) in the oligotrophic surface waters to 350 ( $10$ – $20 \text{ m}^2 \text{ quanta}^{-1}$ ) in the productive areas. This inverse relationship is not always the case.

A preliminary analysis of the values of maximum PQE and pigment composition,  $[\text{Chl } a]/[\text{TPig}]$ , determined using the 12 samples collected for SeaHARRE-2 (the only samples analyzed to date), show good correlations ( $R^2 = 0.72$ ). For  $\sigma\text{PS2}$ , the correlations with  $[\text{Chl } a]/[\text{TPig}]$  were also significant ( $R^2 = 0.69$ ) with a negative slope.

## 7.6 Primary Production

Daily primary production was measured at five BENCAL stations. The primary production integrated through the euphotic zone ranged from 0.62–5.92  $\text{gC m}^{-2} \text{ d}^{-1}$  (Table 14). The highest productivity was found at station 17 in water of  $13.6^\circ\text{C}$ , whereas the lowest production was at station 28 in warmer water of  $16.4^\circ\text{C}$ . Fractionation studies showed a lower percentage contribution by microflagellates to total productivity (10–26%) at the three inshore stations (1, 10, and 17) and a higher contribution (35–63%) at the two offshore stations (28 and 32).

**Table 14.** The daily and vertically-integrated primary production measured during the BENCAL cruise at five stations (the units are  $\text{gC m}^{-3} \text{ d}^{-1}$  and  $\text{gC m}^{-2} \text{ d}^{-1}$ , respectively).

Station No.	Station SDY (Greg.)	Depth [m]	Production	
			Daily	Integ.
1	278 (05Oct02)	0.0	0.077	0.91
		2.0	0.139	
		3.2	0.102	
		4.5	0.094	
		12.5	0.011	
10	281 (08Oct02)	0.0	0.263	3.40
		2.2	0.341	
		4.5	0.333	
		7.3	0.311	
		13.5	0.028	
17	283 (10Oct02)	0.0	0.937	5.92
		2.3	0.845	
		4.8	0.712	
		9.5	0.108	
28	287 (14Oct02)	0.0	0.018	0.62
		3.0	0.046	
		7.2	0.040	
		22.0	0.007	
32	288 (15Oct02)	0.0	0.080	2.02
		1.9	0.243	
		3.8	0.240	
		13.5	0.017	

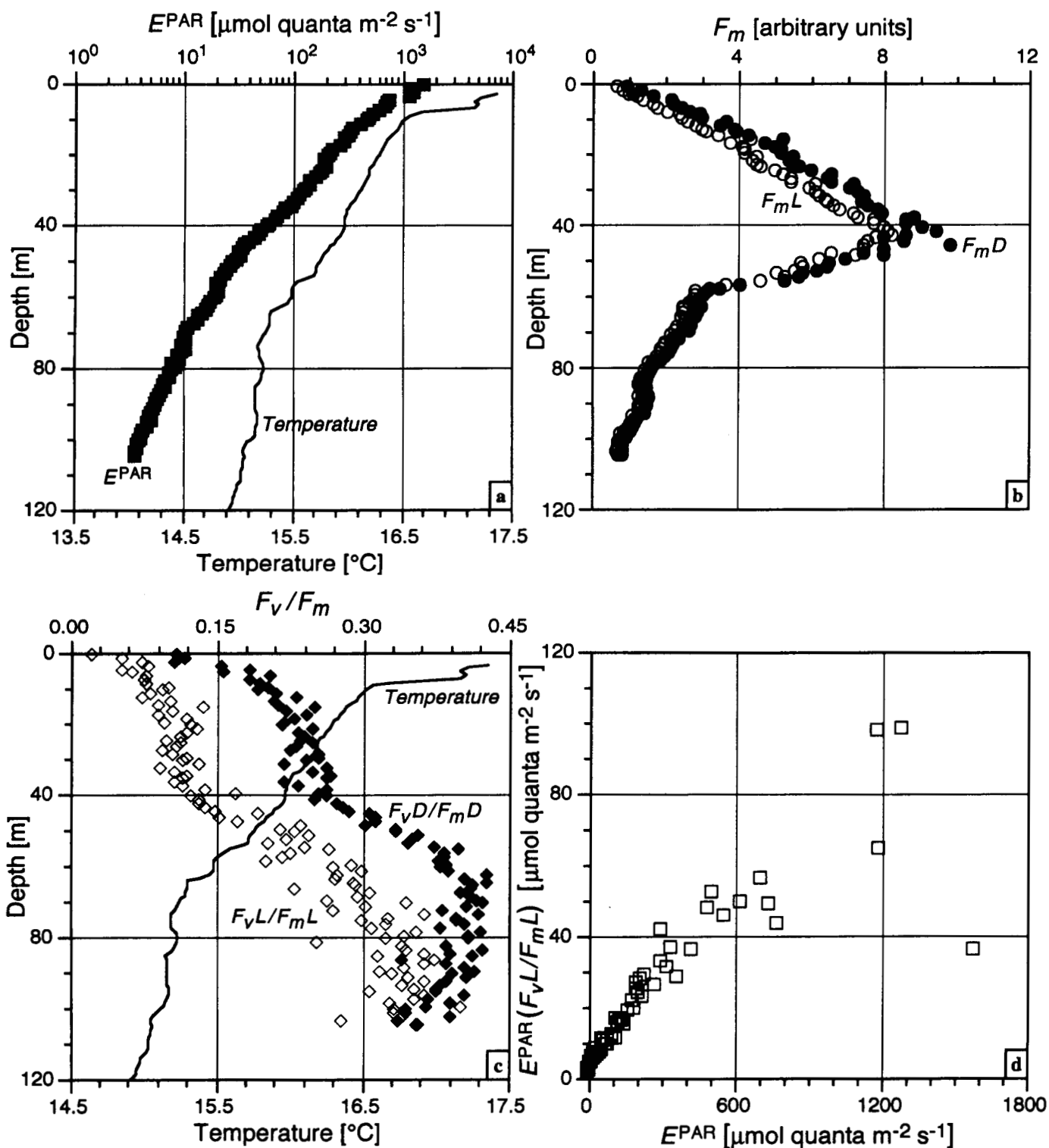


**Fig. 12.** FRRF profiles to 110 m at station 27 on SDY 286 (13Oct02): a)  $E^{PAR}$  (solid squares) and seawater temperature (solid line); b) fluorescence  $F_mD$  (solid circles) and  $F_mL$  (open circles); c)  $F_vD/F_mD$  (solid diamonds),  $F_vL/F_mL$  (open diamonds), and seawater temperature (solid line); d) the product of  $E^{PAR}$  and  $F_vL/F_mL$  versus  $E^{PAR}$  (open squares).

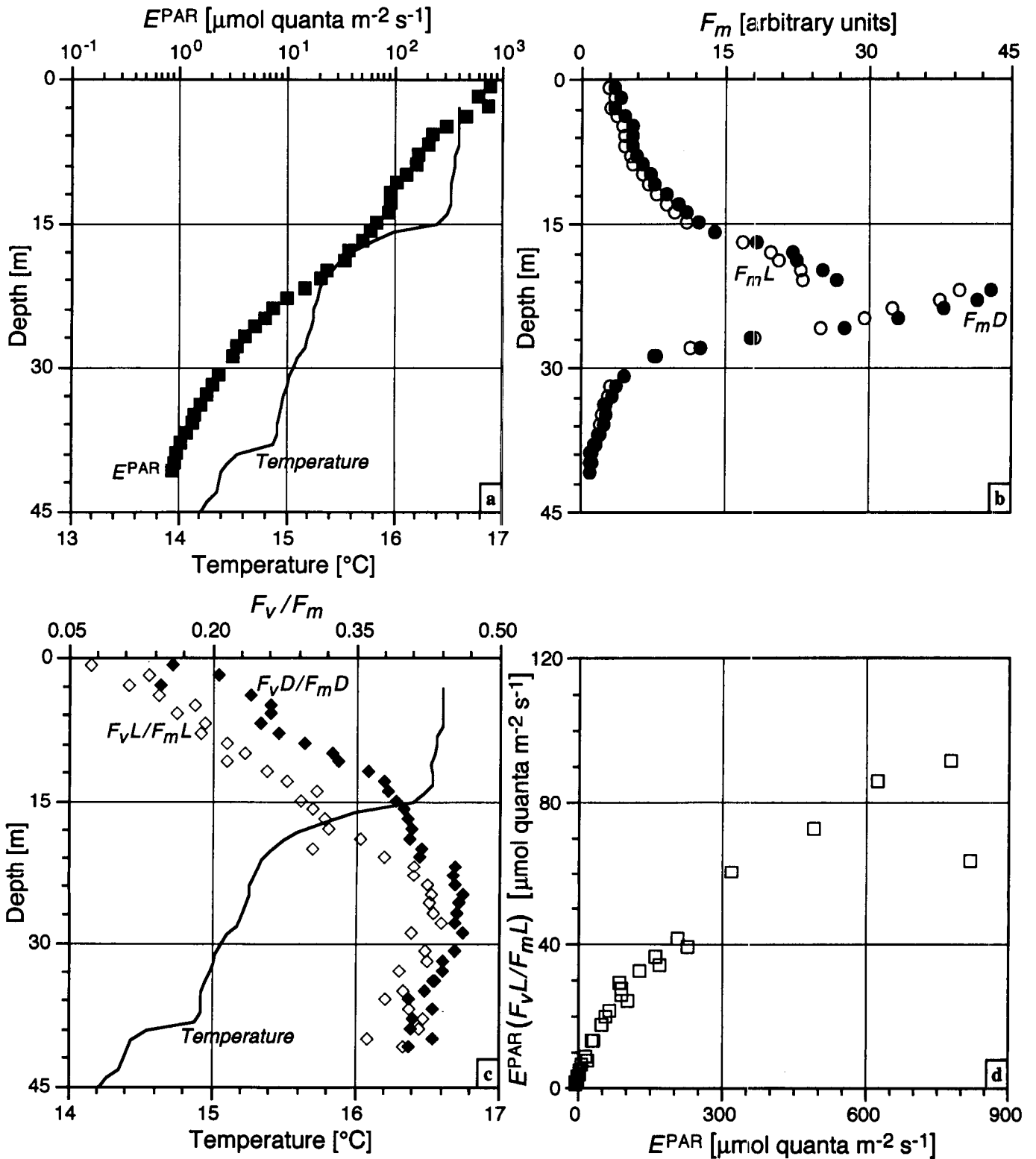


**Fig. 13.** FRRF profiles to 43 m at station 30 on SDY 287 (14Oct02): a)  $E^{PAR}$  (solid squares) and seawater temperature (solid line); b) fluorescence  $F_{mD}$  (solid circles) and  $F_{mL}$  (open circles); c)  $F_{vD}/F_{mD}$  (solid diamonds),  $F_{vL}/F_{mL}$  (open diamonds), and seawater temperature (solid line); d) the product of  $E^{PAR}$  and  $F_{vL}/F_{mL}$  versus  $E^{PAR}$  (open squares).

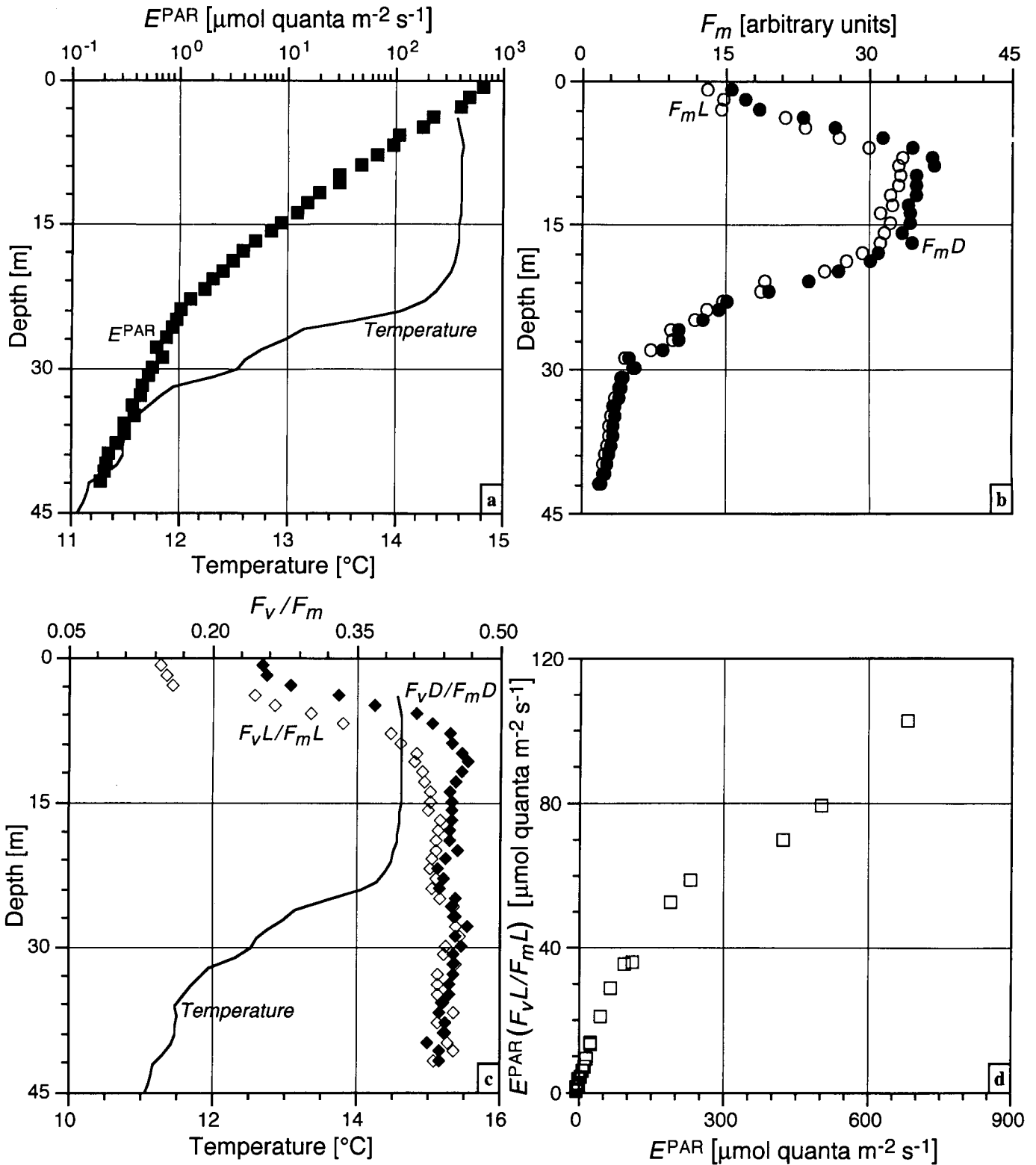


**Fig. 14.** FRRF profiles to 42 m at station 32 on SDY 288 (15Oct02): a)  $E^{\text{PAR}}$  (solid squares) and seawater temperature (solid line); b) fluorescence  $F_mD$  (solid circles) and  $F_mL$  (open circles); c)  $F_vD/F_mD$  (solid diamonds),  $F_vL/F_mL$  (open diamonds), and seawater temperature (solid line); d) the product of  $E^{\text{PAR}}$  and  $F_vL/F_mL$  versus  $E^{\text{PAR}}$  (open squares).

## 8. SUMMARY AND DISCUSSION

The accomplishments of the BENCAL cruise were considerable, although these are only the prelude to the scientific outcomes that are anticipated once the data analyses and interpretations are completed. The list of activities completed successfully is long for such a relatively short cruise, aided by the fine sunny weather, the wide dynamic range of trophic conditions and chlorophyll concentrations of the Benguela ecosystem, the availability of the FRS *Africana*, and the superb support from the captain, officers, and crew.

For the 14 days at sea on *Africana*, *in situ* optical instruments were deployed for all but the first day (4 October). A total of 41 stations were occupied from 5–17 October. There were 39 CTD stations with water samples for pigment profiles from all but 6 casts; 5 casts were for surface water for the pigment intercalibration experiment (SeaHARRE-2), and 1 cast was for a CTD profile only (no water).

Pigments were measured on board by spectrophotometry and filtered samples, frozen in liquid nitrogen, for analysis ashore by HPLC. Additional surface water samples were taken (by pump or bucket) simultaneously with the optical casts during satellite overpasses (filtered and frozen for measurement by HPLC). At 12 stations, 24 surface water samples were filtered for SeaHARRE-2 (triplicate samples for 8 participants). Chlorophyll *a* concentrations (33 stations in addition to SeaHARRE-2) ranged from 0.2–25.7 mg m<sup>-3</sup>, and were distributed rather homogeneously: 8 from 0.2–0.9 mg m<sup>-3</sup>, 11 from 1–5 mg m<sup>-3</sup>, 8 from 5–10 mg m<sup>-3</sup>, 4 from 10–20 mg m<sup>-3</sup>, and 2 greater than 20 mg m<sup>-3</sup>.

The LI-COR spectroradiometer was deployed at 28 stations, mostly when solar illumination conditions were excellent (cloud free). The PML MicroPRO free-fall optical profiler was deployed at 34 stations (all but 7 stations that were either *Q*-cast experiments or aborted stations) for a total of 381 casts. The NASA microNESS free-fall optical profiler was deployed at 37 of the 41 stations (total 555 casts). The THOR free-fall optical profiler was deployed at 16 stations (127 casts) either concurrent with PML or NASA free-fall profilers, or specifically for the *Q*-cast experiments.

There were 47 FRRF profiles at all but four stations, providing rapid, *in situ* measurements of photosynthetic parameters and primary productivity. In addition, two state-of-the-art instruments to measure inherent optical properties were deployed extensively, *in situ* and *in vivo*. There were 48 profiles of the AC-9 and BB-6 at 39 of the 41 stations.

There were 18 deployments of the hyperspectral buoy, which were executed with simultaneous rocket casts and surface reflectance recordings from the TriOS multispectral sensors fitted on the bow of the vessel.

Additional water samples were taken during all optical stations, coincident with the deployments of the AC-9

and BB-6 and filtered for particle absorption spectra and SPM by LOV and PML (intercomparison). At each station, measurements of CDOM were made by spectrophotometry and particle size by Coulter counter, and water samples were preserved for phytoplankton species counts and bacteria counts (UCTT).

There were 9 overpasses of MERIS (2–3 matchups) 19 overpasses of SeaWiFS, and 31 overpasses of MODIS (Terra and Aqua combined). The prospects of significant scientific outcomes from these data when analyses and interpretations are completed are realistically high. Already, preliminary assessments of the matchups of MERIS overpasses and *in situ* data have been presented to the MERIS Calibration and Validation Workshop in December 2002. Excellent comparisons have resulted for quality-assured data free from glint contamination. More intercomparisons are likely when new glint-correction procedures are implemented. The intercomparisons of the four satellite sensors (SeaWiFS, MERIS, MODIS-T, and MODIS-A) are ongoing.

All the HPLC analyses for the SeaHARRE-2 pigment intercomparisons were completed by April 2003, with a preliminary report distributed in April 2003, and a workshop was held in May 2003. The initial findings show excellent comparisons for the significant variables (chlorophyll *a* and the major carotenoids), with some discrepancies noted, and revisions to the measurement protocols already recommended and implemented.

Substantial progress has been achieved on the links between the IOPs measured *in situ* and *in vivo* (in the lab), and linking these to the AOPs will provide a valuable data set for validating bio-optical models or deriving IOP data from remotely sensed observations of ocean color. Similarly, the preliminary analyses of the photosynthetic pigments, optical properties, and photosynthetic parameter values (derived by FRRF) suggests that ultimately, it may be possible to derive these variables and parameters from space sensor data.

### ACKNOWLEDGMENTS

The success of any optical calibration and validation cruise depends upon a first-class ship and crew plus a bit of clear sky during satellite overpass. BENCAL was fortunate to have an excess of the former and enough of the latter to ensure the scientific goals were achieved. The FRS *Africana* is an exemplary research platform, not only because of the spacious and well equipped scientific facilities, but more importantly, because of her fine officers and crew. The scientific party is pleased to acknowledge the high level of professional competence continuously demonstrated by the ship's personnel. In particular, Mike Viljoen (Master), Martin Davies (Chief Engineer), James Cawood, Uben Moodley, Piet Loubser (Navigation Officers), and Patrick Pierce (Bosun) are all thanked for their superb organization and support of shipboard activities. Bernie Taljaard and his team provided an excellent standard of catering and stewarding, which was greatly appreciated by the scientific team.

## BENCAL Cruise Report

MCM, together with Smit Marine South Africa (Pty) Ltd., provided logistical and scientific support, for which Johann Augustyn (Director, Research and Development), Geoff Bailey (Deputy Director, Ocean Environment), Sharon Du Plessis (Ships Logistical Manager), and Ian Calvert (Smit Marine), are gratefully acknowledged. The support of Scarla Weeks and Christo Whittle of OceanSpace CC, University of Cape Town, for processing SeaWiFS data and transmitting daily images to the ship is greatly appreciated. Chris Duncombe Rae, Marcel van den Berg, and Cathy Boucher provided support with the archiving and processing of hydrographic data, plus the production of the cruise track and station plots, while John Jones supported the small-boat operations on *Ecklonia*.

Funding from the regional German GTZ BENEFIT programme to support MCM operations is gratefully acknowledged. The success of the BENCAL cruise would not have been possible without the generous funding support from ESA and NASA.

### APPENDICES

- A. BENCAL Cruise Participants
- B. Scientific Bridge Log
- C. CTD Sampling Log

#### Appendix A

##### *BENCAL Cruise Participants*

The BENCAL cruise participants are presented alphabetically.

James Aiken  
Plymouth Marine Laboratory  
Prospect Place, West Hoe  
Plymouth PL1 3DH  
UNITED KINGDOM  
Voice: 44-1-752-633-429  
Fax: 44-1-752-633-101  
Net: [j.aiken@pml.ac.uk](mailto:j.aiken@pml.ac.uk)

Ray Barlow  
Marine and Coastal Management  
Private Bag X2, Rogge Bay 8012  
Cape Town, SOUTH AFRICA  
Voice: 27-21-402-3327  
Fax: 27-21-425-6976  
Net: [rgbarlow@mcm.wcape.gov.za](mailto:rgbarlow@mcm.wcape.gov.za)

Stewart Bernard  
UCT/Department of Oceanography  
Private Bag, Rondebosch 7700  
Cape Town, SOUTH AFRICA  
Voice: 27-21-650-5775  
Fax: 27-21-650-3979  
Net: [bstewart@ocean.uct.ac.za](mailto:bstewart@ocean.uct.ac.za)

James Brown  
MPO/RSMAS/Univ. of Miami  
4600 Rickenbacker Cswy  
Miami, Florida 33149  
Voice: 305-361-4770  
Fax: 301-361-4622  
Net: [jim.brown@miami.edu](mailto:jim.brown@miami.edu)

Malik Chami  
*Laboratoire d'Océanographie de Villefranche*  
B.P. 08, 06238 Villefranche-sur-Mer  
FRANCE  
Voice: 33-4-93-76-3726  
Fax: 33-4-93-76-3873  
Net: [chami@obs-vlfr.fr](mailto:chami@obs-vlfr.fr)

Hermann Engel  
Marine and Coastal Management  
Private Bag X2, Rogge Bay 8012  
Cape Town, SOUTH AFRICA  
Voice: 27-21-402-3541  
Fax: 27-21-425-6976  
Net: [hengel@mcm.wcape.gov.za](mailto:hengel@mcm.wcape.gov.za)

Alexandra Fawcett  
Saturn Solutions, Ltd.  
Unit 19, Longbridge Industrial Estate  
Floating Bridge Road  
Southampton, SO14 3FL  
UNITED KINGDOM  
Voice: 44-23-80-227-322  
Fax: 44-23-80-227-319  
Net: [a.fawcett@saturnsolutions.co.uk](mailto:a.fawcett@saturnsolutions.co.uk)

James Fishwick  
Plymouth Marine Laboratory  
Prospect Place, West Hoe  
Plymouth PL1 3DH  
UNITED KINGDOM  
Voice: 44-1-752-633-408  
Fax: 44-1-752-633-101  
Net: [j.fishwick@pml.ac.uk](mailto:j.fishwick@pml.ac.uk)

Stanford Hooker  
NASA/GSFC/Code 970.2  
Bldg. 28, Room W126  
Greenbelt, MD 20771  
Voice: 301-286-9503  
Fax: 301-286-0268  
Net: [stan@ardbeg.gsfc.nasa.gov](mailto:stan@ardbeg.gsfc.nasa.gov)

Victor Martinez-Vicente  
Plymouth Marine Laboratory  
Prospect Place, West Hoe  
Plymouth PL1 3DH  
UNITED KINGDOM  
Voice: 44-1-752-633-406  
Fax: 44-1-752-633-101  
Net: [vmv@pml.ac.uk](mailto:vmv@pml.ac.uk)

André Morel  
*Laboratoire d'Océanographie de Villefranche*  
B.P. 08, 06238 Villefranche-sur-Mer  
FRANCE  
Voice: 33-4-93-76-3711  
Fax: 33-4-93-76-3739  
Net: [morel@ccrv.obs-vlfr.fr](mailto:morel@ccrv.obs-vlfr.fr)

Maya Pfaff  
UCT/Department of Zoology  
Private Bag, Rondebosch 7700  
Cape Town, SOUTH AFRICA  
Voice: 27-21-650-3613  
Fax: 27-21-650-3301  
Net: [mpfaff@botzoo.uct.ac.za](mailto:mpfaff@botzoo.uct.ac.za)

Joséphine Ras  
*Laboratoire d'Océanographie de Villefranche*  
 B.P. 08, 06238 Villefranche-sur-Mer  
 FRANCE  
 Voice: 33-4-93-76-3729  
 Fax: 33-4-93-76-3739  
 Net: jras@obs-vlfr.fr

Heather Sessions  
 Marine and Coastal Management  
 Private Bag X2, Rogge Bay 8012  
 Cape Town, SOUTH AFRICA  
 Voice: 27-21-402-3314  
 Fax: 27-21-425-6976  
 Net: heather@mcm.wcape.gov.za

Nonkqubela Silulwane  
 Marine and Coastal Management  
 Private Bag X2, Rogge Bay 8012  
 Cape Town, SOUTH AFRICA  
 Voice: 27-21-430-7006  
 Fax: 27-21-434-2899  
 Net: nonkqu@mcm.wcape.gov.za

## Appendix B

### *Scientific Bridge Log*

The Scientific Bridge Log is presented in Table B1.

## Appendix C

### *CTD Sampling and Bottle Logs*

The CTD Sampling Log is presented in Table C1 and the CTD Bottle Log is presented in Table C2.

## GLOSSARY

- |  |  |
|--|--|
| A/D Analog-to-Digital  | RRRF Fast Repetition Rate Fluorometer  |
| AATSR Advanced Along Track Scanning Radiometer                     | FRS Fisheries Research Ship  |
| AC-9 Absorption and Attenuation Meter                              | GF/F Not an acronym, but a specific type of glass fiber filter manufactured by Whatman.                  |
| ACC Advanced Cosine Collector                                      | GLI Global Imager  |
| AMT Atlantic Meridional Transect                                   | GMT Greenwich Mean Time  |
| AMT-5 The fifth AMT Cruise   | GPS Global Positioning System  |
| AMT-6 The sixth AMT Cruise   | GSFC Goddard Space Flight Center   |
| AOPs Apparent Optical Properties                                   | HOBI Hydro-Optics, Biology, and Instrumentation (Laboratories)   |
| ARC Advanced Radiance Collector                                    | HP Hewlett Packard   |
| BB-6 HydroSCAT-6 (backscattering instrument)                       | HPL Horn Point Laboratory  |
| BENCAL Benguela Calibration (and Validation)                       | HPLC High Performance Liquid Chromatography  |
| BENEFIT Benguela Environment Fisheries Interaction and Training    | H-TSRB Hyperspectral-Tethered Surface Radiometer Buoy  |
| BIO Bedford Institute of Oceanography                              | IAPSO International Association for the Physical Sciences of the Ocean                                   |
| CDOM Colored Dissolved Organic Matter                              | ID Identification  |
| CHORS Center for Hydro-Optics and Remote Sensing                   | IOPs Inherent Optical Properties   |
| C-OPS Combined Operations  | JGOFS Joint Global Ocean Flux Study  |
| CSIRO Commonwealth Scientific and Industrial Research Organisation | JGOFS Joint Global Ocean Flux Study  |
| CT Conductivity, Temperature                                       | LoCNES Low-Cost NASA Environmental Sampling System   |
| CTD Conductivity, Temperature, and Depth                           | LOV <i>Laboratoire d'Océanographie de Villefranche</i> (Laboratory of Oceanography of Villefranche)      |
| CZCS Coastal Zone Color Scanner                                    | MAVT MERIS and AATSR Validation Team   |
| DATA-100 (Satlantic) Data (acquisition) Series 100 (unit)          | MCM Marine and Coastal Management  |
| DHI DHI Institute for Water and Environment                        | MERIS Medium Resolution Imaging Spectrometer   |
| DP Diagnostic Pigments   | microNESS micro NASA Environmental Sampling System   |
| ENVISAT Environmental Satellite                                    | microPRO micro Profiler  |
| ESA European Space Agency  | MODIS Moderate Resolution Imaging Spectroradiometer  |
|  | MODIS-A MODIS on the Aqua spacecraft   |
|  | MODIS-T MODIS on the Terra spacecraft  |
|  | NASA National Aeronautics and Space Administration   |
|  | OCI Ocean Color Irradiance   |
|  | OCR Ocean Color Radiance   |
|  | PAR Photosynthetically Available Radiation   |
|  | PML Plymouth Marine Laboratory   |
|  | PNF Profiling Natural Fluorescence   |
|  | POC Particulate Organic Carbon   |
|  | PPF Pump and Probe Fluorometer   |
|  | PQE Photosynthetic Quantum Efficiency  |
|  | PROSOPE <i>Productivité des Systèmes Océaniques Pélagiques</i> (Productivity of Pelagic Oceanic Systems) |
|  | PS2 Photosystem 2  |
|  | PSD Particulate Size Distribution  |
|  | R/V Research Vessel  |
|  | RAMSES Radiation Measurement Sensor with Enhanced Spectral Resolution                                    |
|  | RSMAS Rosenstiel School for Marine and Atmospheric Science   |
|  | S/N Serial Number  |
|  | SBE Sea-Bird Electronics   |
|  | SCOR Scientific Committee on Oceanographic Research  |
|  | SDY Sequential Day of the Year   |
|  | SeaHARRE SeaWiFS HPLC Analysis Round-Robin Experiment  |
|  | SeaHARRE-1 The First SeaHARRE  |
|  | SeaHARRE-2 The Second SeaHARRE   |

## BENCAL Cruise Report

**Table B1.** A summary of the scientific activities during the BENCAL cruise as recorded in the Scientific Bridge Log. All times are reported in GMT.

Station		Position		Scientific	Station		Position		Scientific		
No.	Time	SDY (Greg.)	Longitude	Latitude	Activity	No.	Time	SDY (Greg.)	Longitude	Latitude	Activity
	1000	277 (04Oct02)			Depart Dock	3	1000	279 (06Oct02)			Sta. 3 closed
1	0639	278 (05Oct02)	18.0668	-32.6613	Sta. 1 opened	4	1045	279 (06Oct02)	18.2540	-32.3298	Sta. 4 opened
	0713				CTD deployed		1055				LI-COR deployed
	0745				CTD onboard		1112				LI-COR recovered
	0815				CTD deployed		1115				PML and NASA rockets deployed (astern)
	0836				CTD onboard		1117				LI-COR deployed
	0852				LI-COR deployed		1128				LI-COR recovered
	0913				LI-COR recovered		1139				FRRF deployed (stbd)
	0915				LI-COR deployed		1155				PML and NASA rockets recovered
	0927				LI-COR recovered		1157				FRRF recovered (stbd)
	1004				FRRF and BB-6 deployed		1201				AC-9 deployed
	1017				FRRF and BB-6 recovered		1219				AC-9 recovered
	1034				PML rocket deployed (astern)		1227				CTD deployed
	1120				PML rocket recovered		1240				CTD recovered
	1128				NASA microNESS deployed (stbd quarter)	4	1244	279 (06Oct02)			Sta. 4 closed
	1153				NASA microNESS recovered	5	1316	279 (06Oct02)	18.2477	-32.3168	Sta. 5 opened
	1158				AC-9 deployed		1319				FRRF deployed
	1213				AC-9 recovered		1325				PML and NASA rockets deployed
1	1216	278 (05Oct02)			Sta. 1 closed		1339				FRRF recovered
2	1218	278 (05Oct02)	18.0672	-32.6590	Sta. 2 opened		1346				AC-9 deployed
	1220				LI-COR deployed (stbd side)		1405				AC-9 recovered
	1235				LI-COR recovered		1418				CTD deployed
	1238				LI-COR deployed (stbd side)		1431				CTD recovered
	1238				NASA rocket deployed (stbd quarter)		1438				H-TSRB deployed (stbd quarter)
	1252				LI-COR recovered		1444				H-TSRB recovered (stbd quarter)
	1254				NASA rocket recovered		1446				Rocket recovered (port quarter)
	1258				FRRF deployed (stbd side)		1449				H-TSRB deployed (port quarter)
	1301				PML rocket deployed (astern)		1510				H-TSRB recovered (port quarter)
	1318				FRRF recovered		1514				Rocket deployed
	1320				PML rocket recovered		1552				Both rockets recovered
	1324				AC-9 deployed	5	1553	279 (06Oct02)			Sta. 5 closed
	1344				AC-9 recovered	6	0632	280 (07Oct02)	18.0990	-32.5975	Sta. 6 opened
	1403				CTD deployed		0635				CTD deployed
	1403				Buoyed rocket deployed		0645				CTD recovered
	1405				CTD at surface		0704				PML and NASA rockets deployed
	1414				CTD on board		0708				LI-COR deployed
	1426				Buoyed rocket recovered		0715				Both rockets recovered
2	1430	278 (05Oct02)			Sta. 2 closed		0722				LI-COR profiler recovered
3	0743	279 (06Oct02)	18.2370	-32.3140	Sta. 3 opened		0724				Rocket deployed
	0746				NASA rocket deployed		0728				LI-COR profiler deployed
	0815				CTD deployed		0733				Rocket recovered
	0844				CTD recovered		0748				LI-COR recovered
	0844				NASA rocket recovered		0752				FRRF deployed
	0849				PML rocket deployed		0800				Both rockets recovered
	0851				LI-COR deployed		0810				FRRF recovered
	0914				LI-COR recovered		0817				AC-9 deployed
	0918				PML rocket deployed		0834				AC-9 recovered
	0921				NASA rocket stuck on ground	6	0834	280 (07Oct02)			Sta. 6 closed
	0923				PML rocket recovered	7	0845	280 (07Oct02)	18.0878	-32.5758	Sta. 7 opened
3	1000	279 (06Oct02)			Sta. 3 closed		0845				PML and NASA rockets deployed

Note: The first rightmost entry is repeated from the bottom leftmost column of the current table.

**Table B1. (cont.)** A summary of the scientific activities during the BENCAL cruise as recorded in the Scientific Bridge Log. All times are reported in GMT.

Station			Position		Scientific	Station			Position		Scientific
No.	Time	SDY (Greg.)	Longitude	Latitude	Activity	No.	Time	SDY (Greg.)	Longitude	Latitude	Activity
7	0845				PML and NASA rockets deployed	9	1640				Rocket recovered
	0847				LI-COR deployed		1642	280 (07Oct02)			Sta. 9 closed
	0854				Rocket recovered	10	0657	281 (08Oct02)	18.1408	-32.6082	Sta. 10 opened
	0859				Second rocket recovered		0702				CTD deployed
	0904				PML and NASA rockets deployed		0715				CTD recovered
	0906				LI-COR deployed		0728				PML and NASA rockets deployed
	0913				Rocket recovered		0730				LI-COR deployed; rockets recovered
	0920				LI-COR recovered		0801				LI-COR recovered
	0924				H-TSRB deployed		0807				FRRF deployed
	0935				Rocket deployed		0819				FRRF recovered
	1011				Rocket recovered		0822				AC-9 deployed
	1015				H-TSRB recovered		0830				H-TSRB deployed
	1025				Rockets deployed (astern)		0835				Rockets deployed
	1026				FRRF deployed (stbd side)		0843				AC-9 recovered
	1043				FRRF recovered (stbd side)		0855				PML and NASA rockets recovered
	1051				AC-9 deployed		0857				H-TSRB recovered
	1110				AC-9 recovered	10	0859	281 (08Oct02)			Sta. 10 closed
	1117				CTD deployed	11	0915	281 (08Oct02)	18.1080	-32.5672	Sta. 11 opened
	1119				Rockets recovered		0919				LI-COR deployed
	1130				CTD recovered		0926				PML and NASA rockets dep., LI-COR rec.
7	1131	280 (07Oct02)				0934					LI-COR deployed
8	1138	280 (07Oct02)	18.0863	-32.5778	Sta. 8 opened	0945					LI-COR recovered
	1140				PML and NASA rockets deployed	0946					PML and NASA rockets deployed
	1144				LI-COR deployed (stbd side)	0951					Profiler deployed
	1202				LI-COR recovered	1003					Rockets recovered
	1208				LI-COR deployed (stbd side)	1004					Profiler recovered
	1217				LI-COR recovered	1008					FRRF deployed
	1220				FRRF deployed	1021					H-TSRB deployed (port quarter)
	1236				FRRF recovered	1022					Rocket deployed (stbd quarter)
	1240				AC-9 deployed	1023					FRRF recovered
	1300				AC-9 recovered	1027					AC-9 deployed
	1301				Rockets recovered	1045					AC-9 recovered
	1308				CTD deployed	1045					Rockets recovered
	1322				CTD recovered	1053					CTD deployed
8	1330	280 (07Oct02)			Sta. 8 closed	1105					CTD recovered
9	1410	280 (07Oct02)	18.0567	-32.5400	Sta. 9 opened	11	1109	281 (08Oct02)			Sta. 11 closed
	1412				PML rocket deployed (stbd quarter)	12	1211	281 (08Oct02)	17.9647	-32.4615	Sta. 12 opened
	1415				NASA rocket deployed (port quarter)		1212				LI-COR deployed; rockets deployed
	1439				AC-9 deployed		1235				LI-COR recovered
	1450				AC-9 recovered		1236				LI-COR deployed (stbd side)
	1510				FRRF deployed (stbd side)		1240				Rockets recovered
	1524				FRRF recovered		1251				LI-COR recovered
	1528				AC-9 deployed		1257				H-TSRB deployed (stbd quarter)
	1547				AC-9 recovered		1259				FRRF deployed (stbd side)
	1551				FRRF deployed		1305				Rockets deployed (astern)
	1613				FRRF recovered		1313				FRRF recovered
	1618				AC-9 deployed		1318				AC-9 deployed
	1633				Rocket recovered		1334				AC-9 recovered
	1636				AC-9 recovered		1339				Rockets recovered
	1640				Rocket recovered		1341				H-TSRB recovered

Note: The first leftmost entry is repeated from the last rightmost column from the previous table, and the first rightmost entry is repeated from the bottom leftmost column of the current table.

BENCAL Cruise Report

**Table B1. (cont.)** A summary of the scientific activities during the BENCAL cruise as recorded in the Scientific Bridge Log. All times are reported in GMT.

No.	Station Time	SDY (Greg.)	Position Longitude	Latitude	Scientific Activity	No.	Station Time	SDY (Greg.)	Position Longitude	Latitude	Scientific Activity
	1341				H-TSRB recovered	15	1025				AC-9 recovered
12	1345				CTD deployed		1039				LI-COR deployed
	1358				CTD recovered		1042				Rocket recovered
12	1359	281 (08Oct02)				1055					LI-COR recovered
13	1403	281 (08Oct02)	17.9683	-32.4600	Sta. 12 closed Sta. 13 opened	1056					LI-COR deployed
	1405				THOR deployed	1113					LI-COR recovered
	1407				Rocket deployed	15	1116	282 (09Oct02)			Sta. 15 closed
	1417				FRRF deployed	16	1253	282 (09Oct02)	17.2307	-30.8067	Sta. 16 opened
	1430				FRRF recovered		1256				FRRF deployed
	1432				AC-9 deployed		1314				PML and NASA rockets deployed
	1501				AC-9 recovered		1320				FRRF recovered
	1503				FRRF deployed		1325				AC-9 deployed
	1525				FRRF recovered		1336				Rocket recovered (stbd side)
	1529				AC-9 deployed		1339				Rocket recovered (prt side)
	1546				AC-9 recovered		1347				AC-9 recovered
	1549				FRRF deployed		1350				LI-COR deployed
	1600				FRRF recovered		1402				LI-COR recovered
	1605				AC-9 deployed		1404				LI-COR deployed
	1617				AC-9 recovered		1420				LI-COR recovered
	1630				Rocket recovered (stbd side)		1424				NASA rocket deployed (port quarter)
	1638				Rocket recovered (prt side)		1435				Rocket recovered (port quarter)
13	1653	281 (08Oct02)			Sta. 13 closed		1439				H-TSRB deployed
14	0601	282 (09Oct02)	17.3507	-30.7550	Sta. 14 opened		1443				Rocket deployed (port quarter)
	0606				CTD deployed		1520				Rocket recovered (port quarter)
	0622				CTD recovered		1524				H-TSRB recovered
	0633				LI-COR deployed		1535				CTD deployed
	0634				LI-COR recovered		1548				CTD recovered
	0636				LI-COR deployed		1608				AC-9 recovered
	0649				LI-COR recovered		1611				FRRF deployed
	0656				NASA rocket deployed (prt)		1618				FRRF recovered
	0657				Rocket recovered (stbd)	16	1620	282 (09Oct02)			Sta. 16 closed
	0700				Rocket recovered (prt)	17	0601	283 (10Oct02)	16.6710	-29.4997	Sta. 17 opened
	0704				FRRF deployed		0606				CTD deployed
	0713				FRRF recovered		0629				CTD recovered
	0718				AC-9 deployed		0641				FRRF deployed
	0731				Rocket recovered (stbd)		0652				FRRF recovered
	0731				AC-9 recovered		0703				AC-9 deployed
	0758				CTD deployed		0724				AC-9 recovered
	0759				CTD recovered		0730				LI-COR deployed
14	0813	282 (9Oct02)			Sta. 14 closed		0730				PML and NASA rockets deployed
15	0858	282 (9Oct02)	17.4537	-30.7320	Sta. 15 opened		0733				LI-COR recovered
	0907				CTD deployed		0733				Rockets recovered
	0922				CTD recovered	17	0736	283 (10Oct02)			Sta. 17 closed
	0930				FRRF deployed	18	0804	283 (10Oct02)	16.6783	-29.4337	Sta. 18 opened
	0945				FRRF recovered		0807				PML and NASA rockets deployed
	0945				AC-9 deployed		0812				LI-COR deployed
	0949				Rocket deployed		0818				PML rocket recovered (stbd)
	1001				AC-9 recovered		0826				LI-COR recovered
	1006				AC-9 deployed		0827				Rockets deployed
	1025				AC-9 recovered		0831				LI-COR deployed

Note: The first leftmost entry is repeated from the last rightmost column from the previous table, and the first rightmost entry is repeated from the bottom leftmost column of the current table.

**Table B1. (cont.)** A summary of the scientific activities during the BENCAL cruise as recorded in the Scientific Bridge Log. All times are reported in GMT.

No.	Station Time	SDY (Greg.)	Position Longitude	Latitude	Scientific Activity	No.	Station Time	SDY (Greg.)	Position Longitude	Latitude	Scientific Activity	
18	0831				LI-COR deployed	20	1352				Rockets deployed	
	0840				Rockets recovered		1356				FRRF deployed	
	0846				LI-COR recovered		1358				Rocket recovered (stbd quarter)	
	0847				NASA and THOR rockets deployed		1416				Rocket recovered (port quarter)	
	0853				FRRF deployed		1408				FRRF recovered	
	0904				FRRF recovered		1411				AC-9 deployed	
	0905				Rockets recovered (small and jumbo)		1421				H-TSRB deployed	
	0908				AC-9 deployed		1428				AC-9 recovered	
	0908				NASA rocket deployed (small)		1458				H-TSRB recovered	
	0909				H-TSRB deployed	20	1459	283 (10Oct02)				Sta. 20 closed
	0912				Rocket deployed (small)	21	1501	283 (10Oct02)	16.7467	-29.4083		Sta. 21 opened
	0915				Rockets deployed		1502				FRRF deployed	
	0924				AC-9 recovered		1503				NASA rocket deployed (port quarter)	
	0932				CTD deployed		1516				FRRF recovered	
	0933				Rockets recovered		1519				AC-9 deployed	
	0938				H-TSRB recovered		1533				AC-9 recovered	
	0936				Rocket recovered (port)		1537				FRRF deployed	
	0946				CTD recovered		1546				FRRF recovered	
18	0948	283 (10Oct02)					1550				AC-9 deployed	
19	1029	283 (10Oct02)	16.6832	-29.4943			1602				AC-9 recovered	
	1031				PML and NASA rockets deployed		1642				Rocket recovered	
	1037				FRRF deployed	21	1645	283 (10Oct02)				Sta. 21 closed
	1046				Rockets recovered	22	0637	284 (11Oct02)	14.8610	-30.0435		Sta. 22 opened
	1056				Rockets deployed		0642				CTD deployed	
	1057				LI-COR deployed (stbd side)		0710				CTD recovered	
	1106				Both rockets recovered		0718				PML and NASA rockets deployed	
	1114				LI-COR recovered		0719				LI-COR deployed	
	1117				Rocket deployed (port quarter)		0736				Rockets recovered	
	1119				Rocket deployed (stbd quarter)		0753				Rockets deployed	
	1121				FRRF deployed		0753				LI-COR recovered	
	1135				FRRF recovered		0756				LI-COR deployed	
	1136				Rocket recovered (stbd quarter)		0807				Rockets recovered	
	1138				Rocket recovered (port quarter)		0816				LI-COR recovered	
	1139				AC-9 deployed (stbd side)		0819				FRRF deployed	
	1141				H-TSRB deployed		0824				Rockets deployed	
	1152				AC-9 recovered		0838				FRRF recovered	
	1205				CTD deployed		0840				H-TSRB deployed	
	1218				H-TSRB recovered		0842				AC-9 deployed	
	1226				CTD recovered		0905				AC-9 recovered	
19	1228	283 (10Oct02)					0935				Rockets recovered	
20	1317	283 (10Oct02)	16.7400	-29.4050			0941				H-TSRB recovered	
	1318				PML and NASA rockets deployed	22	0942	284 (11Oct02)				Sta. 22 closed
	1319				LI-COR deployed	23	1026	284 (11Oct02)	14.9400	-30.0250		Sta. 23 opened
	1325				Both rockets recovered		1041				PML and NASA rockets deployed	
	1330				Rockets deployed		1055				LI-COR deployed	
	1335				LI-COR recovered		1101				Rocket recovered (port)	
	1337				LI-COR deployed		1102				Rocket recovered (stbd)	
	1340				Rockets recovered		1115				LI-COR recovered	
	1352				LI-COR recovered		1117				LI-COR deployed	
20	1352				Rockets deployed	23	1126				LI-COR recovered	

Note: The first leftmost entry is repeated from the last rightmost column from the previous table, and the first rightmost entry is repeated from the bottom leftmost column of the current table.

BENCAL Cruise Report

**Table B1. (cont.)** A summary of the scientific activities during the BENCAL cruise as recorded in the Scientific Bridge Log. All times are reported in GMT.

No.	Time	Station SDY (Greg.)	Position Longitude Latitude	Scientific Activity	No.	Time	Station SDY (Greg.)	Position Longitude Latitude	Scientific Activity
23	1126			LI-COR recovered	26	0900			AC-9 deployed
	1131	284 (11Oct02)		Sta. 23 closed	26	0903			AC-9 recovered
24	1208	284 (11Oct02)	14.8943 -30.1135	Sta. 24 opened		0827			AC-9 deployed
	1214			CTD deployed		0918			NASA rocket recovered
	1236			CTD recovered		0920			Jumbo rocket deployed
	1242			FRRF deployed		0938			H-TSRB recovered
	1245			H-TSRB deployed		0957			Rocket recovered
	1300			FRRF recovered		0958			Jumbo rocket recovered
	1305			AC-9 deployed		0959			AC-9 recovered
	1329			AC-9 recovered	26	1000	286 (13Oct02)		Sta. 26 closed
	1330			H-TSRB recovered	27	1032	286 (13Oct02)	14.4172 -30.5392	Sta. 27 opened
	1335			CTD deployed		1040			NASA rocket deployed (port)
	1342			CTD recovered		1042			PML rocket deployed (stbd)
	1346			FRRF deployed		1048			LI-COR deployed
	1405			NASA rocket deployed		1049			Both rockets recovered
	1408			AC-9 deployed		1116			LI-COR recovered
	1421			NASA rocket recovered		1121			LI-COR deployed
	1429			AC-9 recovered		1134			LI-COR recovered
24	1429	284 (11Oct02)		Sta. 24 closed		1136			Rockets deployed
25	0600	285 (12Oct02)	16.2553 -29.5893	Sta. 25 opened		1140			FRRF deployed
	0606			CTD deployed		1145			Rocket recovered (stbd)
	0626			CTD recovered		1147			All rockets recovered
	0639			LI-COR deployed		1203			FRRF recovered
	0658			LI-COR recovered		1208			AC-9 deployed
	0701			PML and NASA rockets deployed		1234			AC-9 recovered
	0701			AC-9 deployed		1250			CTD deployed
	0720			Rockets recovered		1311			CTD recovered
	0726			AC-9 recovered		1322			FRRF deployed
	0728			FRRF deployed		1327			Rockets deployed
	0746			FRRF recovered		1345			Rocket recovered (stbd)
	0757			CTD deployed		1346			FRRF recovered
	0805			CTD recovered		1355			Rocket recovered (port)
25	0814	285 (12Oct02)		Sta. 25 closed		1406			AC-9 deployed
26	0629	286 (13Oct02)	14.3798 -30.6107	Sta. 26 opened		1436			AC-9 recovered
	0637			CTD deployed		1447			CTD deployed
	0659			CTD recovered		1514			CTD recovered
	0708			PML and NASA rockets deployed	27	1520	286 (13Oct02)		Sta. 27 closed
	0710			LI-COR deployed	28	0605	287 (14Oct02)	15.9980 -29.2387	Sta. 28 opened
	0724			Both rockets recovered		0612			CTD deployed
	0737			LI-COR recovered		0636			CTD recovered
	0739			LI-COR deployed		0643			NASA rocket deployed (port)
	0803			LI-COR recovered		0646			PML rocket deployed (stbd)
	0759			NASA and THOR rockets deployed		0654			FRRF deployed
	0811			FRRF deployed		0707			FRRF recovered
	0830			H-TSRB deployed		0712			Rockets recovered
	0843			FRRF recovered		0714			AC-9 deployed
	0849			AC-9 deployed		0737			AC-9 recovered
	0850			H-TSRB deployed (port)	28	0739	287 (14Oct02)		Sta. 28 closed
	0853			AC-9 recovered	29	0840	287 (14Oct02)	16.0993 -29.0642	Sta. 29 opened
26	0900			AC-9 deployed	29	0841			NASA rocket deployed (port)

Note: The first leftmost entry is repeated from the last rightmost column from the previous table, and the first rightmost entry is repeated from the bottom leftmost column of the current table.

**Table B1. (cont.)** A summary of the scientific activities during the BENCAL cruise as recorded in the Scientific Bridge Log. All times are reported in GMT.

Station			Position		Scientific	Station			Position		Scientific
No.	Time	SDY (Greg.)	Longitude	Latitude	Activity	No.	Time	SDY (Greg.)	Longitude	Latitude	Activity
29	0841				NASA rocket deployed (port)	32	0828				Rockets recovered
29	0842				PML rocket deployed (stbd)	32	0834	288 (15Oct02)			Sta. 32 closed
	0856				Both rockets recovered	33	0858	288 (15Oct02)	16.7740	-29.6577	Sta. 33 opened
	0904				LI-COR deployed		0900				CTD deployed
	0925				LI-COR recovered		0917				CTD recovered
	0929				NASA rocket deployed (port)		0921				PML and NASA rockets deployed
	0930				PML rocket deployed (stbd)		0926				FRRF deployed
	1035				Both rockets recovered		0928				H-TSRB deployed
	1046				FRRF deployed		0940				FRRF recovered
	1101				FRRF recovered		0946				AC-9 deployed
	1104				AC-9 deployed		0956				Rocket recovered (port)
	1123				AC-9 recovered		1003				AC-9 recovered
	1131				CTD deployed		1005				Rocket recovered (stbd)
	1157				CTD recovered		1009				LI-COR deployed
29	1205	287 (14Oct02)					1024				LI-COR recovered
30	1232	287 (14Oct02)	16.1973	-29.0910	Sta. 30 opened		1028				LI-COR deployed
	1245				NASA rocket deployed (port)		1046				LI-COR recovered
	1257				Rockets recovered		1051				NASA and THOR rockets deployed
	1324				Rocket recovered (stbd)		1112				NASA rocket recovered (port)
	1330				THOR rocket deployed		1114				THOR rocket recovered
	1343				All rockets recovered		1117				H-TSRB recovered
	1346				FRRF deployed	33	1117	288 (15Oct02)			Sta. 33 closed
	1358				FRRF recovered	34	1151	288 (15Oct02)	16.8617	-29.6297	Sta. 34 opened
	1418				AC-9 recovered		1154				PML and NASA rockets deployed
	1426				CTD deployed		1205				Rockets recovered
	1443				CTD recovered		1206				LI-COR deployed
30	1445	287 (14Oct02)					1224				LI-COR recovered
31	1453	287 (14Oct02)	16.1950	-29.0867	Sta. 31 opened		1227				LI-COR deployed
	1454				THOR rocket deployed		1240				LI-COR recovered
	1457				NASA rocket deployed		1244				H-TSRB deployed, FRRF deployed
	1642				Rocket recovered (port)		1252				THOR rocket deployed
	1643				Rocket recovered (stbd)		1252				NASA rocket deployed (port)
31	1704	287 (14Oct02)					1255				FRRF recovered
32	0605	288 (15Oct02)	16.6692	-29.6827	Sta. 32 opened		1300				AC-9 deployed
	0613				CTD deployed		1317				AC-9 recovered
	0636				CTD recovered		1321				FRRF deployed
	0647				FRRF deployed		1329				THOR rocket recovered
	0700				FRRF recovered		1330				NASA rocket recovered
	0703				AC-9 deployed		1333				FRRF recovered
	0705				PML and NASA rockets deployed		1335				H-TSRB recovered
	0722				AC-9 recovered		1410				CTD deployed
	0724				Rockets recovered		1427				CTD recovered
	0727				LI-COR deployed	34	1432	288 (15Oct02)			Sta. 34 closed
	0729				LI-COR recovered	35	1459	288 (15Oct02)	16.9067	-29.5933	Sta. 35 opened
	0734				LI-COR deployed		1500				THOR and NASA rocket deployed
	0753				LI-COR recovered		1518				FRRF recovered
	0755				LI-COR deployed		1522				AC-9 deployed
	0809				LI-COR recovered		1540				AC-9 recovered
	0810				PML and NASA rockets deployed		1641				THOR and NASA rocket recovered
32	0828				Rockets recovered	35	1641	288 (15Oct02)			Sta. 35 closed

Note: The first leftmost entry is repeated from the last rightmost column from the previous table, and the first rightmost entry is repeated from the bottom leftmost column of the current table.

BENCAL Cruise Report

**Table B1. (cont.)** A summary of the scientific activities during the BENCAL cruise as recorded in the Scientific Bridge Log. All times are reported in GMT.

Station			Position		Scientific	Station			Position		Scientific
No.	Time	SDY (Greg.)	Longitude	Latitude	Activity	No.	Time	SDY (Greg.)	Longitude	Latitude	Activity
36	0713	289 (16Oct02)	18.2292	-32.0550	Sta. 36 opened	39	0707				AC-9 deployed
	0716				CTD deployed		0707				H-TSRB deployed
	0730				CTD recovered		0713				PML rocket deployed (stbd)
	0736				PML and NASA rockets deployed		0716				NASA rocket deployed (port)
	0737				FRRF deployed		0726				AC-9 recovered
	0750				FRRF recovered		0752				PML rocket recovered (stbd)
	0752				AC-9 deployed		0756				H-TSRB recovered
	0804				PML and NASA rockets recovered		0756				FRRF deployed
	0806				AC-9 recovered		0758				THOR rocket deployed
36	0822	289 (16Oct02)			Sta. 36 closed		0758				NASA rocket recovered (port)
37	1116	289 (16Oct02)	18.1912	-32.0695	Sta. 37 opened		0800				NASA rocket deployed (port)
	1118				FRRF deployed		0803				FRRF recovered
	1118				PML and NASA rockets deployed		0821				NASA rocket recovered (port)
	1125				H-TSRB deployed		0822				THOR rocket recovered
	1131				FRRF recovered		0829				CTD deployed
	1135				AC-9 deployed		0848				CTD recovered
	1152				AC-9 recovered	39	0851	290 (17Oct02)			Sta. 39 closed
	1208				PML and NASA rockets recovered	40	1106	290 (17Oct02)	18.0358	-32.5707	Sta. 40 opened
	1209				LI-COR deployed		1107				NASA rocket deployed (port)
	1224				LI-COR recovered		1108				PML rocket deployed (stbd)
	1225				LI-COR deployed		1120				LI-COR deployed
	1247				LI-COR recovered		1121				PML and NASA rockets recovered
	1302				H-TSRB recovered		1133				LI-COR recovered
	1308				CTD deployed		1138				LI-COR deployed
	1326				CTD recovered		1151				LI-COR recovered
37	1326	289 (16Oct02)			Sta. 37 closed		1155				AC-9 deployed
38	1401	289 (16Oct02)	18.1033	-32.0685	Sta. 38 opened		1212				AC-9 recovered
	1407				PML and NASA rockets deployed		1219				CTD deployed
	1427				LI-COR deployed		1232				CTD recovered
	1427				PML and NASA rockets recovered	40	1232	290 (17Oct02)			Sta. 40 closed
	1431				LI-COR recovered	41	1345	290 (17Oct02)	18.2188	-32.4278	Sta. 41 opened
	1436				LI-COR deployed		1346				PML and NASA rockets deployed
	1449				LI-COR recovered		1352				PML rocket recovered (stbd)
	1452				FRRF deployed		1355				NASA rocket recovered
	1453				THOR and NASA rocket deployed		1408				LI-COR recovered
	1506				FRRF recovered		1410				LI-COR deployed
	1510				AC-9 deployed		1422				LI-COR recovered
	1513				H-TSRB deployed		1425				H-TSRB deployed
	1526				AC-9 recovered		1426				FRRF deployed
	1532				NASA rocket recovered		1427				PML and NASA rockets deployed
	1533				THOR rocket recovered		1434				FRRF recovered
	1551				CTD deployed		1437				AC-9 deployed
	1600				CTD recovered		1451				AC-9 recovered
38	1617	289 (16Oct02)			Sta. 38 closed		1455				PML and NASA rockets recovered
39	0612	290 (17Oct02)	17.6647	-32.6728	Sta. 39 opened		1455				H-TSRB recovered
	0617				CTD deployed		1506				CTD deployed
	0640				CTD recovered		1514				CTD recovered
	0649				FRRF deployed	41	1515	290 (17Oct02)			Sta. 41 closed
39	0701				FRRF recovered		1000	291 (18Oct02)			Arrive Dock

Note: The first leftmost entry is repeated from the last rightmost column from the previous table, and the first rightmost entry is repeated from the bottom leftmost column of the current table.

**Table C1.** A summary of the CTD sampling activities during the BENCAL cruise. On every FRS *Africana* cruise, the bridge records a sequential ship station number (20854–20894 for the BENCAL cruise) and a so-called *grid number* (02–10–01 to 02–10–41). These identifications were displayed on data acquisition screens in the various laboratories during the cruise and are used in the MCM databases, so they are included for completeness. Note that even though there are 41 stations, there are only 39 CTD casts, and the last two digits of the grid number is the same as the station number. For some stations, there were no CTD casts (only optical instrumentation deployments), and at five stations there were two CTD casts. For the latter, the second cast is indicated by the “a” suffix. The stations where only optics was executed are not included. All times are reported in GMT. The CTD Bottle Log, including physical variables recorded at the bottle depths, is presented in Table C2.

No.	Station		Position		Ship Station	Grid Number	CTD Cast	Sampling and Niskin Bottle Notes	
	SDY (Greg.)	Time	Longitude	Latitude					
1	278	(05Oct02)	0817	18.0668	-32.6613	A20854	02-10-01	1	Seven bottles fired.
2	278	(05Oct02)	1405	18.0672	-32.6590	A20855	02-10-02	2	Seven bottles fired.
3	279	(06Oct02)	0817	18.2370	-32.3140	A20856	02-10-03	3	Six bottles fired.
4	279	(06Oct02)	1228	18.2540	-32.3298	A20857	02-10-04	4	Nine bottles fired.
5	279	(06Oct02)	1418	18.2477	-32.3168	A20858	02-10-05	5	Eleven bottles fired.
6	280	(07Oct02)	0635	18.0990	-32.5975	A20859	02-10-06	6	Five bottles fired.
7	280	(07Oct02)	1119	18.0878	-32.5758	A20860	02-10-07	7	Five bottles fired.
8	280	(07Oct02)	1309	18.0863	-32.5778	A20861	02-10-08	8	Seven bottles fired.
10	281	(08Oct02)	0701	18.1408	-32.6082	A20863	02-10-10	9	Six bottles fired.
11	281	(08Oct02)	1053	18.1080	-32.5672	A20864	02-10-11	10	Nine bottles fired.
12	281	(08Oct02)	1346	17.9647	-32.4615	A20865	02-10-12	11	Six bottles fired.
14	282	(09Oct02)	0607	17.3507	-30.7550	A20867	02-10-14	12	Five bottles fired.
14	282	(09Oct02)	0800	17.3488	-30.7528	A20867a	02-10-14a	13	Five bottles fired at 3 m;
								13	no in-water PAR data (cap left on).
15	282	(09Oct02)	0907	17.4537	-30.7320	A20868	02-10-15	14	Nine bottles fired.
16	282	(09Oct02)	1535	17.2307	-30.8067	A20869	02-10-16	15	Eleven bottles fired.
17	283	(10Oct02)	0606	16.6710	-29.4997	A20870	02-10-17	16	Seven bottles fired.
18	283	(10Oct02)	0933	16.6783	-29.4337	A20871	02-10-18	17	Six bottles fired.
19	283	(10Oct02)	1205	16.6832	-29.4943	A20872	02-10-19	18	Eight bottles fired.
22	284	(11Oct02)	0645	14.8610	-30.0435	A20875	02-10-22	19	Seven bottles fired.
24	284	(11Oct02)	1214	14.8943	-30.1135	A20877	02-10-24	20	Eight bottles fired.
24	284	(11Oct02)	1336	14.8998	-30.1247	A20877a	02-10-24a	21	Eleven bottles fired at 10 m.
25	285	(12Oct02)	0607	16.2553	-29.5893	A20878	02-10-25	22	Six bottles fired.
25	285	(12Oct02)	0757	16.2503	-29.5895	A20878a	02-10-25a	23	Four bottles fired at 2 m;
								23	six bottles at 30 m.
26	286	(13Oct02)	0638	14.3798	-30.6107	A20879	02-10-26	24	Seven bottles fired.
								24	No PAR data for bottle 7.
27	286	(13Oct02)	1250	14.4172	-30.5392	A20880	02-10-27	25	Six bottles fired.
27	286	(13Oct02)	1447	14.4260	-30.5365	A20880a	02-10-27a	26	Nine bottles fired at 40 m;
								26	two bottles at 400 m.
28	287	(14Oct02)	0613	15.9980	-29.2387	A20881	02-10-28	27	Seven bottles fired.
29	287	(14Oct02)	1132	16.0993	-29.0642	A20882	02-10-29	28	Seven bottles fired.
30	287	(14Oct02)	1427	16.1973	-29.0910	A20883	02-10-30	29	Six bottles fired.
32	288	(15Oct02)	0612	16.6692	-29.6827	A20885	02-10-32	30	Six bottles fired.
33	288	(15Oct02)	0901	16.7740	-29.6577	A20886	02-10-33	31†	Six bottles fired;
								31†	PAR sensor damaged.
34	288	(15Oct02)	1411	16.8617	-29.6297	A20887	02-10-34	32†	Six bottles fired.
36	289	(16Oct02)	0717	18.2292	-32.0550	A20889	02-10-36	33†	Five bottles fired.
37	289	(16Oct02)	1307	18.1912	-32.0695	A20890	02-10-37	34†	Eleven bottles fired.
38	289	(16Oct02)	1551	18.1033	-32.0685	A20891	02-10-38	35†	Cast only (no bottles fired);
								35†	data extracted at standard depths.
39	290	(17Oct02)	0617	17.6647	-32.6728	A20892	02-10-39	36†	Five bottles fired at 3 m.
39	290	(17Oct02)	0830	17.6505	-32.7025	A20892a	02-10-39a	37†	Six bottles fired.
40	290	(17Oct02)	1219	18.0358	-32.5707	A20893	02-10-40	38†	Six bottles fired.
41	290	(17Oct02)	1503	18.2188	-32.4278	A20894	02-10-41	39†	Five bottles fired.

† No in-water PAR data; the CTD PAR sensor was damaged during cast 31, so it was removed.



**Table C2. (cont.)** A summary of the CTD Bottle Log for the BENCAL cruise. Preliminary physical measures for each cast number (No.) and bottle number (Bo.) are as follows: seawater temperature ( $T_w$ ) units are degrees Celcius, oxygen concentration is in milliliters per liter, turbidity ( $T_n$ ) is in volts, fluorescence ( $F$ ) is in log-transformed volts, subsurface  $E^{PAR}$  and deck cell  $E^{PAR}$  (indicated by  $z$  and  $0^+$ , respectively) are in micromole quanta per square meter per second. The depth of each bottle number,  $Z_n$ , is given in meters. Note, no in-water PAR data were collected for cast 24, bottle 7.

CTD No. Bo.	$Z_n$ [m]	$T_w$ [°C]	$S$	Ox. Con.	$T_n$ [V]	$F$ [V]	$E^{PAR}$		CTD No. Bo.	$Z_n$ [m]	$T_w$ [°C]	$S$	Ox. Con.	$T_n$ [V]	$F$ [V]	$E^{PAR}$			
							$z$	$0^+$								$z$	$0^+$		
14	1	82.0	9.31	34.735	2.15	0.43	0.95	0	2,317	20	1	204.5	10.40	34.851	5.01	0.00	0.51	1	1,541
	2	50.3	10.15	34.782	2.66	0.16	1.17	1	2,542		2	60.0	15.26	35.429	5.20	0.01	1.13	6	1,342
	3	30.4	10.73	34.798	3.44	0.13	1.46	13	2,406		3	35.7	16.25	35.491	5.63	0.02	1.58	33	1,936
	4	17.8	10.96	34.805	3.71	0.13	1.55	93	2,517		4	18.2	16.43	35.492	5.71	0.04	1.63	135	1,500
	5	17.6	10.90	34.803	3.59	0.12	1.54	95	2,379		5	2.8	17.72	35.500	5.65	0.04	1.32	596	1,385
	6	9.3	11.60	34.824	4.49	0.12	1.77	435	2,687		6	3.2	17.75	35.508	5.63	0.05	1.31	756	1,388
	7	9.5	11.14	34.812	4.17	0.13	1.67	452	2,498		7	2.4	18.07	35.505	5.64	0.05	1.30	618	1,397
	8	2.8	11.85	34.830	4.75	0.13	1.62	1,116	2,308		8	3.2	17.28	35.507	5.67	0.05	1.30	679	1,703
	9	3.4	11.85	34.831	4.76	0.13	1.66	1,414	2,156	21	1	10.3	16.67	35.488	5.70	0.04	1.40	325	1,554
15	1	104.1	9.05	34.713	3.23	0.02	0.72	0	156		2	10.1	16.73	35.492	5.70	0.04	1.36	327	1,549
	2	40.8	11.46	34.978	4.26	0.01	1.01	0	158		3	10.5	16.79	35.493	5.69	0.04	1.36	314	1,520
	3	27.7	13.95	34.988	5.35	0.09	1.74	1	192		4	10.5	16.77	35.491	5.69	0.03	1.36	311	1,519
	4	18.3	15.03	34.975	6.06	0.14	1.97	2	196		5	10.8	16.74	35.492	5.69	0.04	1.35	306	1,519
	5	10.3	15.09	34.976	6.10	0.14	1.99	12	206		6	10.5	16.69	35.492	5.69	0.03	1.38	314	1,531
	6	10.0	15.09	34.976	6.10	0.15	1.99	12	209		7	9.7	16.67	35.492	5.69	0.04	1.40	344	1,542
	7	10.4	15.09	34.976	6.10	0.14	2.00	13	209		8	10.2	16.58	35.493	5.70	0.04	1.42	363	1,639
	8	3.0	15.11	34.976	6.11	0.15	2.01	78	219		9	10.6	16.64	35.492	5.70	0.04	1.40	466	2,160
	9	3.1	15.11	34.976	6.10	0.15	2.01	84	219		10	10.6	16.63	35.490	5.70	0.04	1.40	552	2,491
	10	2.9	15.11	34.976	6.11	0.15	2.01	85	221		11	10.5	16.60	35.491	5.69	0.04	1.43	574	2,546
	11	2.6	15.10	34.976	6.10	0.15	2.01	104	233	22	1	163.1	8.89	34.698	2.86	0.07	0.77	0	2,032
16	1	130.1	9.02	34.709	2.59	0.09	0.79	0	702		2	60.0	12.53	35.108	4.53	0.01	1.04	2	2,062
	2	28.1	11.63	34.895	4.22	0.06	1.49	0	1,169		3	40.1	13.83	35.230	4.88	0.02	1.41	7	2,085
	3	28.1	11.63	34.895	4.22	0.06	1.50	0	1,178		4	22.9	15.71	35.274	5.77	0.04	1.78	38	2,094
	4	17.2	13.57	34.873	6.60	0.27	2.68	1	1,520		5	13.7	16.10	35.234	5.90	0.06	1.51	163	2,107
	5	5.7	13.65	34.874	6.62	0.34	2.78	69	2,088		6	1.9	16.18	35.231	5.84	0.05	1.28	1,158	2,121
	6	4.7	13.64	34.874	6.78	0.29	2.74	118	1,321	23	1	30.5	15.56	35.271	5.66	0.04	1.71	14	1,360
	7	2.3	13.64	34.874	6.77	0.29	2.69	568	1,851		2	29.7	15.60	35.267	5.66	0.04	1.70	16	1,378
17	1	122.7	9.23	34.731	2.67	0.19	0.81	0	2,431		3	29.7	15.61	35.266	5.66	0.04	1.71	16	1,384
	2	40.2	12.26	35.057	4.56	0.05	1.43	0	2,435		4	30.0	15.61	35.267	5.66	0.04	1.71	14	1,374
	3	31.4	12.50	34.974	5.27	0.09	2.05	1	2,431		5	30.0	15.60	35.268	5.66	0.04	1.71	14	1,354
	4	20.5	12.88	34.938	5.65	0.13	2.32	4	2,434		6	30.0	15.60	35.267	5.67	0.04	1.71	15	1,359
	5	10.9	14.08	34.915	6.52	0.24	2.58	84	2,433		7	2.3	16.38	35.236	5.83	0.06	1.24	638	1,311
	6	3.0	14.32	34.916	6.58	0.24	2.39	1,303	2,431		8	2.0	16.39	35.236	5.83	0.06	1.31	707	1,315
18	1	126.2	9.06	34.713	2.67	0.14	0.82	0	2,474		9	2.4	16.40	35.236	5.83	0.06	1.29	642	1,314
	2	30.7	11.21	34.880	3.99	0.04	1.09	1	2,467		10	2.9	16.34	35.237	5.83	0.06	1.25	570	1,305
	3	30.9	11.21	34.880	3.98	0.04	1.07	1	2,464	24	1	203.5	13.14	35.153	5.45	0.00	0.54	0	2,234
	4	20.4	13.27	34.915	5.35	0.13	2.06	2	2,480		2	99.7	15.27	35.562	5.41	0.00	0.82	2	2,236
	5	14.5	13.54	34.893	6.05	0.20	2.53	5	2,485		3	80.3	15.38	35.574	5.48	0.01	1.42	4	2,238
	6	7.9	13.77	34.878	7.55	0.36	2.90	108	2,489		4	60.8	15.82	35.586	5.66	0.02	1.57	12	2,239
	7	3.3	14.18	34.885	7.66	0.32	2.57	994	2,489		5	39.9	15.95	35.591	5.70	0.03	1.59	48	2,235
	8	2.4	13.85	34.884	7.67	0.33	2.59	1,520	2,493		6	19.8	16.43	35.601	5.64	0.03	1.41	220	2,246
19	1	205.6	11.34	34.974	5.01	0.01	0.50	0	2,247		7	1.7	16.59	35.607	5.64	0.01	1.05		2,243
	2	100.0	14.35	35.343	4.98	0.01	0.77	1	2,256	25	1	204.0	12.82	35.134	5.21	0.01	0.54	1	2,575
	3	75.5	15.97	35.481	5.60	0.02	1.39	2	2,261		2	80.8	15.23	35.551	5.41	0.00	0.95	8	2,573
	4	50.0	16.34	35.500	5.64	0.04	1.54	10	2,270		3	49.8	15.77	35.596	5.66	0.03	1.66	44	2,590
	5	24.3	16.43	35.502	5.67	0.04	1.62	99	2,281		4	29.9	16.08	35.603	5.76	0.04	1.58	179	2,567
	6	9.5	16.47	35.503	5.67	0.04	1.46	469	2,291		5	10.6	16.70	35.566	5.66	0.04	1.03	736	2,663
	7	2.1	16.51	35.504	5.67	0.04	1.23	1,605	2,288		6	2.0	16.73	35.565	5.66	0.03	0.97	1,793	2,484

BENCAL Cruise Report

**Table C2. (cont.)** A summary of the CTD Bottle Log for the BENCAL cruise. Preliminary physical measures for each cast number (No.) and bottle number (Bo.) are as follows: seawater temperature ( $T_w$ ) units are degrees Celcius, oxygen concentration is in milliliters per liter, turbidity ( $T_n$ ) is in volts, fluorescence ( $F$ ) is in log-transformed volts, subsurface  $E^{PAR}$  and deck cell  $E^{PAR}$  (indicated by  $z$  and  $0^+$ , respectively) are in micromole quanta per square meter per second. The depth of each bottle number,  $Z_n$ , is given in meters. Note, no in-water PAR data were collected for casts 31-39, inclusive (damaged sensor).

CTD No.	Bo.	$Z_n$ [m]	$T_w$ [°C]	S	Ox. Con.	$T_n$ [V]	F [V]	$E^{PAR}$		CTD No.	Bo.	$Z_n$ [m]	$T_w$ [°C]	S	Ox. Con.	$T_n$ [V]	F [V]	$E^{PAR}$	
								$z$	$0^+$									$z$	$0^+$
26	1	402.0	8.79	34.668	4.76	0.00	0.54	0	663	33	1	81.1	9.45	34.756	0.75	0.83	1.02		2,403
	2	402.4	8.79	34.668	4.77	0.00	0.51	0	660		2	30.7	11.04	34.847	2.89	0.05	1.23		2,370
	3	41.7	16.00	35.604	5.72	0.04	1.66	18	874		3	20.3	14.57	34.905	5.61	0.16	2.00		2,475
	4	39.0	16.06	35.597	5.72	0.04	1.65	20	807		4	10.5	15.06	34.891	6.65	0.26	2.43		2,498
	5	40.8	16.02	35.601	5.73	0.04	1.64	20	789		5	2.2	15.14	34.887	7.03	0.28	2.28		2,437
	6	40.4	16.04	35.601	5.72	0.04	1.64	21	803	34	1	91.6	9.23	34.735	0.92	0.89	1.01		2,429
	7	38.7	16.06	35.596	5.72	0.04	1.65	22	825		2	30.4	11.21	34.846	3.11	0.05	1.34		2,430
	8	40.2	16.04	35.601	5.72	0.04	1.65	21	857		3	29.9	11.23	34.846	3.12	0.05	1.37		2,431
	9	40.0	16.04	35.601	5.72	0.13	1.67	22	873		4	20.6	12.49	34.894	3.94	0.07	1.58		2,427
	10	39.9	16.03	35.601	5.72	0.05	1.65	27	1,081		5	19.8	12.64	34.895	4.02	0.06	1.60		2,429
	11	39.5	16.05	35.600	5.73	0.04	1.65	20	801		6	11.4	15.09	34.940	6.34	0.21	2.37		2,428
27	1	165.7	9.11	34.720	2.66	0.07	0.75	0	2,164		7	10.9	15.12	34.939	6.34	0.23	2.38		2,429
	2	69.6	11.81	35.008	4.20	0.01	0.82	0	2,236		8	6.6	16.07	34.941	6.77	0.17	1.77		2,427
	3	40.8	14.45	35.089	5.35	0.07	1.75	1	2,207		9	5.9	16.10	34.938	6.77	0.18	1.77		2,424
	4	25.0	15.47	35.176	5.84	0.07	2.05	11	2,243		10	2.8	16.30	34.937	6.70	0.18	1.58		2,422
	5	16.6	15.80	35.201	6.34	0.08	2.09	67	2,247		11	2.3	16.33	34.937	6.70	0.18	1.57		2,425
	6	7.3	16.40	35.113	6.10	0.10	1.58	377	2,222	35	1	103.0	8.91	34.704	1.79	0.08	0.85		1,473
	7	2.9	16.40	35.113	6.11	0.11	1.50	1,159	2,235		2	100.0	8.91	34.704	1.78	0.07	0.83		1,459
28	1	156.5	9.43	34.754	1.64	0.06	0.89	0	2,391		3	90.0	9.03	34.715	1.62	0.07	0.86		1,481
	2	51.1	12.81	35.041	4.53	0.02	1.08	1	2,403		4	80.0	9.09	34.722	1.59	0.06	0.91		1,466
	3	42.2	14.37	34.987	5.78	0.05	1.78	3	2,408		5	70.0	9.20	34.733	1.33	0.05	0.92		1,464
	4	29.0	15.17	35.080	5.72	0.06	1.91	16	2,293		6	60.0	9.29	34.743	1.25	0.03	1.01		1,477
	5	23.0	15.48	35.099	6.22	0.13	2.22	68	2,432		7	50.0	9.53	34.766	1.66	0.03	1.23		1,491
	6	11.7	16.58	35.078	6.19	0.09	1.70	367	2,441		8	40.0	9.84	34.785	2.90	0.06	1.63		1,484
	7	2.5	16.59	35.078	6.17	0.09	1.41	997	2,447		9	30.0	11.92	34.883	4.27	0.14	1.94		1,477
	8	3.6	16.60	35.078	6.18	0.09	1.41	1,384	2,441		10	20.0	14.88	34.951	5.98	0.16	1.88		1,489
29	1	152.5	9.44	34.756	1.73	0.06	0.89	0	2,304		11	10.0	15.16	34.934	6.28	0.14	1.65		1,494
	2	39.2	13.32	35.133	4.55	0.02	1.05	2	2,280		12	3.0	16.79	34.943	6.00	0.17	1.87		1,525
	3	26.9	15.20	35.112	5.55	0.05	1.78	7	2,281	36	1	3.0	16.13	35.038	6.40	0.22	1.98		556
	4	19.7	15.73	35.130	6.14	0.12	2.12	35	2,274		2	3.3	16.14	35.038	6.41	0.21	2.02		558
	5	9.4	16.59	35.098	6.20	0.09	1.78	268	2,272		3	3.6	16.14	35.038	6.41	0.22	2.00		560
	6	3.8	16.62	35.098	6.19	0.09	1.61	960	2,283		4	3.5	16.14	35.038	6.41	0.24	2.01		562
30	1	138.4	8.98	34.706	2.53	0.06	0.80	0	2,050		5	3.6	16.14	35.039	6.40	0.21	2.00		564
	2	31.7	11.98	35.009	4.10	0.03	1.38	1	2,150	37	1	204.9	7.74	34.585	4.22	0.08	0.67		1,915
	3	21.7	14.45	35.005	6.08	0.16	2.36	3	2,119		2	35.1	13.39	35.035	4.24	0.08	1.38		1,850
	4	10.5	14.62	34.986	6.22	0.18	2.36	59	2,140		3	24.3	15.40	35.118	5.79	0.16	2.05		1,802
	5	4.0	14.64	34.987	6.23	0.17	2.18	526	2,148		4	15.8	15.73	35.095	6.14	0.19	2.15		1,809
	6	1.9	14.64	34.987	6.24	0.18	2.11	1,117	2,146		5	7.5	16.11	35.047	6.41	0.23	1.99		1,845
31	1	123.5	9.05	34.716	2.35	0.37	0.87		2,434		6	3.4	16.13	35.044	6.40	0.21	1.82		1,880
	2	28.2	12.48	35.084	4.29	0.05	1.57		2,428	38	1	54.5	9.88	34.793	0.78	0.33	1.02		2,422
	3	21.2	13.14	34.913	6.20	0.19	2.65		2,434		2	20.1	12.91	34.945	4.10	0.06	1.41		2,309
	4	14.7	13.26	34.922	6.17	0.19	2.66		2,430		3	15.5	14.30	34.910	5.15	0.09	1.77		2,534
	5	7.5	13.52	34.931	6.70	0.19	2.67		2,424		4	13.1	14.58	34.910	6.24	0.21	2.42		2,018
	6	2.3	13.70	34.857	5.18	0.17	2.14		2,417		5	9.8	14.97	34.915	7.23	0.27	2.33		2,118
32	1	113.6	9.42	34.754	1.84	1.62	1.03		2,305		6	3.1	16.31	34.955	6.75	0.18	1.85		1,918
	2	40.3	10.65	34.881	3.52	0.03	1.22		2,286	39	1	52.4	10.13	34.805	1.09	0.57	1.11		2,063
	3	30.4	11.75	34.943	4.45	0.12	2.10		2,289		2	20.8	13.58	34.888	4.51	0.12	1.38		2,043
	4	16.4	12.29	34.880	6.00	0.21	2.57		2,289		3	12.0	15.09	34.912	5.06	0.30	1.83		2,025
	5	8.0	12.71	34.865	8.34	0.26	2.82		2,293		4	6.7	15.45	34.899	5.48	0.40	2.15		2,031
	6	2.9	14.15	34.860	8.18	0.23	2.68		2,287		5	3.4	16.67	34.922	8.16	0.36	1.96		2,015

SeaWiFS Sea-viewing Wide Field-of-view Sensor  
 SIMBIOS Sensor Intercomparison and Merger for Biological and Interdisciplinary Oceanic Studies  
 SPM Suspended Particulate Matter  
 THOR Three-Headed Optical Recorder  
 UCT University of Cape Town  
 UNESCO United Nations Educational, Scientific, and Cultural Organization  
 UV Ultraviolet  
 WETLabs Western Environmental Technology Laboratories (Inc.)

## SYMBOLS

$a(\lambda)$  Spectral absorption coefficient.  
 $A(\lambda)$  Spectral absorbance.  
 $a_d(\lambda)$  Spectral absorption coefficient of detritus.  
 $a_p(\lambda)$  Spectral absorption coefficient of particulate matter.  
 $a_T(\lambda)$  Total spectral absorption (water excluded).  
 $a_y(\lambda)$  Yellow substance (*gelbstoff*) spectral absorption.  
 $a_\phi(\lambda)$  Phytoplankton spectral absorption.  
 $b_b(\lambda)$  Spectral backscattering coefficient.  
 $b_{b_p}(\lambda)$  Particulate spectral backscattering.  
 $b_{b_T}(\lambda)$  Total spectral backscattering (water included).  
 $b_{b_w}(\lambda)$  Molecular (water) spectral backscattering coefficient.  
 $b_T(\lambda)$  Total spectral scattering (water excluded).  
 $C_a$  Chlorophyll *a* concentration.  
 $C_a^S$  Spectrophotometrically determined chlorophyll *a* concentration.  
 $c_T(\lambda)$  Total spectral attenuation (water excluded).  
 $CC$  Cloud cover.  
 $dr$  Radius interval.  
 $E^{\text{PAR}}$  PAR.  
 $E_0^{\text{PAR}}$  PAR measured as scalar irradiance.  
 $E_d(z, \lambda)$  Spectral downward irradiance.  
 $E_d(0^+, \lambda)$  Spectral downward irradiance measured just above the sea surface (the global solar irradiance).  
 $E_d(0^-, \lambda)$  Spectral downward irradiance measured just below the sea surface.  
 $E_u(z, \lambda)$  Spectral upward irradiance.  
 $F$  Fluorescence.  
 $F(r)$  The number of particles of radius  $r$ .  
 $F_m$  Maximal fluorescence yield.  
 $F_m D$  Maximal fluorescence yield in the dark chamber.  
 $F_m L$  Maximal fluorescence yield in the light chamber.  
 $F_o$  Ambient fluorescence yield.  
 $F_o D$  Ambient fluorescence yield in the dark chamber.  
 $F_o L$  Ambient fluorescence yield in the light chamber.  
 $F_v$  Variable fluorescence.  
 $F_v D$  Variable fluorescence in the dark chamber.  
 $F_v L$  Variable fluorescence in the light chamber.  
 $G$  Geometrical cross-sectional area of particles per unit volume.  
 $H$  Wave height.  
 $K_d(\lambda)$  Spectral diffuse attenuation coefficient for downward irradiance.  
 $K_u(\lambda)$  Spectral diffuse attenuation coefficient for upward irradiance.

$L_i(\lambda)$  Spectral sky radiance.  
 $L_T(\lambda)$  Spectral total radiance.  
 $L_u(\lambda)$  Spectral upwelling radiance.  
 $L_u(z_0)$  Spectral upwelling near-surface radiance.  
 $n$  The bottle number.  
 $N$  The number of parameters.  
 $N_B$  Bacteria counts.  
 $N_C$  Coulter counts.  
 $N_F$  The number of free-fall (microNESS, LoCNESS, plus microPRO) casts.  
 $N_P$  Phytoplankton counts.  
 $P_l$  Path length of spectrophotometer cuvette.  
 $Q(\lambda)$  The (bidirectional)  $Q$ -factor:  $Q(\lambda) = E_u(\lambda)/L_u(\lambda)$ .  
 $r$  Radius.  
 $r_{\text{eff}}$  The effective radius.  
 $R(\lambda)$  Spectral irradiance reflectance.  
 $R^2$  Square of the linear correlation coefficient.  
 $s$  The exponential slope.  
 $S$  Salinity.  
 $T_n$  Turbidity.  
 $T_w$  Seawater temperature.  
 $V_e$  Volume of extract.  
 $V_f$  Volume filtered.  
 $W$  Wind speed.  
 $z$  Depth.  
 $Z_D$  The depth of a sample.  
 $Z_n$  Bottle number depth ( $n$  indicates the bottle).  
 $\vartheta$  The nadir viewing angle.  
 $\vartheta'$  The zenith viewing angle measured from nadir ( $\pi - \vartheta$ ).  
 $\lambda$  Wavelength.  
 $\lambda_i$  A particular wavelength.  
 $\lambda_h$  Wavelength for hyperspectral instruments.  
 $\rho_a$  Air-water Fresnel reflectance.  
 $\rho_w$  Water-air Fresnel reflectance.  
 $\sigma_{\text{PS2}}$  Size of the cross-section of PS2.  
 $\tau$  Turnover time of PS2.  
 $\varphi$  The two-axis tilt with respect to the vertical axis.  
 $v_{\text{eff}}$  Effective variance.

## REFERENCES

- Aiken, J., 2001: Fluorometry as a Biological Sensor. In: *Encyclopaedia of Ocean Sciences*. J.H. Steele, K.K. Turekian and S.A. Thorpe, Eds., Academic Press, San Diego, California, 1,073–1,081.
- , D.G. Cummings, S.W. Gibb, N.W. Rees, R. Woodd-Walker, E.M.S. Woodward, J. Woolfenden, S.B. Hooker, J-F. Berthon, C.D. Dempsey, D.J. Suggett, P. Wood, C. Donlon, N. González-Berítez, I. Huskin, M. Quevedo, R. Barciela-Fernandez, C. de Vargas, and C. McKee, 1998: AMT-5 Cruise Report. *NASA Tech. Memo. 1998-206892*, Vol. 2, S.B. Hooker and E.R. Firestone, Eds., NASA Goddard Space Flight Center, Greenbelt, Maryland, 113 pp.

## BENCAL Cruise Report

- , G.F. Moore, C.C. Trees, S.B. Hooker, and D.K. Clark, 1995: The SeaWiFS CZCS-Type Pigment Algorithm. *NASA Tech. Memo. 104566, Vol. 29*, S.B. Hooker and E.R. Firestone, Eds., NASA Goddard Space Flight Center, Greenbelt, Maryland, 34 pp.
- Barber, J., S. Malkin, and A. Telfer, 1989: The origin of chlorophyll fluorescence *in vivo* and its quenching of the photosystem II reaction center. *Phil. Trans. R. Soc. Ser. B*, **323**, 227–239.
- Barlow, R.G., 1982: Phytoplankton ecology in the southern Benguela current. I. Biochemical composition. *J. Exp. Mar. Biol. Ecol.*, **63**, 209–227.
- , D.G. Cummings, and S.W. Gibb, 1997: Improved resolution of mono- and divinyl chlorophylls *a* and *b* and zeaxanthin and lutein in phytoplankton extracts using reverse phase C-8 HPLC. *Mar. Ecol. Prog. Ser.*, **161**, 303–307.
- , J. Aiken, H.E. Sessions, S. Lavender, and J. Mantel, 2001: Phytoplankton pigment, absorption and ocean colour characteristics in the southern Benguela ecosystem. *S. Afr. J. Sci.*, **97**, 230–238.
- Bricaud, A., A. Morel, and L. Prieur, 1981: Absorption by dissolved organic matter of the sea (yellow substance) in the UV and visible domains. *Limnol. Oceanogr.*, **26**, 43–53.
- , A.L. Bedhomme, and A. Morel, 1988: Optical properties of diverse phytoplanktonic species: Experimental results and theoretical interpretation. *J. Plankton Res.*, **10**, 851–873.
- , and D. Stramski, 1990: Spectral absorption coefficients of living phytoplankton and nonalgal biogenous matter: A comparison between the Peru upwelling area and Sargasso Sea. *Limnol. Oceanogr.*, **35**, 562–582.
- Brown, P.C., S.J. Painting, and K.L. Cochrane, 1991: Estimates of phytoplankton and bacterial biomass and production in the northern and southern Benguela ecosystems. *S. Afr. J. Sci.*, **11**, 537–564.
- Buiteveld, H., J.H.H. Hakvoort, and M. Donze, 1994: The optical properties of pure water. *Ocean Optics XIII*, J.S. Jaffe, Ed., Proc. SPIE, **2258**, 174–183.
- Carder, K.L., F.R. Chen, Z.P. Lee, S. Hawes, and D. Kamykowski, 1999: Semi-analytic MODIS algorithms for chlorophyll *a* and absorption with bio-optical domains based on nitrate-depletion temperatures. *J. Geophys. Res.*, **104**, 5,403–5,421.
- Claustre, H., A. Morel, S.B. Hooker, M. Babin, D. Antoine, K. Oubelkheir, A. Bricaud, K. Leblanc, B. Quéguiner, and S. Maritorena, 2002: Is desert dust making oligotrophic waters greener? *Geophys. Res. Lett.*, **29**, 107-1–107-4.
- , S.B. Hooker, L. Van Heukelem, J-F. Berthon, R. Barlow, J. Ras, H. Sessions, C. Targa, C.S. Thomas, D. van der Linde, and J-C. Marty, 2003: An intercomparison of HPLC phytoplankton methods using *in situ* samples: Application to remote sensing and database activities. *Mar. Chem.*, (submitted).
- Duncombe Rae, C.M., 1991: Agulhas retroflection rings in the South Atlantic: an overview. *S. Afr. J. Sci.*, **11**, 327–344.
- Falkowski, P.G., and D.A. Kiefer, 1985: Chlorophyll-*a* fluorescence in phytoplankton: Relationships to photosynthesis and biomass. *J. Plankton. Res.*, **7**, 715–731.
- Garver, S.A., and D.A. Siegel, 1997: Inherent optical property inversion of ocean color spectra and its biogeochemical interpretation. 1. Time series from the Sargasso Sea. *J. Geophys. Res.*, **102**, 18,607–18,625.
- Garzoli, S.L., P.L. Richardson, C.M. Duncombe Rae, D.M. Fratantoni, G.J. Goni, and A.J. Roubicek, 1999: Three Agulhas rings observed during the Benguela Current Experiment. *J. Geophys. Res.*, **104**, 20,971–20,985.
- Grasshoff, K., M. Ehrhardt, and K. Kremling, 1983: *Methods of Seawater Analysis*. Second edition. Verlag Chemie, Weinheim, 419 pp.
- Hansen, J.E., and L.D. Travis, 1974: Light scattering in planetary atmospheres. *Space Sci. Rev.*, **16**, 527–610.
- Hobbie, J.E., R.J. Daley, and S. Jasper, 1977: Use of Nucleopore filters for counting bacteria by fluorescence microscopy. *Appl. Environ. Microbio.*, **33**, 1,225–1,228.
- HOBILabs, 2002: *HydroSCAT-6 Spectral Backscattering Sensor, Users Manual*. Hydro-Optics, Biology and Instrumentation Laboratories, Inc., Moss Landing, California, 63 pp.
- Hooker, S.B., and W.E. Esaias, 1993: An overview of the SeaWiFS project. *Eos, Trans., Amer. Geophys. Union*, **74**, 241–246.
- , G. Zibordi, G. Lazin, and S. McLean, 1999: The SeaBOARR-98 Field Campaign. *NASA Tech. Memo. 1999-206892, Vol. 3*, S.B. Hooker and E.R. Firestone, Eds., NASA Goddard Space Flight Center, Greenbelt, Maryland, 40 pp.
- , and S. Maritorena, 2000: An evaluation of oceanographic radiometers and deployment methodologies. *J. Atmos. Ocean. Technol.*, **17**, 811–830.
- , H. Claustre, J. Ras, L. Van Heukelem, J-F. Berthon, C. Targa, D. van der Linde, R. Barlow, and H. Sessions, 2000: The First SeaWiFS HPLC Analysis Round-Robin Experiment (SeaHARRE-1). *NASA Tech. Memo. 2000-206892, Vol. 14*, S.B. Hooker and E.R. Firestone, Eds., NASA Goddard Space Flight Center, Greenbelt, Maryland, 42 pp.
- Hutchings, L., 1992: Fish harvesting in a variable, productive environment—searching for rules or searching for exceptions? *S. Afr. J. Sci.*, **12**, 297–318.
- Jeffrey, S.W., and G.F. Humphrey, 1975: New spectrophotometric equations for determining chlorophylls *a*, *b*, *c*<sub>1</sub> and *c*<sub>2</sub> in higher plants, algae and natural phytoplankton. *Biochem. Physiol. Pflanzen*, **167**, 191–194.

- , R.F.C. Mantoura, and S.W. Wright, 1997: *Phytoplankton Pigments in Oceanography: Guidelines to Modern Methods*. UNESCO Publishing, Paris, 661 pp.
- JGOFS, 1994: Protocols for the Joint Global Ocean Flux Study Core Measurements. Intergovernmental Oceanographic Commission, Scientific Committee on Oceanic Research. *Manual and Guides, UNESCO, 29*, 91–96.
- Kirk, J.T.O., 1994: *Light and Photosynthesis in Aquatic Ecosystems*, 2nd Ed. Cambridge University Press, Cambridge, 509 pp.
- Kirkwood, D.S., 1994: The SAN plus segmented flow analyzer: Seawater analysis. Publication No. 07300194. *Ministry of Agriculture, Fisheries and Food (MAFF)*. Lowestoft, UK. 34 pp.
- Kishino, M., N. Okami, and S. Ichimura, 1985: Estimation of the spectral absorption coefficients of phytoplankton in the sea. *Bull. Mar. Sci.*, **37**, 634–642.
- Kolber, Z., and P.G. Falkowski, 1993: Use of active fluorescence to estimate phytoplankton photosynthesis *in situ*. *Limnol. Oceanogr.*, **38**, 1,646–1,665.
- , O. Prasil, and P.G. Falkowski, 1998: Measurements of variable fluorescence using fast repetition rate techniques: Defining methodology and experimental protocols. *Biochimica et Biophysica Acta*, **1,367**, 88–106.
- Kou, L., D. Labrie, and P. Chylek, 1993: Refractive indices of water and ice in the 0.65–2.5 mm spectral range. *Appl. Opt.*, **32**, 3,531–3,540.
- Kuring, N., M.R. Lewis, T. Platt, and J.E. O'Reilly, 1990: Satellite-derived estimates of primary production on the northwest Atlantic continental shelf. *Cont. Shelf Res.*, **10**, 461–484.
- Maffione, R.A., and D.R. Dana, 1997: Instruments and methods for measuring the backward-scattering coefficient of ocean waters. *Appl. Opt.*, **36**, 6,057–6,067.
- Mitchell, B.G., and D.A. Kiefer, 1988: Chlorophyll *a* specific absorption and fluorescence excitation spectra for light-limited phytoplankton. *Deep-Sea Res.*, **35**, 639–663.
- , M. Kahru, J. Wieland, and M. Stramska, 2002: "Determination of spectral absorption coefficients of particles, dissolved material and phytoplankton for discrete water samples." In: Mueller, J.L., and 39 Coauthors, *Ocean Optics Protocols for Satellite Ocean Color Sensor Validation, Revision 3, Volume 2. NASA Tech. Memo. 2002-210004/Rev3-Vol2*, NASA Goddard Space Flight Center, Greenbelt, Maryland, 231–257.
- Mitchell-Innes, B.A., and A. Winter, 1987: Coccolithophores: A major phytoplankton component in mature upwelled waters off the Cape Peninsula, South Africa in March 1983. *Mar. Biol.*, **95**, 25–30.
- Mobley, C.D., 1994: *Light and Water: Radiative Transfer in Natural Waters*. Academic Press, San Diego, California, 592 pp.
- Moore, C., J.R.V. Zaneveld, and J.C. Kitchen, 1992: Preliminary results from an in-situ spectral absorption meter. *Ocean Optics XI, Proc. SPIE*, **1750**, 330–337.
- Morel, A., 1988: Optical modeling of the upper ocean in relation to its biogenous matter content (case 1 water). *J. Geophys. Res.*, **93**, 10,749–10,768
- , and Y. Ahn, 1991: Optics of heterotrophic nanoflagellates and ciliates: A tentative assessment of their scattering role in oceanic waters compared to those of bacterial and algal cells. *J. Mar. Res.*, **49**, 177–202.
- , and D. Antoine, 2000: *Pigment index retrieval in Case 1 waters*. MERIS ATBD 2.9, ESA Doc. No. PO-TN-MEL-GS-0005, 9-1-9-20. [World Wide Web page.] From URL: [http://envisat.esa.int/instruments/meris/pdf/atbd\\_2\\_09.pdf](http://envisat.esa.int/instruments/meris/pdf/atbd_2_09.pdf) European Space Agency, Issue 4, Rev. 2, 26 pp.
- , and S. Maritorena, 2001: Bio-optical properties of oceanic waters: A reappraisal. *J. Geophys. Res.*, **106**, 7,163–7,180.
- Mueller, J.L., 2003: "Overview of measurement and data analysis methods." In: Mueller, J.L., and 17 Coauthors, *Ocean Optics Protocols for Satellite Ocean Color Sensor Validation, Revision 4, Volume III: Radiometric Measurements and Data Analysis Protocols. NASA Tech. Memo. 2003-211621/Rev4-Vol.III*, NASA Goddard Space Flight Center, Greenbelt, Maryland, 1–6.
- , and R.W. Austin, 1995: *Ocean Optics Protocols for SeaWiFS Validation, Revision 1. NASA Tech. Memo. 104566, Vol. 25*, S.B. Hooker, E.R. Firestone, and J.G. Acker, Eds., NASA Goddard Space Flight Center, Greenbelt, Maryland, 67 pp.
- , and C.C. Trees, 1997: "Revised SeaWiFS prelaunch algorithm for the diffuse attenuation coefficient  $K(490)$ ." In: Yeh, E-n., R.A. Barnes, M. Darzi, L. Kumar, E.A. Early, B.C. Johnson, and J.L. Mueller, *Case Studies for SeaWiFS Calibration and Validation, Part 4. NASA Tech. Memo. 104566, Vol. 41*, S.B. Hooker and E.R. Firestone, Eds., NASA Goddard Space Flight Center, Greenbelt, Maryland, 18–21.
- Nelson, G., and L. Hutchings, 1983: The Benguela upwelling area. *Prog. Oceanogr.*, **12**, 333–356.
- , A.J. Boyd, J.J. Agenbag, and C.M. Duncombe Rae, 1998: An upwelling filament north-west of Cape Town, South Africa. *S. Afr. J. Sci.*, **19**, 75–88.
- O'Reilly, J.E., and 24 Coauthors, 2000: *SeaWiFS Postlaunch Calibration and Validation Analyses, Part 3. NASA Tech. Memo. 2000-206892, Vol. 11*, S.B. Hooker and E.R. Firestone, Eds., NASA Goddard Space Flight Center, 49 pp.
- Pegau, W.S., D. Gray, and J.R.V. Zaneveld, 1997: Absorption of visible and near-infrared light in water: The dependence on temperature and salinity. *Appl. Opt.*, **36**, 6,035–6,046.
- Pitcher, G.C., A.J. Boyd, D.A. Horstman, and B.A. Mitchell-Innes, 1998: Subsurface dinoflagellate populations, frontal blooms and the formation of red tide in the southern Benguela upwelling system. *Mar. Ecol. Prog. Ser.*, **172**, 253–264.

## BENCAL Cruise Report

- Platt, T., C.M. Caverhill, and S. Sathyendranath, 1991: Basin-scale estimates of oceanic primary production by remote sensing: The North Atlantic. *J. Geophys. Res.*, **96**, 15,147–15,159.
- Pope, R.M., and E.S. Fry, 1997: Absorption spectrum (380–700 nm) of pure water II, Integrating cavity measurements, *Appl. Opt.*, **36**, 8,710–8,723.
- Robins, D.B., A.J. Bale, G.F. Moore, N.W. Rees, S.B. Hooker, C.P. Gallienne, A.G. Westbrook, E. Marañón, W.H. Spooner, and S.R. Laney, 1996: AMT-1 Cruise Report and Preliminary Results. *NASA Tech. Memo. 104566*, Vol. 35, S.B. Hooker and E.R. Firestone, Eds., NASA Goddard Space Flight Center, Greenbelt, Maryland, 87 pp.
- Schiller, H., and R. Doerffer, 1999: Neural network for emulation of an inverse model—operational derivation of Case II water properties from MERIS data. *Int. J. Remote Sens.*, **20**, 1,735–1,746.
- Shannon, L.V., 1985: The Benguela ecosystem. Part I. Evolution of the Benguela, physical features and processes. *Oceanogr. Mar. Biol. Ann. Rev.*, **23**, 105–182.
- , and G. Nelson, 1996: The Benguela: Large scale features and processes and system variability. In: Wefer, G., W.H. Berger, G. Siedler, and D.J. Webb, Eds., *The South Atlantic: Present and Past Circulation*. Springer, Berlin, 163–210.
- Smayda, T.J., 1978: Estimating cell numbers. What to count? In: Sournia, A., Ed., *Phytoplankton Manual*, UNESCO Monographs on Oceanographic Methodology, **6**, 165–166.
- Strickland, J.D.H., and T.R. Parsons, 1972: "Determination of dissolved oxygen." In: A Practical Handbook of Seawater Analysis. *Fish. Res. Board Can. Bull.*, **167**, 21–26.
- Vidussi, F., H. Claustre, J. Bustillos-Guzmán, C. Cailliau, and J-C Marty, 1996: Determination of chlorophylls and carotenoids of marine phytoplankton: Separation of chlorophyll *a* from divinyl-chlorophyll *a* and zeaxanthin from lutein. *J. Plankton Res.*, **18**, 2,377–2,382.
- , —, B.B. Manca, A. Luchetta, and J-C. Marty, 2001: Phytoplankton pigment distribution in relation to upper thermocline circulation in the eastern Mediterranean Sea during winter. *J. Geophys. Res.*, **106**, 19,939–19,956.
- WETLabs, 2000: *AC-9 Protocol Document, Revision D*. Western Environmental Technology Laboratories (WETLabs), Philomath, Oregon, 47 pp.
- Wright, S.W., S.W. Jeffrey, F.C. Mantoura, C.A. Llewellyn, T. Bjørnland, D. Repeta, and N. Welschmeyer, 1991: Improved HPLC method for the analysis of chlorophylls and carotenoids from marine phytoplankton. *Mar. Ecol. Prog. Ser.*, **77**, 183–196.
- Zaneveld, J.R.V., J.C. Kitchen, and C.C. Moore, 1994: Scattering error correction of reflecting tube absorption meters. *Ocean Optics XII*, S. Ackleson, Ed., Proc. SPIE, **2258**, 44–55.
- , E. Boss, and P.A. Hwang, 2001: The influence of coherent waves on the remotely sensed reflectance. *Optics Express*, **9**, 260–266.

## THE SEAWiFS POSTLAUNCH TECHNICAL REPORT SERIES

### Vol. 1

Johnson, B.C., J.B. Fowler, and C.L. Cromer, 1998: The SeaWiFS Transfer Radiometer (SXR). *NASA Tech. Memo. 1998-206892*, Vol. 1, S.B. Hooker and E.R. Firestone, Eds., NASA Goddard Space Flight Center, Greenbelt, Maryland, 58 pp.

### Vol. 2

Aiken, J., D.G. Cummings, S.W. Gibb, N.W. Rees, R. Woodd-Walker, E.M.S. Woodward, J. Woolfenden, S.B. Hooker, J-F. Berthon, C.D. Dempsey, D.J. Suggett, P. Wood, C. Donlon, N. González-Benítez, I. Huskin, M. Quevedo, R. Barciela-Fernandez, C. de Vargas, and C. McKee, 1998: AMT-5 Cruise Report. *NASA Tech. Memo. 1998-206892*, Vol. 2, S.B. Hooker and E.R. Firestone, Eds., NASA Goddard Space Flight Center, Greenbelt, Maryland, 113 pp.

### Vol. 3

Hooker, S.B., G. Zibordi, G. Lazin, and S. McLean, 1999: The SeaBOARR-98 Field Campaign. *NASA Tech. Memo. 1999-206892*, Vol. 3, S.B. Hooker and E.R. Firestone, Eds., NASA Goddard Space Flight Center, Greenbelt, Maryland, 40 pp.

### Vol. 4

Johnson, B.C., E.A. Early, R.E. Eplee, Jr., R.A. Barnes, and R.T. Caffrey, 1999: The 1997 Prelaunch Radiometric Calibration of SeaWiFS. *NASA Tech. Memo. 1999-206892*, Vol. 4, S.B. Hooker and E.R. Firestone, Eds., NASA Goddard Space Flight Center, Greenbelt, Maryland, 51 pp.

### Vol. 5

Barnes, R.A., R.E. Eplee, Jr., S.F. Biggar, K.J. Thome, E.F. Zalewski, P.N. Slater, and A.W. Holmes 1999: The SeaWiFS Solar Radiation-Based Calibration and the Transfer-to-Orbit Experiment. *NASA Tech. Memo. 1999-206892*, Vol. 5, S.B. Hooker and E.R. Firestone, Eds., NASA Goddard Space Flight Center, 28 pp.

### Vol. 6

Firestone, E.R., and S.B. Hooker, 2000: SeaWiFS Postlaunch Technical Report Series Cumulative Index: Volumes 1–5. *NASA Tech. Memo. 2000-206892*, Vol. 6, S.B. Hooker and E.R. Firestone, Eds., NASA Goddard Space Flight Center, Greenbelt, Maryland, 14 pp.

### Vol. 7

Johnson, B.C., H.W. Yoon, S.S. Bruce, P-S. Shaw, A. Thompson, S.B. Hooker, R.E. Eplee, Jr., R.A. Barnes, S. Maritorena, and J.L. Mueller, 1999: The Fifth SeaWiFS Intercalibration Round-Robin Experiment (SIRREX-5), July 1996. *NASA Tech. Memo. 1999-206892*, Vol. 7, S.B. Hooker and E.R. Firestone, Eds., NASA Goddard Space Flight Center, 75 pp.

- Vol. 8
- Hooker, S.B., and G. Lazin, 2000: The SeaBOARR-99 Field Campaign. *NASA Tech. Memo. 2000-206892, Vol. 8*, S.B. Hooker and E.R. Firestone, Eds., NASA Goddard Space Flight Center, 46 pp.
- Vol. 9
- McClain, C.R., E.J. Ainsworth, R.A. Barnes, R.E. Eplee, Jr., F.S. Patt, W.D. Robinson, M. Wang, and S.W. Bailey, 2000: SeaWiFS Postlaunch Calibration and Validation Analyses, Part 1. *NASA Tech. Memo. 2000-206892, Vol. 9*, S.B. Hooker and E.R. Firestone, Eds., NASA Goddard Space Flight Center, 82 pp.
- Vol. 10
- McClain, C.R., R.A. Barnes, R.E. Eplee, Jr., B.A. Franz, N.C. Hsu, F.S. Patt, C.M. Pietras, W.D. Robinson, B.D. Schieber, G.M. Schmidt, M. Wang, S.W. Bailey, and P.J. Werdell, 2000: SeaWiFS Postlaunch Calibration and Validation Analyses, Part 2. *NASA Tech. Memo. 2000-206892, Vol. 10*, S.B. Hooker and E.R. Firestone, Eds., NASA Goddard Space Flight Center, 57 pp.
- Vol. 11
- O'Reilly, J.E., S. Maritorena, M.C. O'Brien, D.A. Siegel, D. Toole, D. Menzies, R.C. Smith, J.L. Mueller, B.G. Mitchell, M. Kahru, F.P. Chavez, P. Strutton, G.F. Cota, S.B. Hooker, C.R. McClain, K.L. Carder, F. Müller-Karger, L. Harding, A. Magnuson, D. Phinney, G.F. Moore, J. Aiken, K.R. Arrigo, R. Letelier, and M. Culver 2000: SeaWiFS Postlaunch Calibration and Validation Analyses, Part 3. *NASA Tech. Memo. 2000-206892, Vol. 11*, S.B. Hooker and E.R. Firestone, Eds., NASA Goddard Space Flight Center, 49 pp.
- Vol. 12
- Firestone, E.R., and S.B. Hooker, 2000: SeaWiFS Postlaunch Technical Report Series Cumulative Index: Volumes 1-11. *NASA Tech. Memo. 2000-206892, Vol. 12*, S.B. Hooker and E.R. Firestone, Eds., NASA Goddard Space Flight Center, Greenbelt, Maryland, 24 pp.
- Vol. 13
- Hooker, S.B., G. Zibordi, J-F. Berthon, S.W. Bailey, and C.M. Pietras, 2000: The SeaWiFS Photometer Revision for Incident Surface Measurement (SeaPRISM) Field Commissioning. *NASA Tech. Memo. 2000-206892, Vol. 13*, S.B. Hooker and E.R. Firestone, Eds., NASA Goddard Space Flight Center, Greenbelt, Maryland, 24 pp.
- Vol. 14
- Hooker, S.B., H. Claustre, J. Ras, L. Van Heukelem, J-F. Berthon, C. Targa, D. van der Linde, R. Barlow, and H. Sessions, 2000: The First SeaWiFS HPLC Analysis Round-Robin Experiment (SeaHARRE-1). *NASA Tech. Memo. 2000-206892, Vol. 14*, S.B. Hooker and E.R. Firestone, Eds., NASA Goddard Space Flight Center, Greenbelt, Maryland, 42 pp.
- Vol. 15
- Hooker, S.B., G. Zibordi, J-F. Berthon, D. D'Alimonte, S. Maritorena, S. McLean, and J. Sildam, 2001: Results of the Second SeaWiFS Data Analysis Round Robin, March 2000 (DARR-00). *NASA Tech. Memo. 2001-206892, Vol. 15*, S.B. Hooker and E.R. Firestone, Eds., NASA Goddard Space Flight Center, Greenbelt, Maryland, 71 pp.
- Vol. 16
- Patt, F.S., 2002: Navigation Algorithms for the SeaWiFS Mission. *NASA Tech. Memo. 2002-206892, Vol. 16*, S.B. Hooker and E.R. Firestone, Eds., NASA Goddard Space Flight Center, Greenbelt, Maryland, 17 pp.
- Vol. 17
- Hooker, S.B., S. McLean, J. Sherman, M. Small, G. Lazin, G. Zibordi, and J.W. Brown, 2002: The Seventh SeaWiFS Intercalibration Round-Robin Experiment (SIRREX-7), March 1999. *NASA Tech. Memo. 2002-206892, Vol. 17*, S.B. Hooker and E.R. Firestone, Eds., NASA Goddard Space Flight Center, Greenbelt, Maryland, 69 pp.
- Vol. 18
- Firestone, E.R., and S.B. Hocker, 2002: SeaWiFS Postlaunch Technical Report Series Cumulative Index: Volumes 1-17. *NASA Tech. Memo. 2002-206892, Vol. 18*, S.B. Hooker and E.R. Firestone, Eds., NASA Goddard Space Flight Center, Greenbelt, Maryland, 28 pp.
- Vol. 19
- Zibordi, G., J-F. Berthon, J.P. Doyle, S. Grossi, D. van der Linde, C. Targa, and L. A. berotanza 2002: Coastal Atmosphere and Sea Time Series (CoASTS), Part 1: A Tower-Based Long-Term Measurement Program. *NASA Tech. Memo. 2002-206892, Vol. 19*, S.B. Hooker and E.R. Firestone, Eds., NASA Goddard Space Flight Center, Greenbelt, Maryland, 29 pp.
- Vol. 20
- Berthon, J-F., G. Zibordi, J.P. Doyle, S. Grossi, D. van der Linde, and C. Targa, 2002: Coastal Atmosphere and Sea Time Series (CoASTS), Part 2: Data Analysis. *NASA Tech. Memo. 2002-206892, Vol. 20*, S.B. Hooker and E.R. Firestone, Eds., NASA Goddard Space Flight Center, Greenbelt, Maryland, 25 pp.
- Vol. 21
- Zibordi, G., D. D'Alimonte, D. van der Linde, J-F. Berthon, S.B. Hooker, J.L. Mueller, G. Lazin, and S. McLean, 2002: The Eighth SeaWiFS Intercalibration Round-Robin Experiment (SIRREX-8), September-December 2001. *NASA Tech. Memo. 2002-206892, Vol. 21*, S.B. Hooker and E.R. Firestone, Eds., NASA Goddard Space Flight Center, Greenbelt, Maryland, 39 pp.
- Vol. 22
- Patt, F.S., R.A. Barnes, R.E. Eplee, Jr., B.A. Franz, W.D. Robinson, G.C. Feldman, S.W. Bailey, J. Gales, P.J. Werdell, M. Wang, R. Frouin, R.P. Stumpf, R.A. Arnone, R.W. Gould, Jr., P.M. Martinolich, V. Ransibrahmanakul, J.E. O'Reilly, and J.A. Yoder, 2003: Algorithm Updates for the Fourth SeaWiFS Data Reprocessing, *NASA Tech. Memo. 2003-206892, Vol. 22*, S.B. Hooker and E.R. Firestone, Eds., NASA Goddard Space Flight Center, Greenbelt, Maryland, 74 pp.

## BENCAL Cruise Report

### Vol. 23

Hooker, S.B., G. Zibordi, J-F. Berthon, D. D'Alimonte, D. van der Linde, and J.W. Brown, 2003: Tower-Perturbation Measurements in Above-Water Radiometry. *NASA Tech. Memo. 2003-206892, Vol. 23*, S.B. Hooker and E.R. Firestone, Eds., NASA Goddard Space Flight Center, Greenbelt, Maryland, 35 pp.

### Vol. 24

Firestone, E.R., and S.B. Hooker, 2003: SeaWiFS Postlaunch Technical Report Series Cumulative Index: Volumes 1-23. *NASA Tech. Memo. 2003-206892, Vol. 24*, S.B. Hooker and E.R. Firestone, Eds., NASA Goddard Space Flight Center, Greenbelt, Maryland, 35 pp.

### Vol. 25

Doyle, J.P., S.B. Hooker, G. Zibordi, and D. van der Linde, 2003: Validation of an In-Water, Tower-Shading Correction Scheme. *NASA Tech. Memo. 2003-206892, Vol. 25*, S.B. Hooker and E.R. Firestone, Eds., NASA Goddard Space Flight Center, Greenbelt, Maryland, 32 pp.

### Vol. 26

Zibordi, G., D. D'Alimonte, D. van der Linde, S.B. Hooker, and J.W. Brown, 2003: New Laboratory Methods for Characterizing the Immersion Factors of Irradiance Sensors. *NASA Tech. Memo. 2003-206892, Vol. 26*, S.B. Hooker and E.R. Firestone, Eds., NASA Goddard Space Flight Center, Greenbelt, Maryland, 34 pp.

### Vol. 27

Barlow, R., H. Sessions, N. Silulwane, H. Engel, S.B. Hooker, J. Aiken, J. Fishwick, V. Vicente, A. Morel, M. Chami, J. Ras, S. Bernard, M. Pfaff, J.W. Brown, and A. Fawcett, 2003: BENCAL Cruise Report. *NASA Tech. Memo. 2003-206892, Vol. 27*, S.B. Hooker and E.R. Firestone (Eds.), NASA Goddard Space Flight Center, Greenbelt, Maryland, 64 pp.

# REPORT DOCUMENTATION PAGE

Form Approved  
OMB No. 0704-0188

Public reporting burden for this collection of information is estimated to average 1 hour per response, including the time for reviewing instructions, searching existing data sources, gathering and maintaining the data needed, and completing and reviewing the collection of information. Send comments regarding this burden estimate or any other aspect of this collection of information, including suggestions for reducing this burden, to Washington Headquarters Services, Directorate for Information Operations and Reports, 1215 Jefferson Davis Highway, Suite 1204, Arlington, VA 22202-4302, and to the Office of Management and Budget, Paperwork Reduction Project (0704-0188), Washington, DC 20503.

<b>1. AGENCY USE ONLY (Leave blank)</b>		<b>2. REPORT DATE</b> September 2003	<b>3. REPORT TYPE AND DATES COVERED</b> Technical Memorandum	
<b>4. TITLE AND SUBTITLE</b> SeaWiFS Postlaunch Technical Report Series Volume 27: BENCAL Cruise Report			<b>5. FUNDING NUMBERS</b>	
<b>6. AUTHOR</b> Ray Barlow, Heather Sessions, Nonkqubela Silulwane, Hermann Engel, Stanford B. Hooker, James Fishwick, Victor Martinez-Vicente, André Morel, Malik Chami, Joséphine Ras, Stewart Bernard Maya Pfaff, James W. Brown, and Alexandra Fawcett  Series Editors: Stanford B. Hooker and Elaine R. Firestone				
<b>7. PERFORMING ORGANIZATION NAME(S) AND ADDRESS(ES)</b> Laboratory for Hydrospheric Processes Goddard Space Flight Center Greenbelt, Maryland 20771			<b>8. PERFORMING ORGANIZATION REPORT NUMBER</b> 2003-01909-0	
<b>9. SPONSORING/MONITORING AGENCY NAME(S) AND ADDRESS(ES)</b> National Aeronautics and Space Administration Washington, D.C. 20546-0001			<b>10. SPONSORING/MONITORING AGENCY REPORT NUMBER</b> TM-2003-206892, Vol. 27	
<b>11. SUPPLEMENTARY NOTES</b> E.R. Firestone: Science Applications International Corporation, Beltsville, Maryland; R. Barlow, H. Sessions, N. Silulwane, and H. Engel: Marine and Coastal Management, Cape Town, South Africa; J. Aiken, J. Fishwick, and V. Martinez-Vicente: Plymouth Marine Laboratory, Plymouth, United Kingdom; A. Morel, M. Chami, and J. Ras: <i>LOV Observatoire Océanologique de Villefranche</i> , Villefranche-sur-Mer, France; S. Bernard and M. Pfaff: University of Cape Town, Cape Town, South Africa; J.W. Brown: RSMAS University of Miami, Miami, Florida; A. Fawcett: Saturn Solutions, Ltd., Southampton, United Kingdom				
<b>12a. DISTRIBUTION/AVAILABILITY STATEMENT</b> Unclassified-Unlimited Subject Category 48 Report is available from the Center for AeroSpace Information (CASI), 7121 Standard Drive, Hanover, MD 21076-1320; (301)621-0390			<b>12b. DISTRIBUTION CODE</b>	
<b>13. ABSTRACT (Maximum 200 words)</b> This report documents the scientific activities on board the South African Fisheries Research Ship (FRS) <i>Africana</i> during an ocean color calibration and validation cruise in the Benguela upwelling ecosystem (BENCAL), 4-17 October 2002. The cruise, denoted <i>Africana</i> voyage 170, was staged in the southern Benguela between Cape Town and the Orange River within the region 14-18.5°E, 29-34°S, with 15 scientists participating from seven different international organizations. Uniquely in October 2002, four high-precision ocean color sensors were operational, and these included the Moderate Resolution Imaging Spectro-radiometer (MODIS) instruments on the Aqua and Terra spacecraft, the Medium Resolution Imaging Spectrometer (MERIS), and the Sea-viewing Wide Field-of-view Sensor (SeaWiFS). SeaWiFS imagery was transmitted daily to the ship to assist in choosing the vessel's course and selecting stations for bio-optical deployments. There were four primary objectives of the cruise. The first was to conduct bio-optical measurements with above- and in-water optical instruments to vicariously calibrate the satellite sensors. The second was to interrelate diverse measurements of the apparent optical properties (AOPs) at satellite sensor wavelengths with inherent optical properties (IOPs) and bio-optically active constituents of seawater such as particles, pigments, and dissolved compounds. The third was to determine the interrelationships between optical properties, phytoplankton pigment composition, photosynthetic rates, and primary production, while the fourth objective was to collect samples for a second pigment round-robin intercalibration experiment. Weather conditions were generally very favorable, and a range of hyperspectral and fixed wavelength AOP instruments were deployed during daylight hours. Various IOP instruments were used to determine the absorption, attenuation, scattering, and backscattering properties of particulate matter and dissolved substances, while a Fast Repetition Rate Fluorometer (FRRF) was deployed to acquire data on phytoplankton photosynthetic activity. Hydrographic profiling was conducted routinely during the cruise, and seawater samples were collected for measurements of salinity, oxygen, inorganic nutrients, pigments, particulate organic carbon, suspended particulate material, and primary production. Location of stations and times of optical deployments were selected to coincide with satellite overpasses whenever possible, and to cover a large range in trophic conditions.				
<b>14. SUBJECT TERMS</b> SeaWiFS, Oceanography, BENCAL, Cruise Report, Remote Sensing, Hydrographic Data			<b>15. NUMBER OF PAGES</b> 64	
			<b>16. PRICE CODE</b>	
<b>17. SECURITY CLASSIFICATION OF REPORT</b> Unclassified	<b>18. SECURITY CLASSIFICATION OF THIS PAGE</b> Unclassified	<b>19. SECURITY CLASSIFICATION OF ABSTRACT</b> Unclassified	<b>20. LIMITATION OF ABSTRACT</b> Unlimited	